NASA Technical Paper 1589

Exploratory Study of the Effects of Wing-Leading-Edge Modifications on the Stall/Spin Behavior of a Light General Aviation Airplane

Staff of Langley Research Center
Hampton, Virginia

NASA

National Aeronautics
and Space Administration

**Scientific and Technical
Information Branch**

1979

CONTENTS

SUMMARY

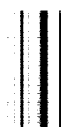An exploratory study was conducted to determine the effects of several wing-leading-edge modifications on the stalling and spinning characteristics of a light, general aviation airplane. Configurations with full-span and segmented leading-edge flaps and full-span and segmented leading-edge droop were tested. Studies were conducted with wind-tunnel models at NASA Langley Research Center, with an outdoor radio-controlled model at West Point, Virginia, and with a full-scale airplane at NASA Wallops Flight Center. This report summarizes some of the more important information generated in the study.

The study showed that wing-leading-edge modifications can produce large effects (both beneficial and detrimental) on stall/spin characteristics, particularly on spin resistance. During the study, an outboard wing modification was conceived and tested which significantly improved lateral stability at stall, spin resistance, and developed spin characteristics. Also, radio-controlled model and full-scale flight results correlated well for all comparable configurations tested.

The results obtained from wind-tunnel tests, radio-controlled model tests, and airplane flight tests are individually presented and discussed herein.

INTRODUCTION

Joseph R. Chambers

At the present time, stalling and spinning are major causal factors in
fatal general aviation accidents, accounting for over 28 percent of the total
number of fatalities (refs. 1 and 2). Examination of the circumstances involved
suggests that the majority of these general aviation stall/spin accidents occur
at low altitude and involve a sequence of inadvertent loss of longitudinal or
lateral-directional control, spin entry, and ground impact before the spin
becomes fully developed. The NASA Langley Research Center has initiated a broad
research program encompassing a wide variety of wind-tunnel and flight testing
techniques to develop the technology required to improve the stalling and spin-
ning characteristics of light general aviation airplanes. References 3 to 7
present some results obtained thus far in the Langley stall/spin research pro-
gram from studies of the fully developed spin and spin recovery. In recognition
of the potential danger associated with inadvertent stalls at low altitude, the
stall/spin research program includes studies to define concepts which improve
the stall characteristics and spin resistance of this class of airplane in addi-
tion to studies of the fully developed spin and spin recovery.

One well-known factor which has a significant influence on lateral stabil-
ity and controllability at the stall is the tendency of unswept wings to experi-
ence unstable damping in roll and autorotation near stall. Unstable damping in
roll can result in rapid rolling and yawing motions which the pilot may find
difficult to control, particularly in the low-altitude, high-work-load environ-
ment of the terminal area. The high angular rates which may result from unstable
damping in roll also lead to autorotation which can propel the airplane to
higher angular rates and angles of attack where the vehicle may exhibit a
developed spin mode.

It has long been recognized that wing-leading-edge modifications, such as
slots, slats, or flaps, can significantly alter the damping-in-roll character-
istics of wings near the stall. The early research of Weick and others
(refs. 8 to 12) identified the potential aerodynamic benefits of such modifica-
tions; however, many of the concepts proposed by the early research efforts
proved to be infeasible because of attendant degradation in aerodynamic perfor-
mance, excessive complexity in terms of construction and maintenance, and cost.
Also, although certain types of leading-edge high-lift devices improved stall
behavior, they actually aggravated spin characteristics in several instances
and resulted in degraded spin recovery.

Recently, the potential advantages at the stall afforded by wing-leading-
edge modifications have been reexamined by the University of Michigan and NASA
Ames Research Center (refs. 13 and 14) in an attempt to eliminate these earlier
deficiencies. The concept involved in their research was to modify portions of
the wing leading edge to control local stall progression and produce a "flat-
top" lift curve which would be expected to minimize or eliminate loss of damping

3

in roll at the stall. Limited wind-tunnel studies indicated that the concept offered considerable promise in achieving a flat-top lift curve. This report documents studies that have been conducted at Langley to more fully explore the potential of segmented leading-edge devices for improving both stalling and spinning characteristics.

In the Langley program, wind-tunnel tests explored the effects of several wing-leading-edge modifications on the static aerodynamic characteristics of models of a representative low-wing general aviation airplane. Particular emphasis was placed on the variation of lift-curve slope of the total configuration with angle of attack near stall. The static tests also included unique tests in which the outer wing panel of the model was mounted to the inner wing panel via a strain-gauge balance to permit documentation and analysis of the aerodynamic characteristics of the outer wing panel. Dynamic (forced-oscillation) wind-tunnel force tests were also conducted to assess the influence of the leading-edge modifications on damping in roll at high angles of attack.

The favorable results indicated by the static and dynamic wind-tunnel tests encouraged a free-flight investigation of the stalling and spinning behavior of a radio-controlled model to permit an evaluation of the effectiveness of the modifications in flight. After results of the model flight tests indicated very significant improvements in stall/spin characteristics, full-scale airplane flight tests were conducted at NASA Wallops Flight Center. The results of this series of tests are summarized in the following three parts of this report.

The reader is cautioned that this investigation was exploratory and limited to a single configuration and that additional wind-tunnel and in-flight research is required to optimize beneficial effects and further define the phenomena discussed herein. In particular, the influence of these leading-edge modifications on aerodynamic performance and operational utility must be determined as well as the general applicability of such concepts to other wing planforms and airfoils. However, the limited results obtained thus far indicate that significant improvements in stalling characteristics and spin resistance may be obtainable by certain types of segmented wing-leading-edge modifications.

4

REFERENCES

1. Silver, Brent W.: Statistical Analysis of General Aviation Stall Spin Accidents. [Preprint] 760480, Soc. Automot. Eng., Apr. 1976.

2. Ellis, David R.: A Study of Lightplane Stall Avoidance and Suppression. Rep. No. FAA-RD-77-25, Feb. 1977.

3. Bowman, James S., Jr.; Stough, Harry P.; Burk, Sanger M., Jr.; and Patton, James M., Jr.: Correlation of Model and Airplane Spin Characteristics for a Low-Wing General Aviation Research Airplane. AIAA Paper 78-1477, Aug. 1978.

4. Burk, Sanger M., Jr.; Bowman, James S., Jr.; and White, William L.: Spin-Tunnel Investigation of the Spinning Characteristics of Typical Single-Engine General Aviation Airplane Designs. I - Low-Wing Model A: Effect of Tail Configurations. NASA TP-1009, 1977.

5. Burk, Sanger M., Jr.; Bowman, James S., Jr.; and White, William L.: Spin-Tunnel Investigation of the Spinning Characteristics of Typical Single-Engine General Aviation Airplane Designs. II - Low-Wing Model A: Tail Parachute Diameter and Canopy Distance for Emergency Spin Recovery. NASA TP-1076, 1977.

6. Bihrle, William, Jr.; Barnhart, Billy; and Pantason, Paul: Static Aero-dynamic Characteristics of a Typical Single-Engine Low-Wing General Aviation Design for an Angle-of-Attack Range of -8° to 90°. NASA CR-2971, 1978.

7. Bihrle, William, Jr.; Hultberg, Randy S.; and Mulcay, William: Rotary Balance Data for a Typical Single-Engine Low-Wing General Aviation Design for an Angle-of-Attack Range of 30° to 90°. NASA CR-2972, 1978.

8. Weick, Fred E.; and Wenzinger, Carl J.: Effect of Length of Handley Page Tip Slots on the Lateral-Stability Factor, Damping in Roll. NACA TN No. 423, 1932.

9. Weick, Fred E.; and Wenzinger, Carl J.: Wind-Tunnel Research Comparing Lateral Control Devices, Particularly at High Angles of Attack. VII - Handley Page Tip and Full-Span Slots With Ailerons and Spoilers. NACA TN No. 443, 1933.

10. Weick, Fred E.; and Wenzinger, Carl J.: Wind-Tunnel Research Comparing Lateral Control Devices, Particularly at High Angles of Attack. I - Ordinary Ailerons on Rectangular Wings. NACA Rep. No. 419, 1932.

11. Weick, Fred Ernest; Sevelson, Maurice S.; McClure, James G.; and Flanagan, Marion D.: Investigation of Lateral Control Near the Stall. Flight Investigation With a Light High-Wing Monoplane Tested With Various Amounts of Washout and Various Lengths of Leading-Edge Slot. NACA TN-2948, 1953.

12. Weick, Fred Ernest; and Abramson, H. Norman: Investigation of Lateral Control Near the Stall. Flight Tests With High-Wing and Low-Wing Monoplanes of Various Configurations. NACA TN-3676, 1956.

13. Kroeger, R. A.; and Feistel, T. W.: Reduction of Stall-Spin Entry Tendencies Through Wing Aerodynamic Design. [Paper] 760481, Soc. Automot. Eng., Apr. 1976.

14. Feistel, T. W.; Anderson, S. B.; and Kroeger, R. A.: A Method for Localizing Wing Flow Separation at Stall To Alleviate Spin Entry Tendencies. AIAA Paper 78-1476, Aug. 1978.

I. WIND-TUNNEL TESTS

Daniel J. DiCarlo; Joseph L. Johnson, Jr.;
Sanger M. Burk, Jr.; and Sue B. Grafton

SUMMARY

Low-speed wind-tunnel tests of a low-wing general aviation airplane have
shown that the lift-curve shape and aerodynamic damping in roll near and above
stall angles of attack could be significantly improved by wing-leading-edge
modifications such as leading-edge flaps and droop. In particular, the results
of static and dynamic (forced-oscillation) tests indicated that the onset of
unstable damping in roll could be delayed to high angles of attack by outboard
leading-edge modifications. Static tests in which the outer wing panel was
mounted to the inner wing panel through a strain-gauge balance indicated that
the outer wing panel with a drooped leading edge acted as a low-aspect-ratio
wing which significantly delayed wing-tip stall and improved lateral stability.
The data obtained in the wind-tunnel tests suggested that the stalling and spin
resistance of the airplane configurations would probably be significantly
improved by outer-wing leading-edge modifications.

INTRODUCTION

This part of the report presents the results of low-speed wind-tunnel
studies and dynamic force tests to determine the effects of segmented wing-
leading-edge devices on the lift characteristics, roll-rate damping, and other
aerodynamic characteristics of a low-wing general aviation airplane at high
angles of attack. Simple small-scale model wind-tunnel tests identified candi-
date wing configurations for further study in radio-controlled model tests and
in airplane flight tests. During the wind-tunnel studies, a large number of
segmented and full-span leading-edge devices (flaps, slats, and droop) and other
wing modifications were tested. Wind-tunnel tests of the more promising config-
urations are presented here in the form of nondimensional force and moment coef-
ficients, lateral-directional dynamic derivatives, and flow-visualization photo-
graphs to aid in qualitatively assessing the aerodynamic behavior associated
with such modifications.

SYMBOLS

All aerodynamic data except for lift and drag are presented with respect to
a body system of axes with a center-of-gravity position of 25 percent of the
wing mean aerodynamic chord. Measurements were made in the U.S. Customary Units
and equivalent values in the International System of Units (SI) were determined
using conversion factors given in reference 1.

b	wing span, m (ft)
$\bar{c}$	wing mean aerodynamic chord, m (ft)
C_D	drag coefficient, $F_D/q_\infty S$
C_L	lift coefficient, $F_L/q_\infty S$
$C_{L,max}$	maximum lift coefficient
C_l	rolling-moment coefficient, $M_X/q_\infty Sb$
C_m	pitching-moment coefficient, $M_Y/q_\infty S\bar{c}$
C_n	yawing-moment coefficient, $M_Z/q_\infty Sb$
C_R	resultant aerodynamic coefficient, $\sqrt{C_L^2 + C_D^2}$
C_Y	side-force coefficient, $F_Y/q_\infty S$
F_D	drag force, N (lb)
F_L	lift force, N (lb)
F_Y	side force, N (lb)
M_X	rolling moment, positive for right wing down, m-N (ft-lb)
M_Y	pitching moment, positive for nose up, m-N (ft-lb)
M_Z	yawing moment, positive for nose right, m-N (ft-lb)
p	rolling velocity, positive for right wing down, rad/sec
q_∞	free-stream dynamic pressure, N/m^2 (lb/ft^2)
S	wing area, m^2 (ft^2)
V	velocity, m/sec (ft/sec)
α	angle of attack, deg or rad
β	angle of sideslip, deg or rad

A dot over symbol indicates derivative with respect to time, and Δ denotes incremental change in a parameter.

8

Dynamic derivatives:

Dynamic derivatives are defined as follows:

$$C_{l_p} = \frac{\partial C_l}{\partial \frac{pb}{2V}} \qquad C_{l_\beta} = \frac{\partial C_l}{\partial \beta}$$

$$C_{l_{\dot\beta}} = \frac{\partial C_l}{\partial \frac{\dot\beta b}{2V}} \qquad C_{n_\beta} = \frac{\partial C_n}{\partial \beta}$$

$$C_{n_p} = \frac{\partial C_n}{\partial \frac{pb}{2V}} \qquad C_{Y_\beta} = \frac{\partial C_Y}{\partial \beta}$$

$$C_{n_{\dot\beta}} = \frac{\partial C_n}{\partial \frac{\dot\beta b}{2V}}$$

Roll out-of-phase derivatives:

The term roll out-of-phase derivative refers to an oscillatory derivative that is based on the components of forces and moments 90° out of phase with the angle of roll produced in the forced-oscillation tests.

$$C_{l_p} + C_{l_{\dot\beta}} \sin \alpha$$

$$C_{n_p} + C_{n_{\dot\beta}} \sin \alpha$$

MODELS

Static low-speed wind-tunnel tests were conducted using the 1/5-scale model of the low-wing airplane shown in figure 1. This model had movable control surfaces which permitted maximum aileron deflections of 25° up to 20° down, rudder deflections of ±25°, and elevator deflections of -25° (trailing edge up) and +15° (trailing edge down). Forced-oscillation tests were conducted with the 1/3-scale model shown in figure 2. For this model, the control surfaces were immovable and remained at their zero-deflection, or neutral, positions. Both models were constructed of fiberglass, balsa, and aluminum, and their propellers were removed for these tests.

9

During the static force test program, the 1/5-scale model was modified to permit measurements of the aerodynamic forces produced by the outer wing panels. As shown in figure 3, the left outer wing panel was cut from the model and mounted to the inner wing panel via a strain-gauge balance within the wing structure. The wing parting line was sealed with flexible material for these tests. This technique permitted a comparison of aerodynamic characteristics of the outer wing panel (measured by the wing balance) and the complete configuration (measured by the main balance).

LEADING-EDGE MODIFICATIONS

One wing-leading-edge modification studied was the leading-edge flap arrangement shown in figure 4. The flap section was of conventional design, based on the leading-edge airfoil coordinates of the basic wing airfoil. The upper leading-edge surface was extended forward to a position resulting in a deflection angle of 45° relative to the chord plane. The coordinates of the basic wing, a modified NACA 64_2-415 airfoil, are given in table I. Configurations tested included a continuous full-span leading-edge flap and a segmented arrangement with a gap extending from the 46-percent to the 57-percent semispan location.

Tests were also conducted to evaluate the effects of segmented leading-edge droop, the geometry of which is shown in figure 5. The coordinates for this drooped leading-edge design are given in table II. Locations of the spanwise segments tested were the same as those described for the segmented leading-edge flaps.

TEST TECHNIQUES AND CONDITIONS

Static Force Tests

The static force tests were conducted at the Langley Research Center in a low-speed wind tunnel having a 3.6 m (12 ft) octagonal test section. Figure 6 is a photograph of the 1/5-scale model in the tunnel test section. Aerodynamic forces and moments were measured with an internally mounted strain-gauge balance with the model unpowered and the propeller removed. The tests were conducted at a Reynolds number of 0.3×10^6 based on the mean aerodynamic chord of the wing. The data were measured over a range of angle of attack from -10° to 50° for sideslip angles of 0° and $\pm 5^\circ$. Tests were also conducted to determine aileron effectiveness near the stall.

Tests to determine the individual aerodynamic behavior of the outer wing panel were conducted for the basic model and for the model modified with leading-edge droop.

Tuft flow-visualization studies were conducted during the static force tests to provide a qualitative indication of the stall patterns produced by the wing modifications.

10

Forced-Oscillation Tests

Forced-oscillation tests in roll were conducted using the 1/3-scale model in the 9 by 18 m (30 by 60 ft) test section of the Langley full-scale tunnel. These tests, designed to measure the aerodynamic damping in roll of the model, were conducted using the test setup illustrated in figure 7. The model was mounted to a pivoted sting assembly with an internal strain gauge. The model-sting combination was forced to oscillate in roll by a variable-frequency electric motor through a flywheel and bell-crank assembly. The frequency of the oscillations was varied by the speed of the motor; the amplitude of the oscillations was varied by adjusting the bell-crank attachment point along the diameter of the flywheel; and the angle of attack of the model was varied by rotating the entire apparatus about a vertical axis by use of a turntable. The oscillatory balance outputs were analyzed to separate the forces and moments into components in phase with, and 90° out of phase with, the angular displacement of the model. The out-of-phase components were then used to compute the damping and cross derivatives due to rolling. Additional information regarding the testing technique is presented in reference 2.

The forced-oscillation tests were conducted for a range of angle of attack from 0° to 30°, for an oscillation frequency of 0.3 Hz, and for amplitude of ±15°. The tests were conducted at a Reynolds number of 0.55 × 10⁶ based on the mean aerodynamic chord of the wing.

RESULTS AND DISCUSSION

Before discussing the results of the wind-tunnel tests conducted on the model, it is appropriate to briefly review some fundamentals of stall-related autorotation of an airplane in roll. The concept of autorotation of an unswept wing is illustrated in figures 8 and 9. Figure 8 shows typical variations of lift coefficient and drag coefficient with angle of attack for an unswept wing. For angles of attack below the stall (up to point B), C_L increases with increasing α; the reverse is true for angles of attack beyond the stall. As shown in figure 9, if an unswept wing with forward velocity is subjected to a rate of roll p in the clockwise direction, a chordwise section x-x of the right wing (at a distance y from the wing center line) encounters an increase in local incidence of py/V, and the corresponding section x'-x' of the left wing has its incidence decreased by an equal amount. If a wing with the section lift curve shown in figure 8 is operating at point A below the stall, the lift of the downgoing right wing is increased and that of the upgoing left wing is decreased, and an opposing, or damping, rolling moment is produced. Thus, stable damping in roll is provided below the stall. For flight above the stall (point C), the lift of the upgoing wing is increased relative to the downgoing wing, and a propelling, or autorotative, moment is produced.

As shown in figure 10, the autorotative aerodynamic rolling moment is a nonlinear function of roll rate, so that as the spin rate increases, the propelling moments can become equal to zero whereby the wing establishes a steady autorotation in roll. Thus, to rigorously analyze autorotation, several types

11

of wind-tunnel tests may be necessary ranging from conventional static force tests to forced-oscillation tests and rotary spin balance tests.

Of interest to the present investigation is the classical interpretation of static aerodynamic data to predict the damping-in-roll characteristics of straight wings near the stall. The relationship between autorotative tendencies and variations of C_L and C_D with α was defined in early research by Glauert (ref. 3) and Knight (ref. 4). As discussed in reference 4, strip theory analysis indicates that autorotation is encountered when the variation of the total resultant force coefficient of a wing with angle of attack becomes negative, that is, when

$$\frac{dC_R}{d\alpha} < 0$$

Correlation of calculated and experimental ranges of autorotation for two wing models (ref. 4) is presented in figure 11. Results predicted by Knight's criterion were in fair agreement with experimental results for the biplane model with zero stagger, which also exhibited autorotation at extremely high angles of attack. However, the correlation was poor for the monoplane wing model because of unaccounted for variations in span loading. Data presented later in this section of the present report give some insight into such span loading effects.

Static Force Tests

Representative static longitudinal characteristics of the 1/5-scale model are given in figures 12 and 13. Figure 12(a) shows results for the basic model, for the model with a full-span leading-edge flap, and for the model with the segmented leading-edge flap (fig. 4). For the basic wing, the data indicate a stall angle of attack of about 10° followed by a large negative lift-curve slope from $\alpha = 10^O$ to $\alpha = 15^O$. The autorotation criterion described previously predicts autorotative tendencies over this angle-of-attack region, as shown in figure 12(b). With the addition of full-span flaps, the stall angle of attack and maximum lift coefficient were increased, as expected. Again at the stall, a negative lift-curve slope was exhibited and potential autorotation was predicted for $\alpha = 20^O$ to $\alpha = 26^O$.

When a portion of the leading-edge flap was removed, the data obtained for the resulting segmented flap configuration indicated a primary and secondary stall, or a "double-peaked" lift curve. The primary stall occurred near a lift coefficient of 1.1 and was characterized by a flat-top segment over the angle-of-attack range from about 10° to 17°, followed by a positive lift-curve slope to a secondary stall at $\alpha = 30^O$. The primary stall was related to the stall of the inboard wing section, while the secondary stall was associated with the stall of the outer wing panel. It is interesting to note that the primary stall occurred at about the same values of $C_{L,max}$ and α as those for the basic wing with no leading-edge modifications; the secondary stall occurred at a higher angle of attack and about the same $C_{L,max}$ as the model with a full-span flap.

12

The segmented flap data indicate a delay of any autorotative tendency to an angle of attack of 30°, which is 20° higher than that for the basic wing and 10° higher than that for the wing with a full-span flap. Thus, roll instability could possibly be removed from the trimmable flight envelope of the airplane. With the double-peaked lift curve, the initial stall buffet might serve as a stall warning. If sufficient control is available to trim the airplane to higher angles of attack, the positive lift-curve slope after the initial stall should be indicative of increased lateral stability which would prevent auto-rotation and inadvertent spin entry.

Although the aerodynamic effect produced by the segmented leading-edge flap would be expected to improve stall/spin characteristics, such a modification would probably be considered infeasible because of cruise performance degradation (fixed flap) or complexity and cost (movable flap). Thus, tests were conducted with the leading-edge droop configuration which tended to minimize flow separation and alleviate the problems with performance and cost. The static force data and resultant autorotation criterion for the basic wing with full-span and segmented leading-edge droop are presented in figure 13. The segmented drooped leading edge resulted in a double-peaked lift curve and autorotational predictions similar to the leading-edge flap results.

Although elimination of autorotation is a highly desirable achievement, the impact of wing modifications on roll control effectiveness is also a matter of concern. The effect of the segmented leading-edge flap on roll control is shown in figure 14. The incremental rolling and yawing moments produced by right roll control indicate that the roll control effectiveness was significantly improved at high angles of attack with the segmented leading-edge flap.

Also of interest are the effects of such wing modifications on lateral-directional stability. The static lateral-directional stability derivatives based on values of the coefficients at $\beta = \pm 5°$ for the 1/5-scale model are presented in figure 15 as a function of angle of attack. Results are shown for the model with and without the segmented leading-edge flap. As shown, the basic configuration was directionally stable $\left(\text{positive } C_{n_\beta}\right)$ up to an angle of attack of about 23° and exhibited stable dihedral effect $\left(\text{negative } C_{l_\beta}\right)$ throughout the the test angle-of-attack range. The segmented leading-edge flap significantly improved the directional stability with an attendant reduction in stable dihedral effect near the primary stall ($\alpha = 10°$). At the secondary stall ($\alpha = 30°$), the segmented flap improved C_{n_β} but produced unstable values of C_{l_β} at a slightly higher angle of attack. Though no lateral-directional data were obtained for the drooped leading-edge configurations, similar results would be expected.

Flow-Visualization Tests

Tuft flow-visualization studies were conducted to gain insight into the effects of the leading-edge devices investigated on the airflow behavior over the wing. Representative upper surface tuft patterns for the basic wing and the segmented leading-edge flap configurations are shown in figure 16. The tufts indicate a classical straight-wing stall pattern on the basic wing: flow

13

separation begins at the inboard section of the trailing edge ($\alpha = 4^{\circ}$ and 8°) and progresses outboard and toward the leading edge, with a fully developed stall indicated at $\alpha = 12^{\circ}$. The flow breakdown at $\alpha = 12^{\circ}$ has spread onto the aileron, causing the reduction in roll control effectiveness noted in the previously discussed static force data.

Unlike the basic-wing patterns, the flow on the wing with the segmented leading-edge flap appears to separate initially on the trailing edge behind the flap cutout section ($\alpha = 8^{\circ}$), with the detachment moving toward the leading edge as the angle of attack is increased to about 12°, the initial stall point. Beyond this angle of attack, the flow patterns over the outer wing panel are more favorable than those for the basic wing. This flow remains attached up to $\alpha = 30^{\circ}$, as expected on the basis of the static force data of figure 12. Flow over the ailerons is improved as was indicated by the aileron control effectiveness data of figure 14.

Forced-Oscillation Tests

Although static wind-tunnel data may provide some insight into potential autorotative tendencies, a more accurate assessment of such tendencies is afforded by wind-tunnel forced-oscillation tests. The results of forced-oscillation tests for the 1/3-scale model in both the basic and segmented-flap configurations are shown in figure 17. As expected, the onset of autorotation was indicated when the roll damping parameter $\left(C_{l_p} + C_{l_{\dot{\beta}}} \sin \alpha\right)$ for the basic model became unstable (positive) at and beyond the stall angle of attack. When the segmented leading-edge flap was added to the model, the roll damping was maintained to $\alpha = 30^{\circ}$, as was expected from the preceding analysis of static force data.

The correlation between the dynamic measurements and the trends expected from the static data is extremely good. For example, with the segmented leading edge, the damping in roll decreases near the primary stall, then increases as the lift-curve slope (fig. 12) increases toward the secondary stall at $\alpha = 30^{\circ}$. Finally, after the secondary stall, the roll damping becomes unstable, as expected from the negative lift-curve slope.

As previously stated, a valid representation of the autorotative moments acting on the model during spin entry would require data obtained under steady-state rolling conditions because of nonlinear variations in C_l with roll rate. However, the foregoing dynamic data are useful in analyzing the initial tendency of an airplane to enter autorotation. On the basis of results shown in figure 17, the model with segmented leading-edge flaps would not be expected to autorotate for angles of attack up to $\alpha = 30^{\circ}$, in contrast to the basic configuration, which should begin to autorotate near $\alpha = 14^{\circ}$.

Outer-Wing Tests

It is generally accepted that the outer wing determines, to a large degree, the lateral stability of an unswept wing at high angles of attack. To obtain

14

information regarding the contribution of the outer wing panels to the aerodynamic characteristics of the model at the stall and higher angles of attack, a series of tests was conducted using the 1/5-scale model with the outer wing panel mounted to the inner wing panel through a strain-gauge balance (fig. 3). The results of these tests are summarized in figure 18. As shown by the data, the outer panel for the basic wing stalled at $\alpha = 10^{\circ}$ and its lift-curve slope was negative above the stall. With full-span leading-edge droop on the wing, the maximum lift coefficient of the outer panel was increased and the stall angle of attack was slightly increased. With only outboard droop, the results obtained were similar to those discussed previously for the complete model; that is, the outer panel exhibited the double-peaked lift curve and the secondary stall occurred near $\alpha = 30^{\circ}$.

In view of the tuft flow-visualization photographs of figure 16, which show the outer panel apparently acting as a low-aspect-ratio wing, an additional test was conducted in which the outer panel was removed from the wing and tested individually as a wing (with leading-edge droop) with an aspect ratio of 1.5. As shown in figure 18, the lift of the isolated panel with leading-edge droop was much lower below stall than that obtained when the panel was in proximity to the inner wing; however, the maximum lift coefficient and the stall angle of attack of the wing were about the same under both conditions. Thus, it would appear that the outer-wing-panel contribution to lateral stability (avoidance of autorotation) was provided by the span loading produced by the leading-edge modification which caused the panel to act as a low-aspect-ratio wing.

SUMMARY OF RESULTS

The results of a wind-tunnel investigation to determine the influence of wing-leading-edge modifications on the stall/spin behavior of a single-engine, low-wing, general aviation airplane may be summarized as follows:

1. A segmented leading-edge flap or leading-edge droop modification produced a lift curve which was double peaked, having an initial stall at an angle of attack $\alpha = 10^{\circ}$ and a second stall at $\alpha = 30^{\circ}$.

2. The double-peaked lift curve associated with the leading-edge modifications extended the angle-of-attack region of stable roll damping by 20°, from $\alpha = 10^{\circ}$ to $\alpha = 30^{\circ}$.

3. Addition of the segmented leading-edge flap improved roll control (aileron) effectiveness at the higher angles of attack.

4. The outer wing panel, with the addition of a drooped leading edge, acted as a low-aspect-ratio wing which resulted in a significant delay in wing-tip stall and improved lateral stability.

These improvements in lateral stability and control characteristics, associated with the leading-edge modifications, are expected to increase the spin resistance of the configuration.

REFERENCES

1. Standard for Metric Practice. E 380-76, American Soc. Testing & Mater., 1976.

2. Chambers, Joseph R.; and Grafton, Sue B.: Static and Dynamic Longitudinal Stability Derivatives of a Powered 1/9-Scale Model of a Tilt-Wing V/STOL Transport. NASA TN D-3591, 1966.

3. Glauert, H.: The Rotation of an Airfoil About a Fixed Axis. R. & M. No. 595, British A.C.A., 1919.

4. Knight, Montgomery: Wind Tunnel Tests on Autorotation and the "Flat Spin." NACA Rep. 273, 1927.

TABLE I.- COORDINATES OF MODIFIED NACA 64$_2$-415 AIRFOIL

$$\begin{bmatrix} \text{Stations and ordinates given in} \\ \text{percent of airfoil chord} \end{bmatrix}$$

Upper surface		Lower surface	
Station	Ordinates	Station	Ordinates
0	0	0	0
.299	1.291	.701	-1.091
.526	1.579	.974	-1.299
.996	2.038	1.504	-1.610
2.207	2.883	2.793	-2.139
4.673	4.121	5.327	-2.857
7.162	5.075	7.838	-3.379
9.662	5.864	10.338	-3.796
14.681	7.122	15.319	-4.430
19.714	8.066	20.286	-4.882
24.756	8.771	25.244	-5.191
29.803	9.260	30.197	-5.372
34.853	9.541	35.147	-5.421
39.904	9.614	40.096	-5.330
44.954	9.414	45.046	-5.034
50.000	9.016	50.000	-4.604
55.040	8.456	54.960	-4.076
60.072	7.762	60.000	-3.698
65.096	6.954	65.000	-3.281
70.111	6.055	70.000	-2.865
75.115	5.084	75.000	-2.343
80.109	4.062	80.000	-1.875
85.092	3.020	85.000	-1.458
90.066	1.982	90.000	-.990
95.032	.976	95.000	-.573
100.000	0	100.000	0

TABLE II.- COORDINATES OF DROOPED LEADING-EDGE AIRFOIL

$$\left[\begin{array}{c}\text{Stations and ordinates given in}\\\text{percent of airfoil chord}\end{array}\right]$$

Station	Ordinate		Station	Ordinate	
	Upper surface	Lower surface		Upper surface	Lower surface
0	0	0	29.41	11.357	-2.805
.45	1.719	-1.493	36.20	11.584	-2.964
.90	2.489	-1.946	40.72	11.538	-3.032
1.35	3.167	-2.149	45.25	11.303	-2.986
1.80	3.710	-2.172	49.77	10.851	-2.760
2.26	4.208	-2.172	54.30	10.226	-2.489
2.71	4.570	-2.181	61.09	9.050	-2.127
3.62	5.385	-2.199	65.61	8.190	-1.878
4.52	5.973	-2.217	70.14	7.195	-1.629
6.79	7.104	-2.262	74.66	6.615	-1.357
9.05	7.896	-2.353	79.19	5.113	-1.086
11.31	8.588	-2.398	85.97	3.439	-.724
15.84	9.638	-2.511	90.50	2.353	-.543
20.36	10.407	-2.579	95.02	1.176	-.181
24.89	10.950	-2.692	100.00	0	0

18
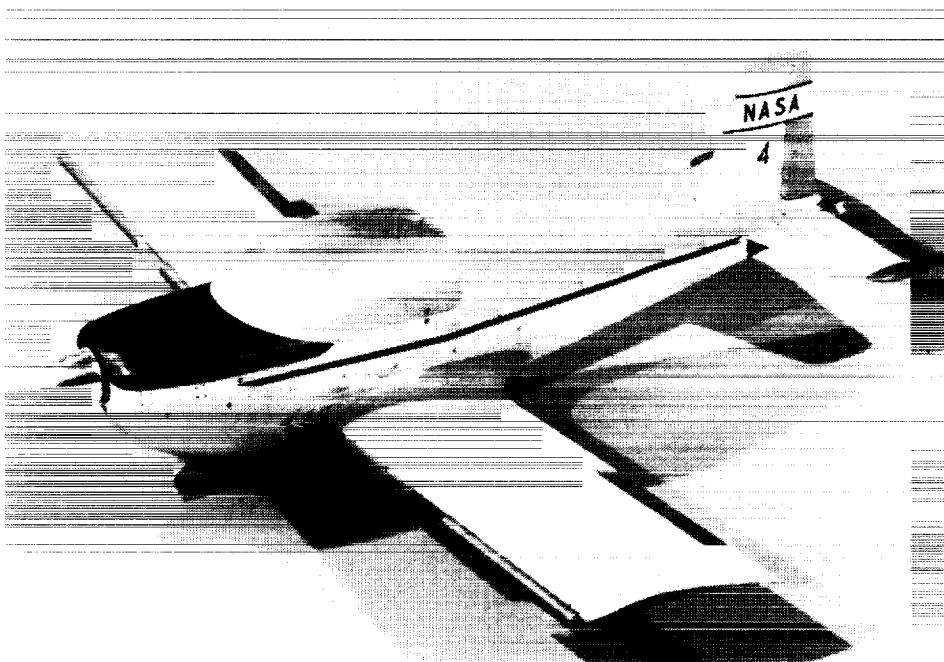
L-78-1000

Figure 1.- 1/5-scale force test model,
with segmented leading-edge flap.

L-78-3372

Figure 2.- 1/3-scale static and dynamic force test model,
with outboard leading-edge flap.
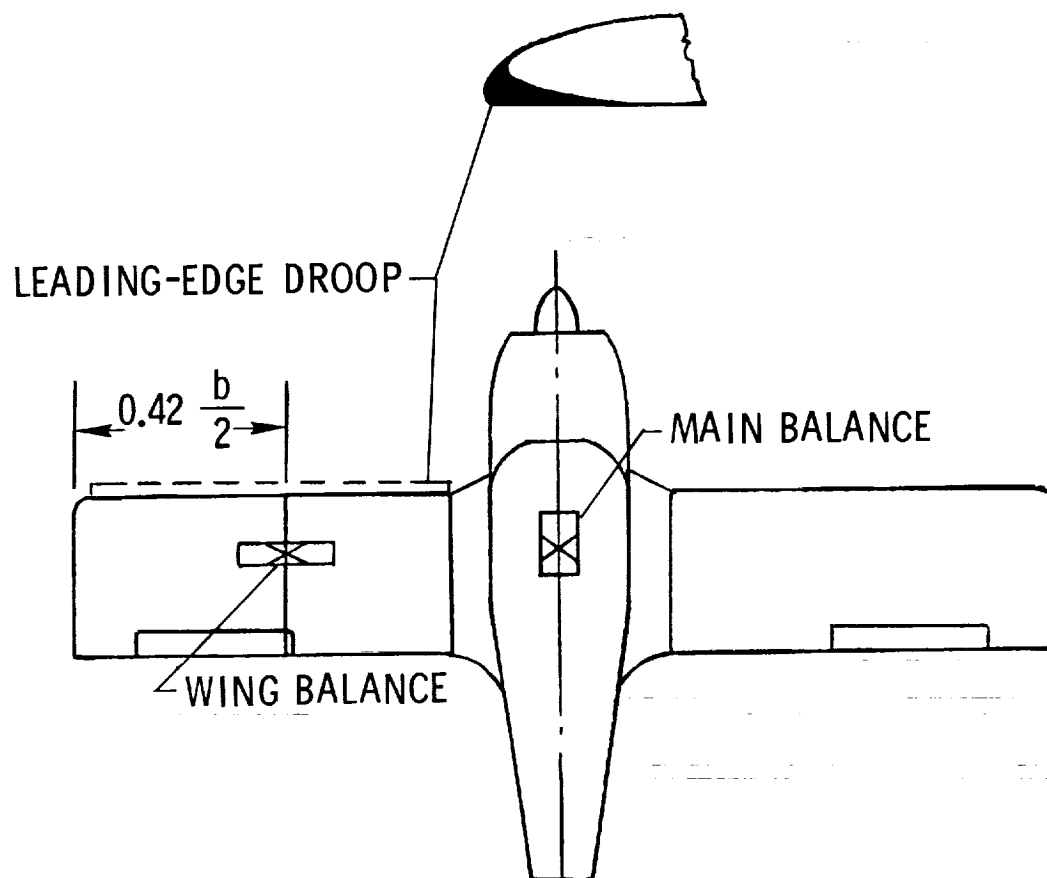
Figure 3.- Details of installation of outer-wing-panel balance.
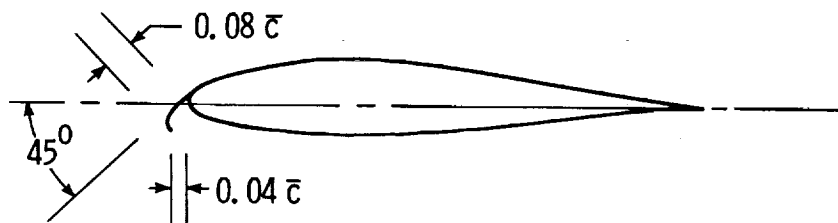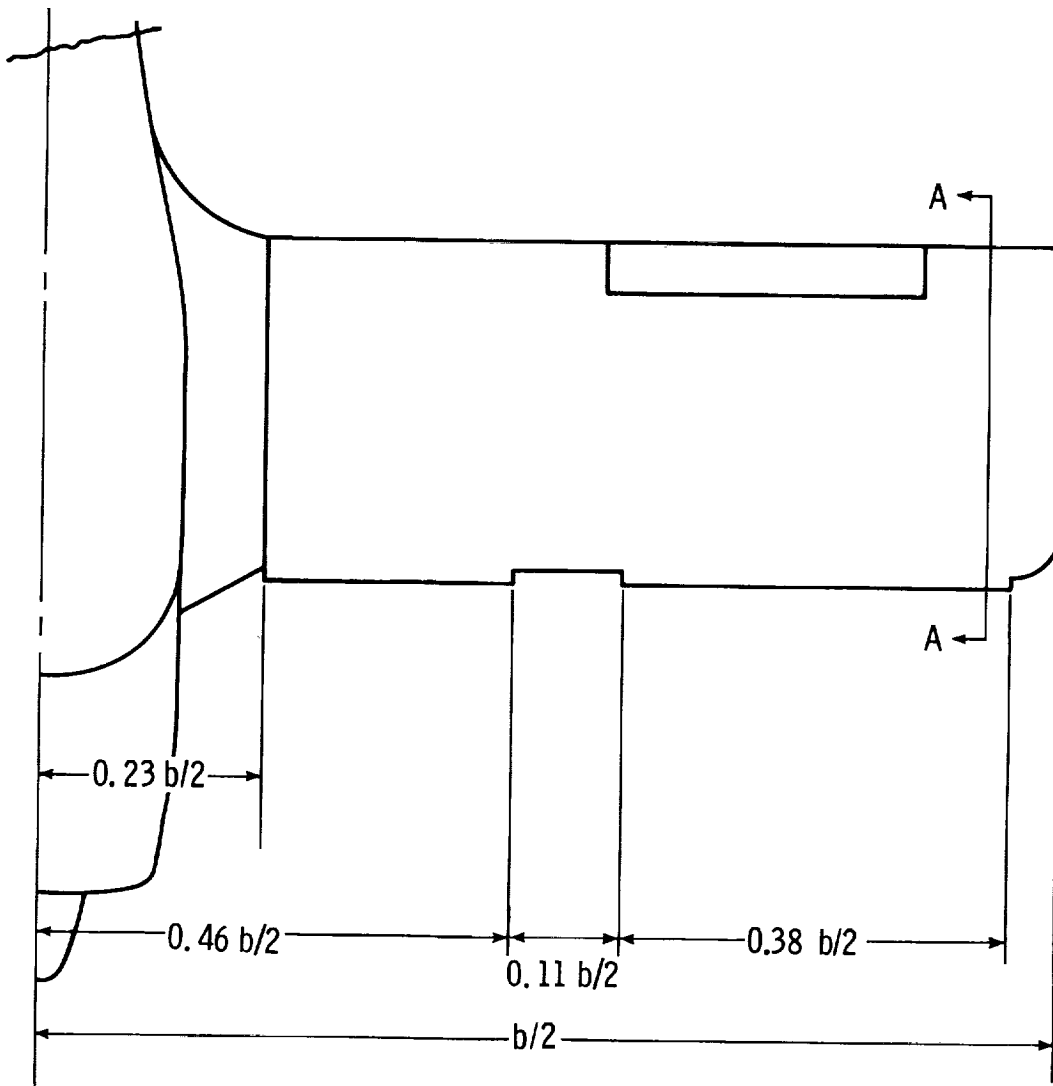
Figure 4.- Segmented leading-edge flap geometry.
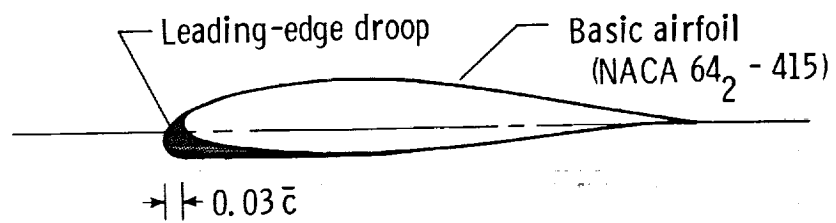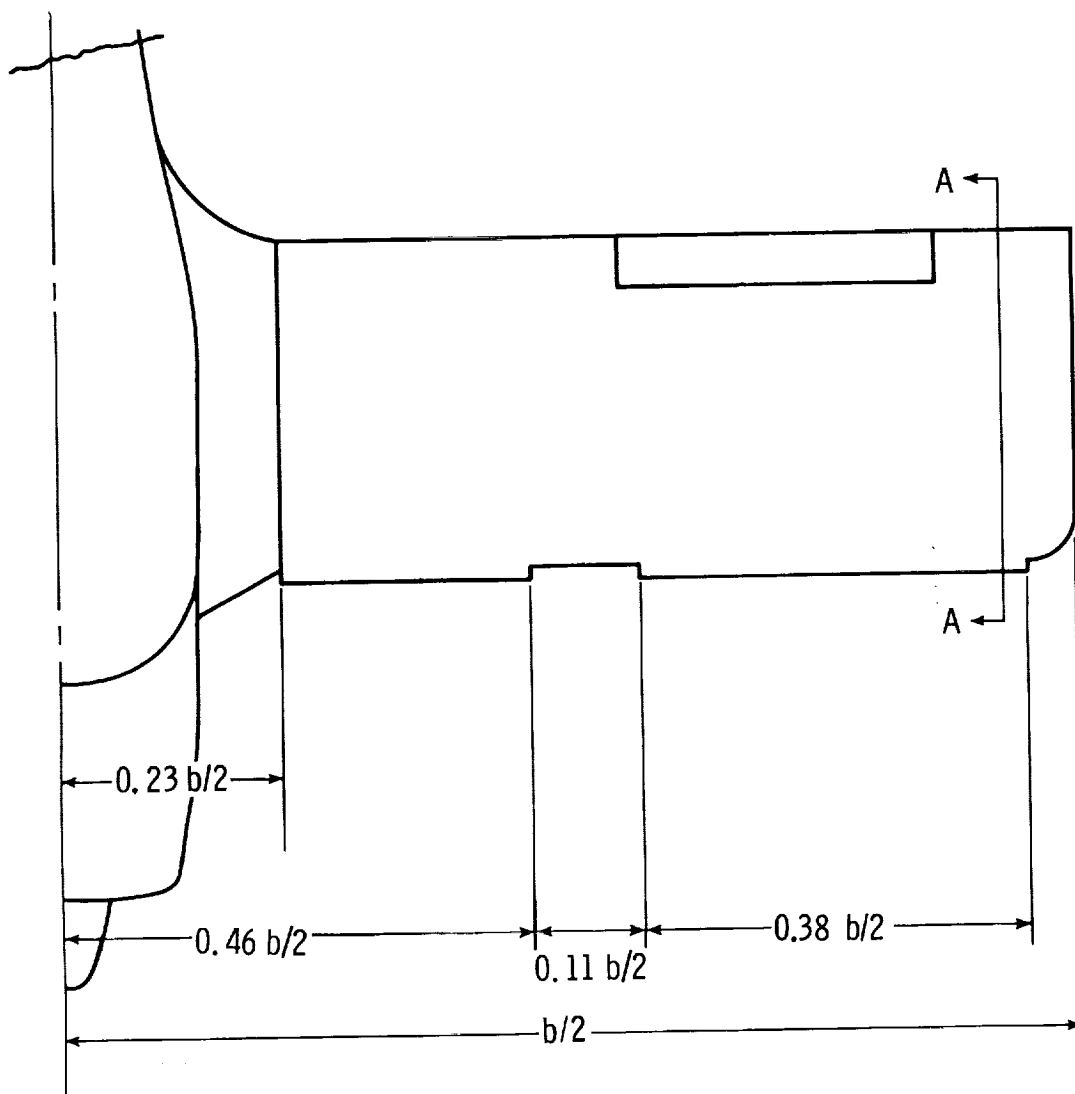
Figure 5.- Segmented leading-edge droop geometry.

L-78-2727

Figure 6.- 1/5-scale model in low-speed tunnel.
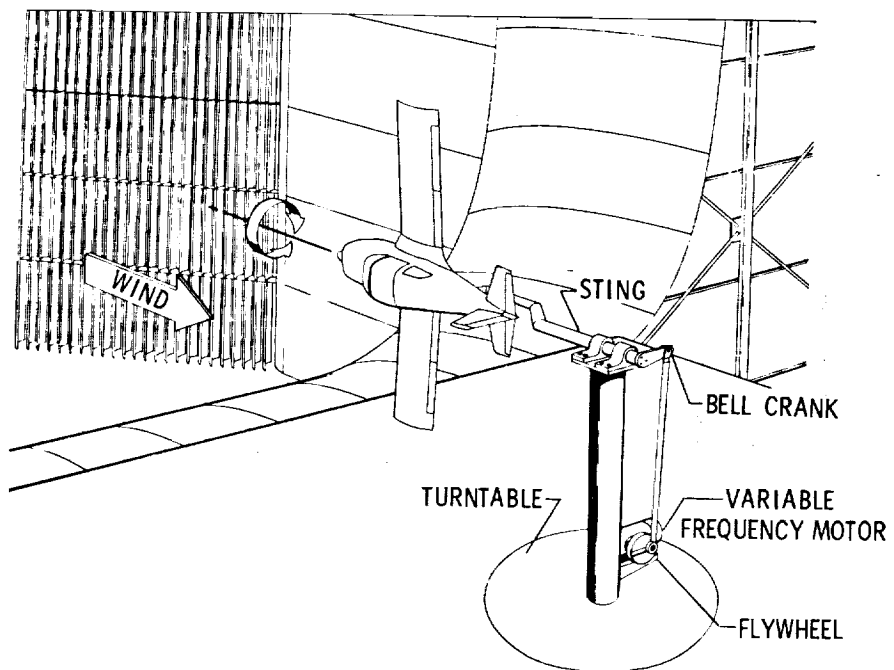
Figure 7.- Forced-oscillation test setup for
roll degree of freedom.
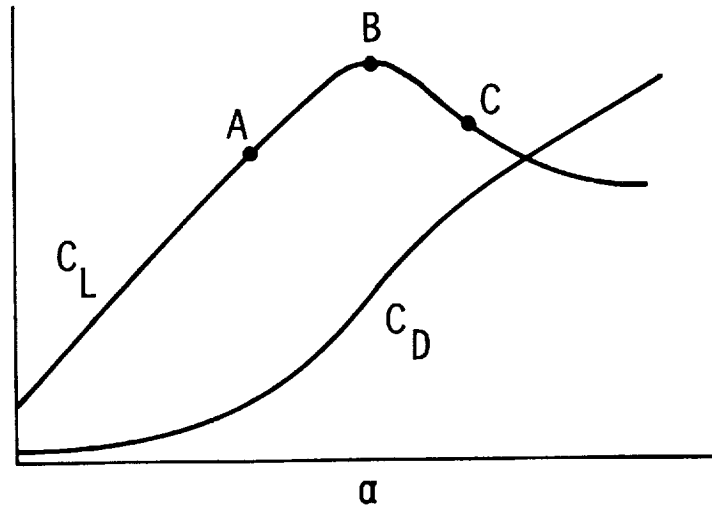
Figure 8.- Typical variations of C_L and C_D
with α for unswept wing.
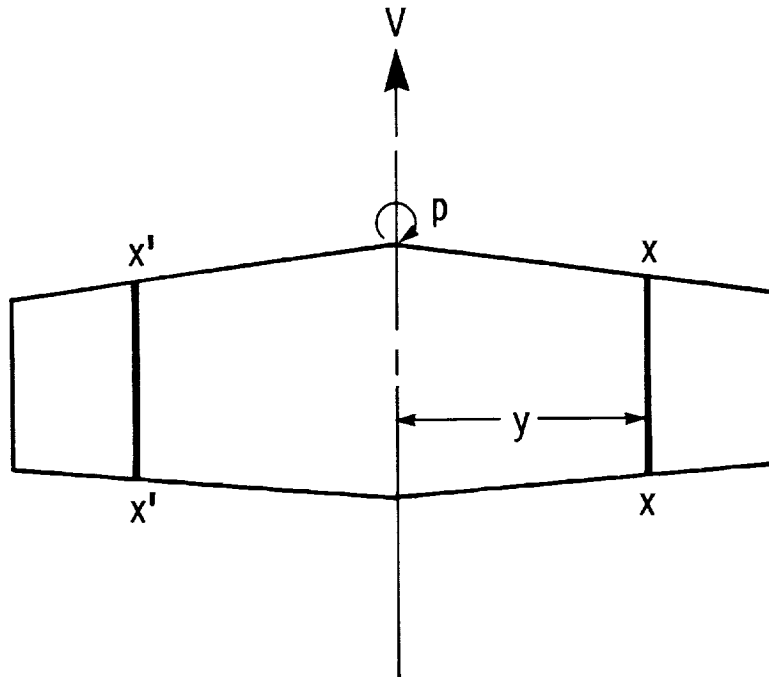
Figure 9.- Unswept wing with rolling motion.
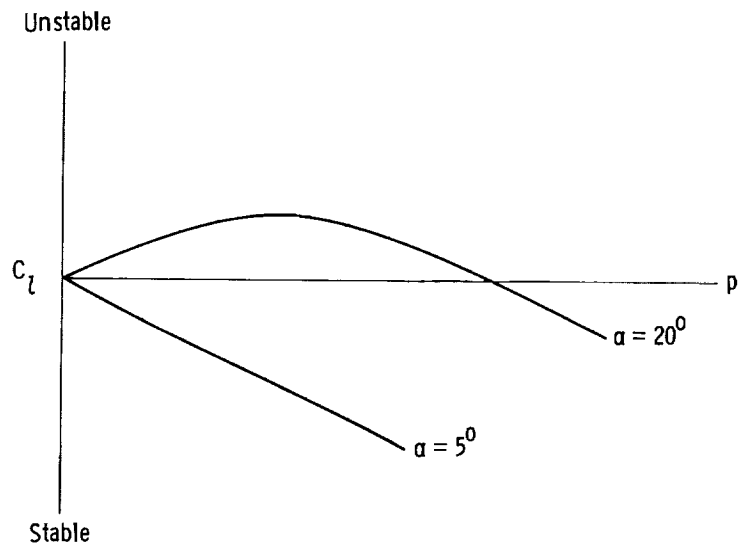
Figure 10.- Nonlinear variation of autorotative
rolling moment with roll rate.
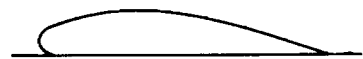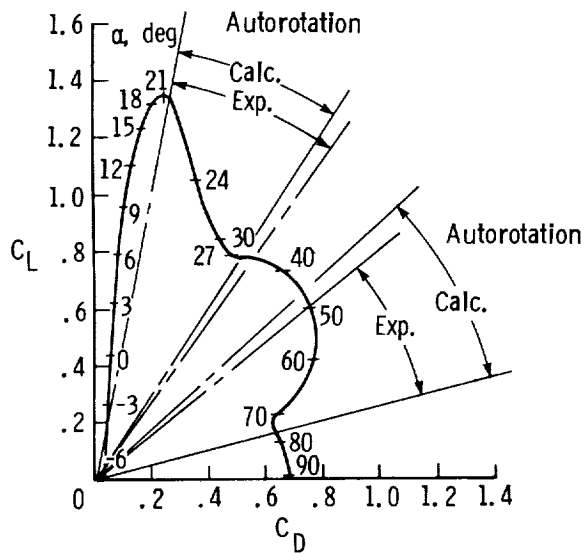
(a) Göttingen 387-FB biplane.   (b) NACA M1 monoplane.
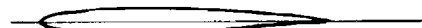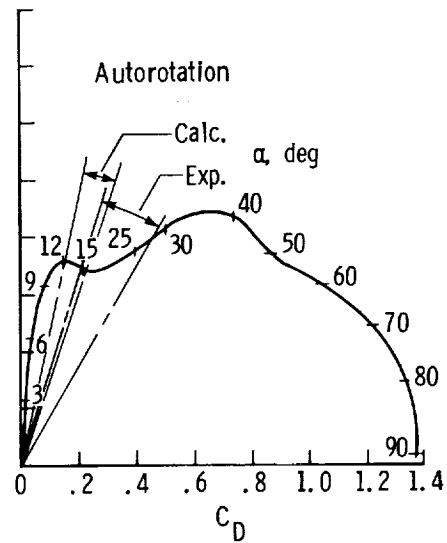
Figure 11.- Correlation of experimental and predicted autorotation
tendencies for two model wings.   Reynolds number = 1.5×10^6;
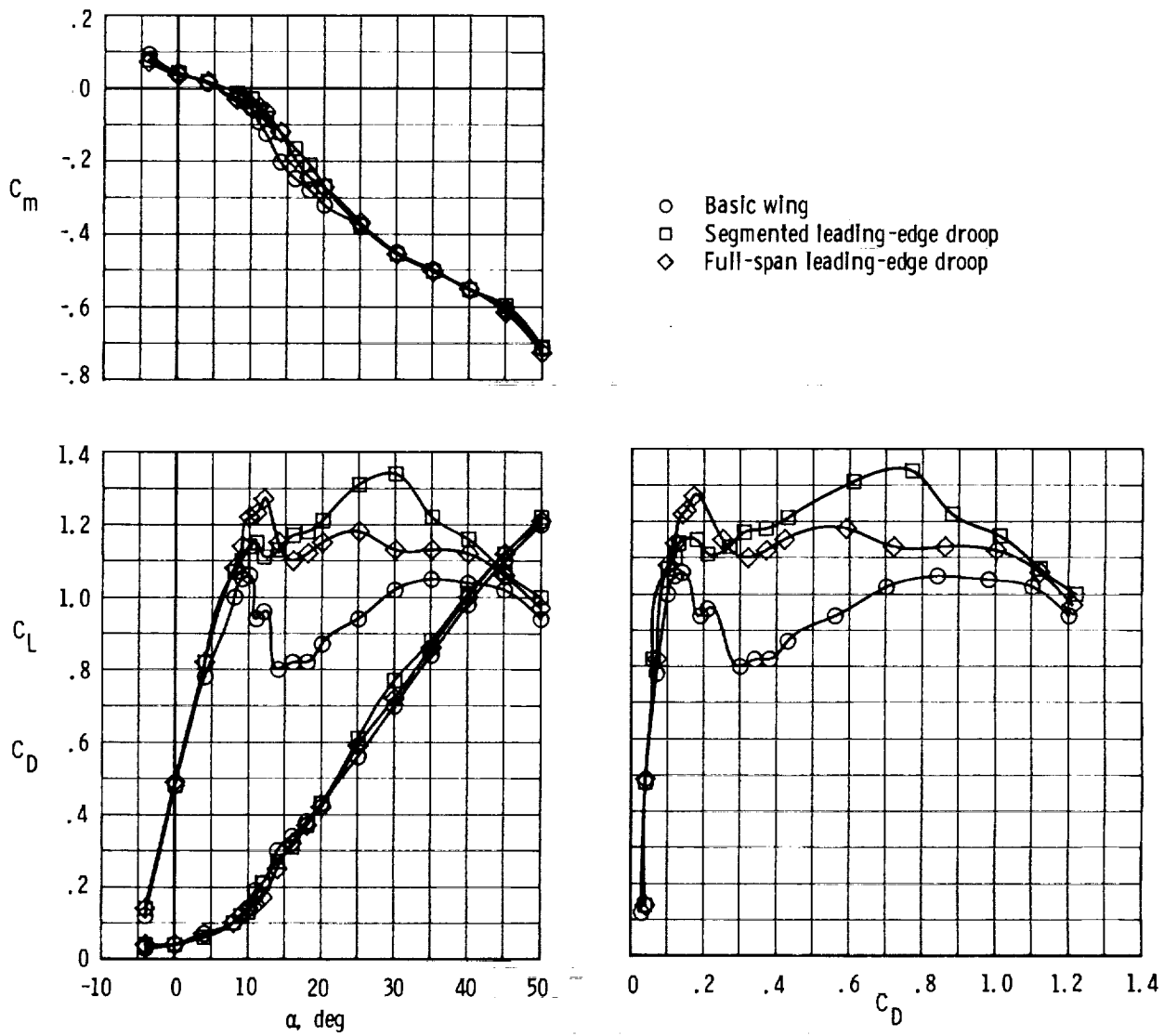Aspect ratio = 6.   (Adapted from ref. 4.)

26
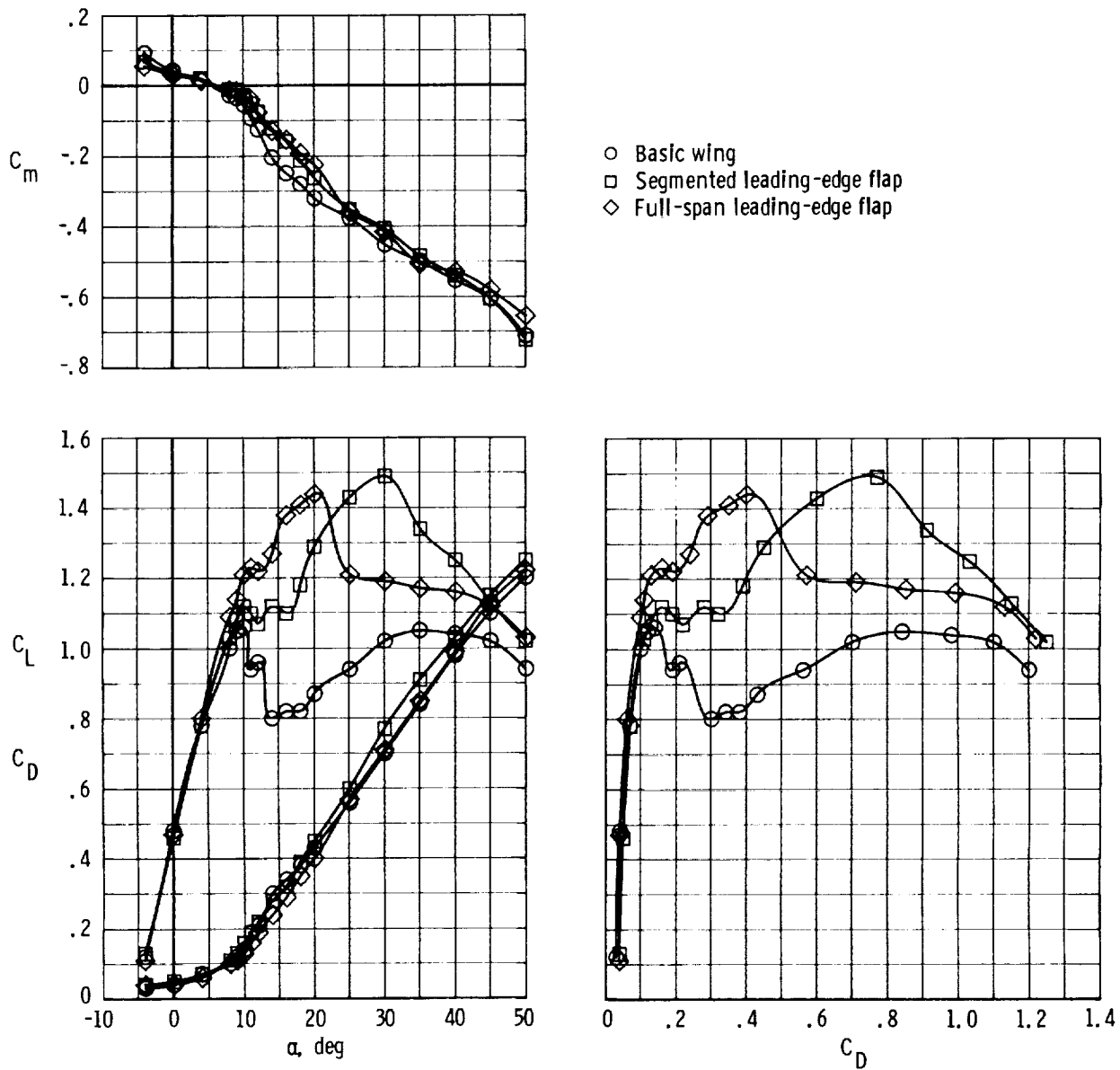
(a) Static longitudinal characteristics.

Figure 12.- Comparison of static force data for leading-edge flap
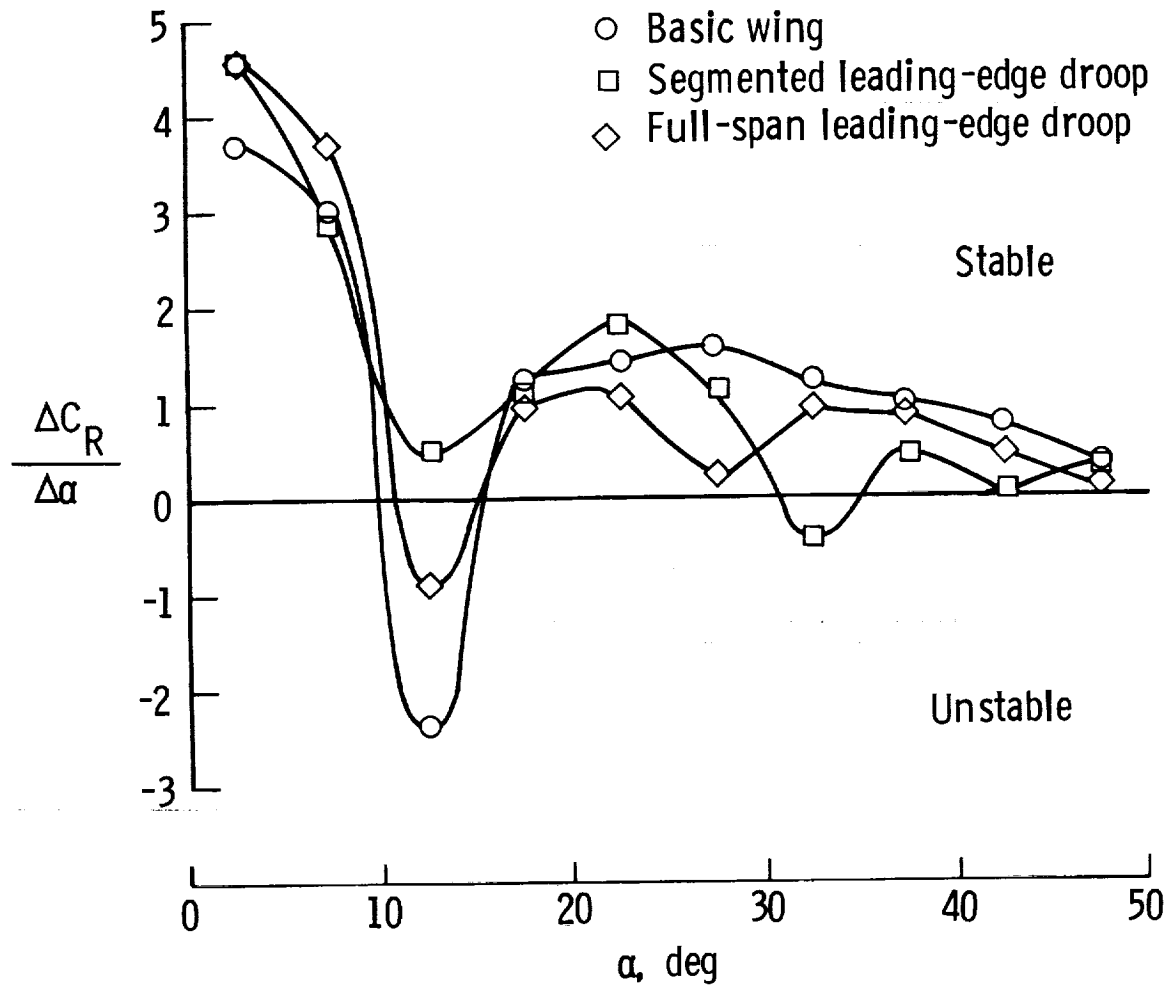configurations. 1/5-scale model in low-speed tunnel.

27
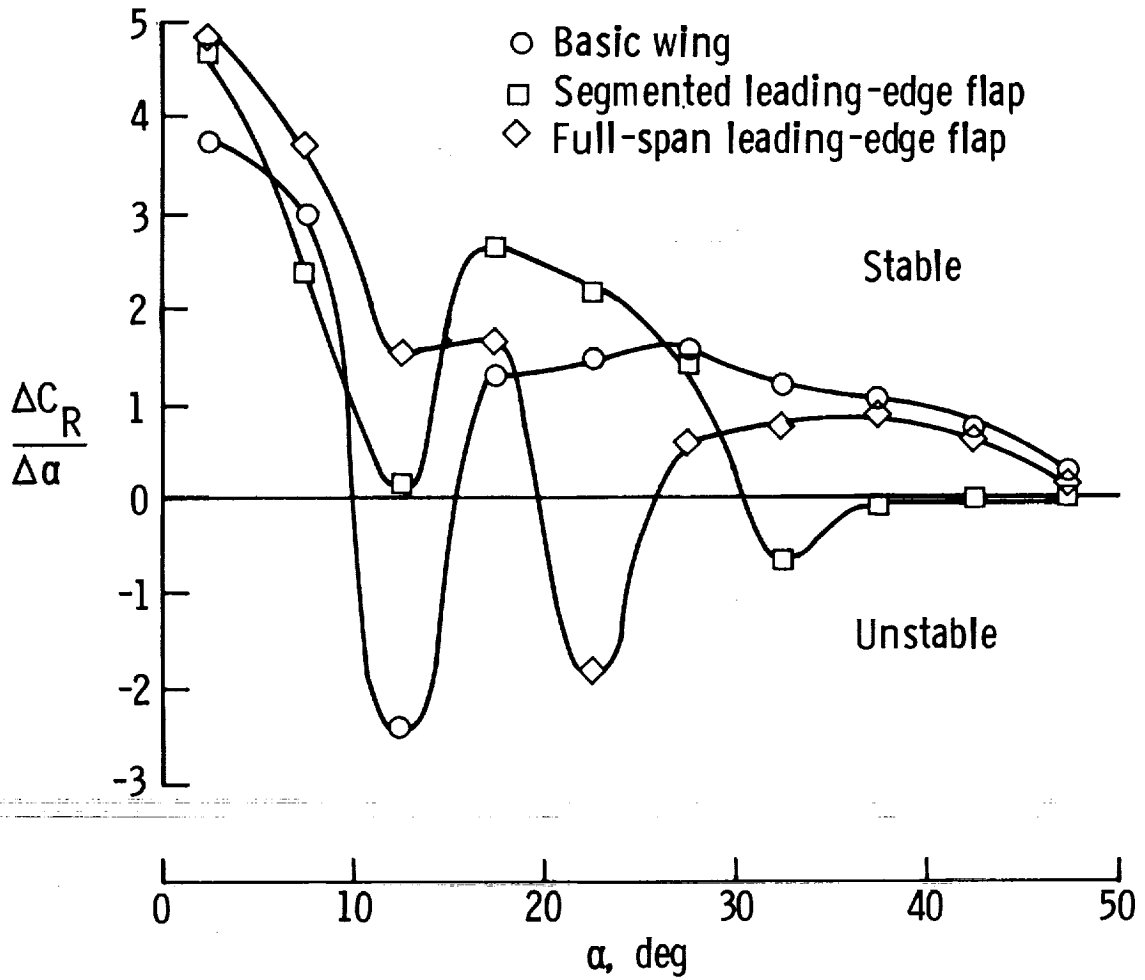
(b) Autorotation stability curves.

Figure 12.- Concluded.

Key:
○ Basic wing
□ Segmented leading-edge droop
◇ Full-span leading-edge droop

(a) Static longitudinal characteristics.

Figure 13.- Comparison of static force data for leading-edge droop configurations. 1/5-scale model in low-speed tunnel.

(b) Autorotation stability curves.
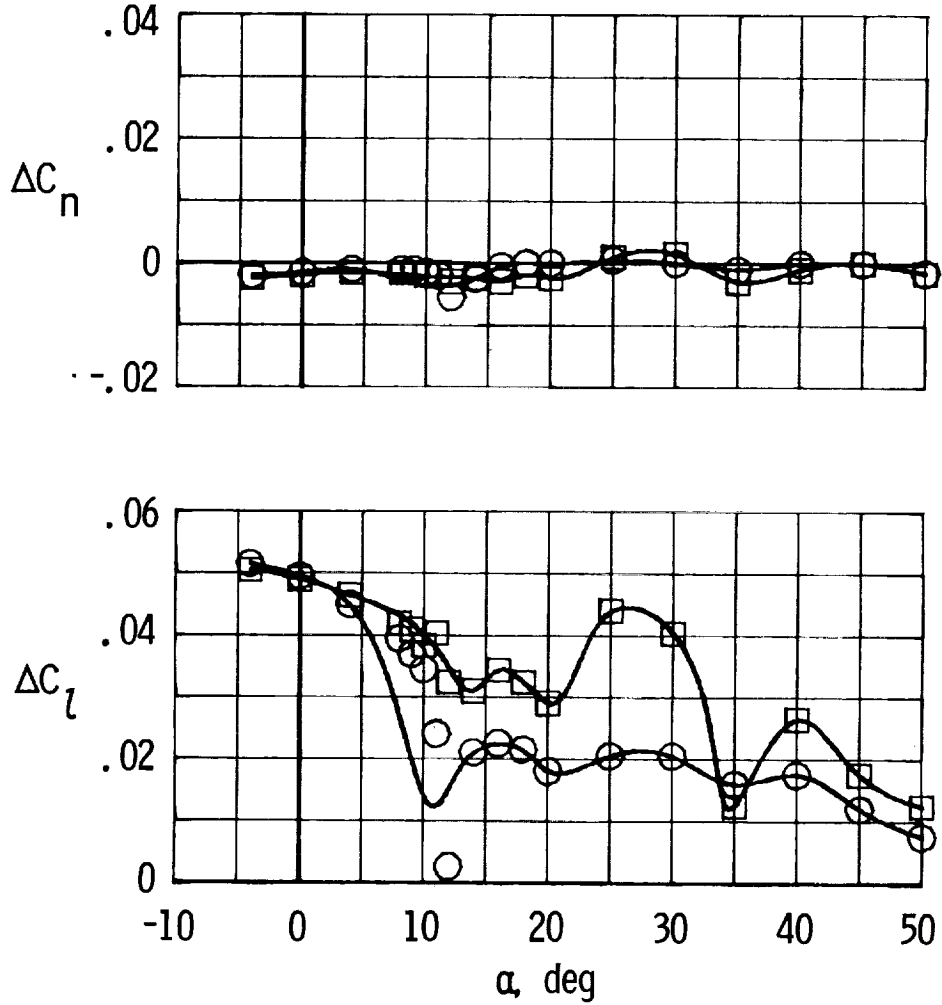
Figure 13.- Concluded.

Figure 14.- Effect of aileron control on lateral-directional moments with and without segmented leading-edge flap. 1/5-scale model in low-speed tunnel; maximum aileron deflection for right roll.
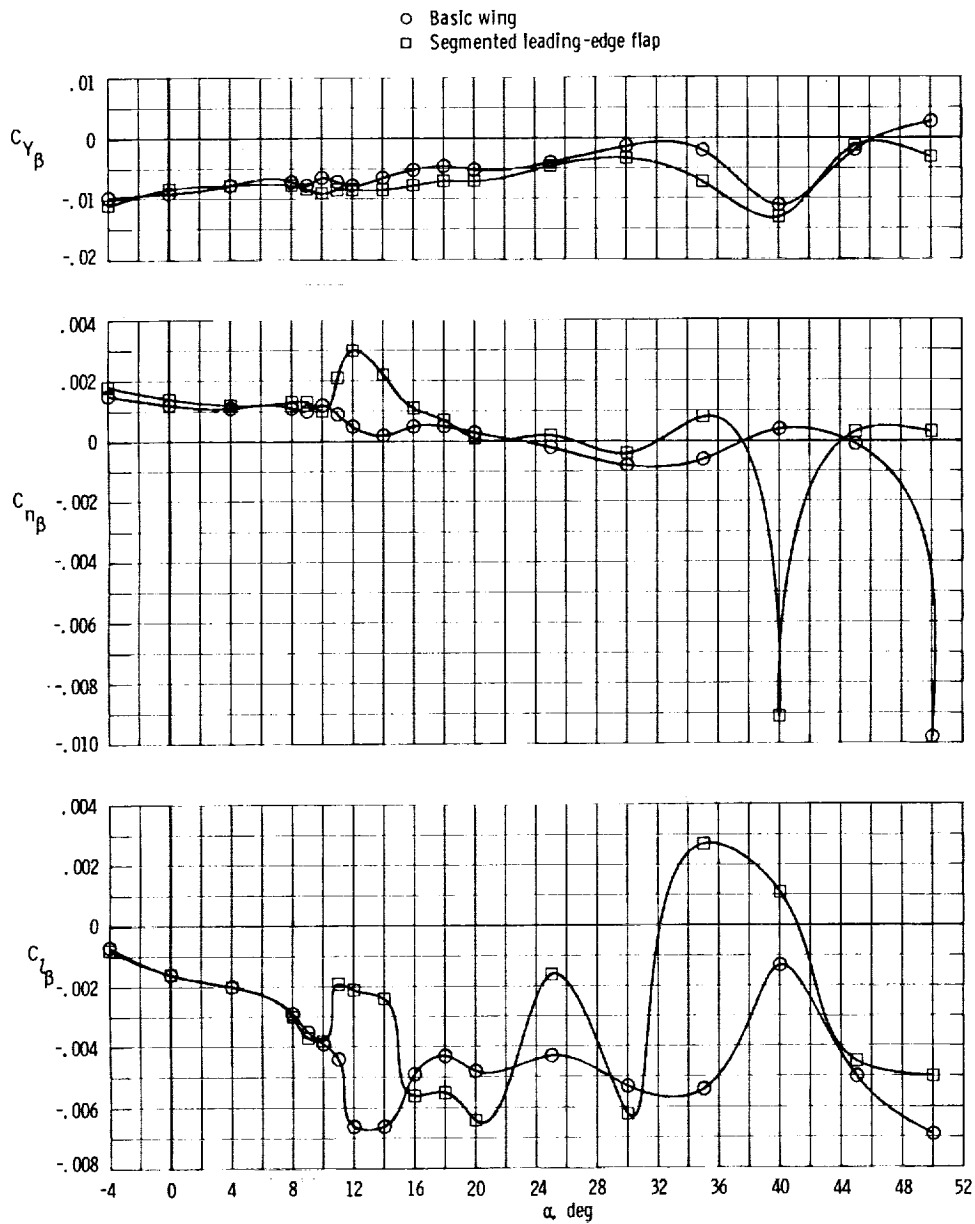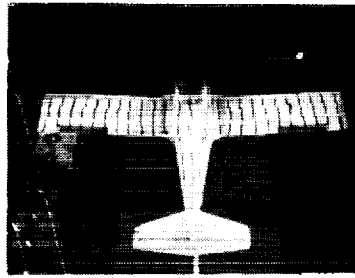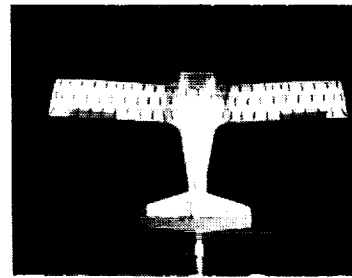
Figure 15.- Variation of static lateral-directional stability
derivatives with angle of attack. 1/5-scale model.

$\alpha = 0^{\circ}$ $\alpha = 0^{\circ}$

$\alpha = 4^{\circ}$ $\alpha = 4^{\circ}$

$\alpha = 8^{\circ}$ $\alpha = 8^{\circ}$

$\alpha = 12^{\circ}$ $\alpha = 12^{\circ}$
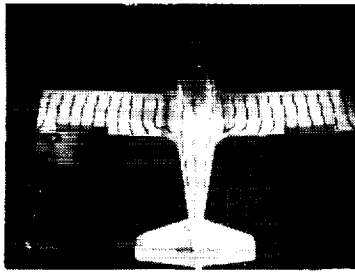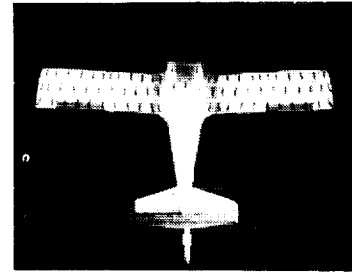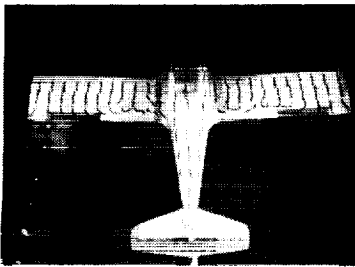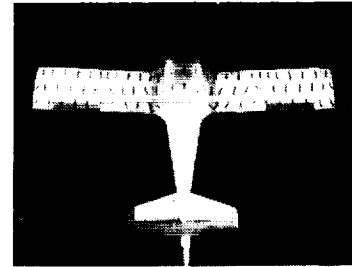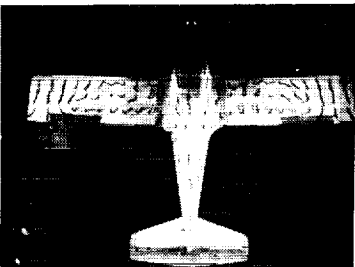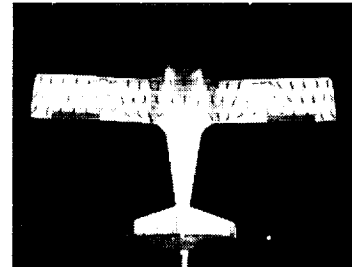
Basic wing   Segmented leading-edge flap

L-79-346

Figure 16.- Tuft flow-visualization patterns at several angles of attack for wing with and without segmented leading-edge flap.

$\alpha = 16^0$ $\alpha = 16^0$

$\alpha = 20^0$ $\alpha = 20^0$

$\alpha = 30^0$ $\alpha = 30^0$

$\alpha = 40^0$ $\alpha = 40^0$
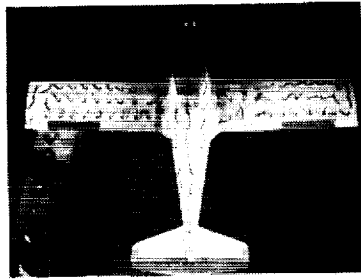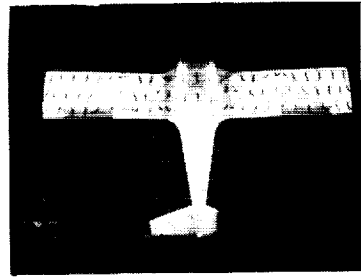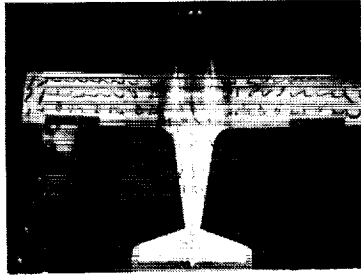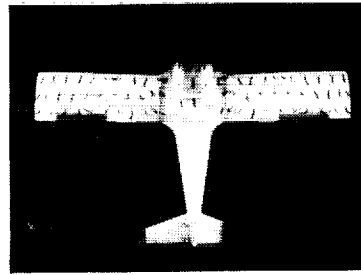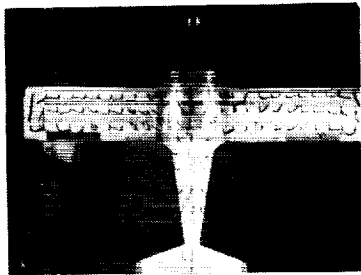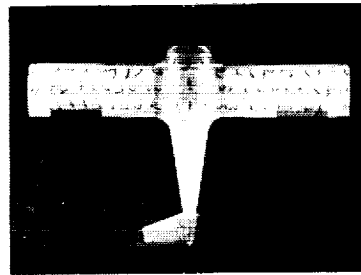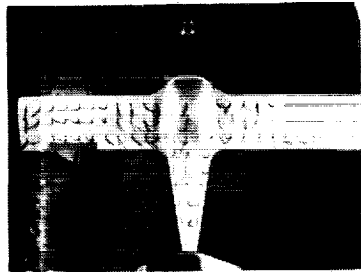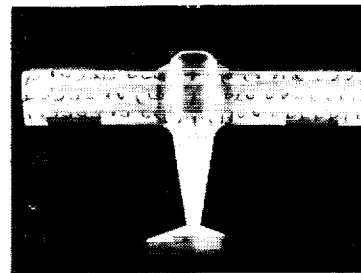
Basic wing   Segmented leading-edge
flap

L-79-347

Figure 16.- Concluded.

34
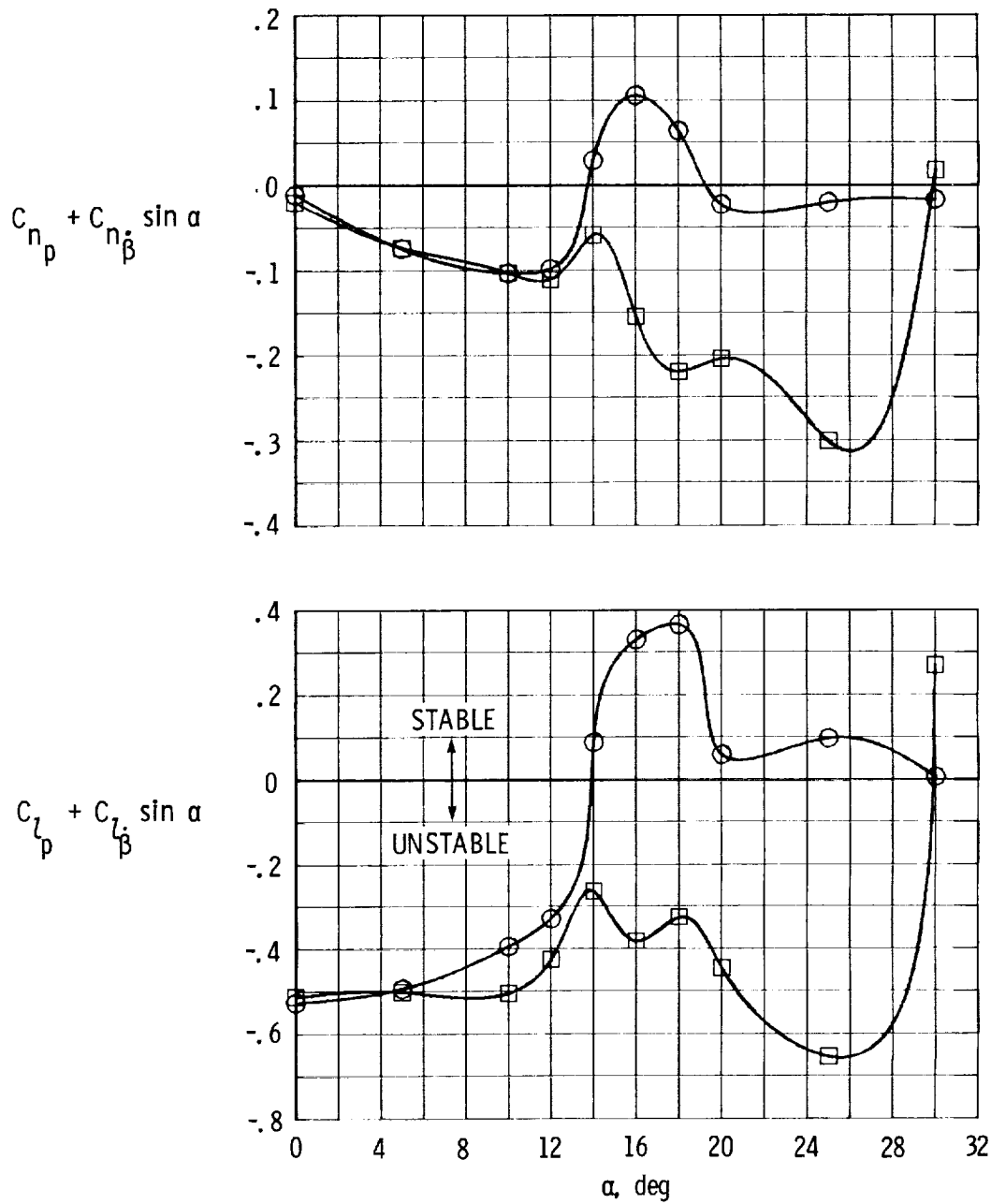
Figure 17.- Variation of lateral-directional damping parameters with angle of attack for wing with and without segmented leading-edge flap. Amplitude = ±15°; frequency = 0.3 cycles/sec.
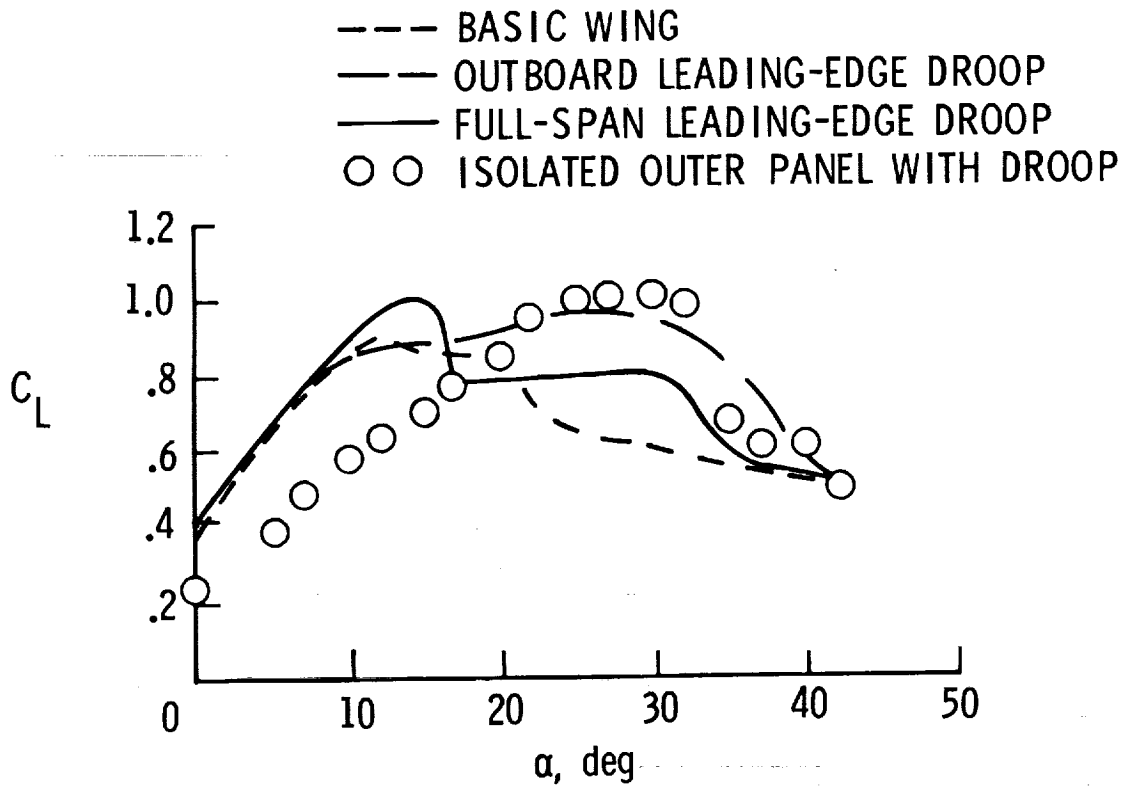
Figure 18.- Aerodynamic characteristics of outer-wing-panel lift
for various wing-leading-edge arrangements.

II. RADIO-CONTROLLED MODEL TESTS

Sanger M. Burk, Jr.; and David B. Robelen

SUMMARY

Stall and spin tests were conducted with a 1/5-scale powered radio-controlled model to determine the effects of wing-leading-edge modifications. The modifications tested included full-span, partial-span, and segmented leading-edge droop and flaps.

The basic configuration (no leading-edge modification) tended to roll off during 1g and accelerated stalls before the elevator could be deflected full up and exhibited two developed spin modes. One spin mode was moderately flat, could be entered using normal prospin controls, and could be terminated satisfactorily. The second mode was fast and flat with poor or no recovery; however, the model was reluctant to enter this mode with normal prospin controls. The addition of full-span leading-edge droop greatly reduced the resistance of the model to enter the unrecoverable flat spin mode. A partial-span outer-panel modification significantly improved the stall and spin characteristics of the model. With the outer-panel modification, stalls could be conducted with the elevator deflected full up without a tendency for the model to roll off, and the model did not exhibit either spin associated with the basic configuration. Instead, it had only a very slow, steep spin mode from which recovery was effected immediately when controls were relaxed.

INTRODUCTION

Static and dynamic wind-tunnel tests of the low-wing general aviation airplane indicated a potential for significant improvements in stall/spin characteristics by modifying the wing leading edge. Subsequently, stalling and spinning tests of a powered, dynamically scaled radio-controlled model of the airplane were conducted to further evaluate the potential benefits and to assess the validity of the analysis of wind-tunnel data.

This part of the report discusses the results obtained in the radio-controlled model tests with emphasis on characteristics noted during 1g and accelerated stalls and deliberate spin entry attempts. The model used in the tests was not instrumented, and the results obtained, consisting of pilot observations and motion picture records, were mainly qualitative.

SYMBOLS

Dimensional quantities are presented both in the International System of Units (SI) and in U.S. Customary Units. Measurements were made in U.S. Customary

37

Units and equivalent dimensions were determined using conversion factors given in reference 1.

b   wing span, m (ft)

$\bar{c}$ wing mean aerodynamic chord, m (ft)

g   acceleration due to gravity, 9.8 m/sec^2 (32 ft/sec^2)

I_X moment of inertia about longitudinal body axis, kg-m^2 (slug-ft^2)

I_Y moment of inertia about lateral body axis, kg-m^2 (slug-ft^2)

m   mass of model, kg (slugs)

S   wing area, m^2 (ft^2)

μ model relative density $\left(\dfrac{m}{\rho S b}\right)$

ρ air density, kg/m^3 (slugs/ft^3)

DESCRIPTION OF MODEL

A 1/5-scale powered radio-controlled model was used for the flight tests. The dynamically scaled model was identical to the model used for the wind-tunnel tests. The model and the test crew are shown in figure 1. The mass and dimensional characteristics of the model are presented in table I in terms of values corresponding to the full-scale airplane.

The model was powered by a conventional model-airplane engine which developed approximately 1.1 kW (1.5 horsepower). An emergency spin-recovery parachute was attached to the tail of the model in case a spin could not be terminated by use of the aerodynamic control surfaces. The parachute size and line length were determined by tests of a 1/11-scale model of this configuration in the Langley spin tunnel (ref. 2).

The radio control system used to fly the model was a proportional control unit and operated the rudder, elevator, ailerons, throttle setting, and spin-recovery parachute.

Maximum control deflections used on the model during the tests (measured in a plane normal to the hinge lines) were

Rudder deflection, deg . . . . 25 right, 25 left
Elevator deflection, deg . . . . 25 up, 15 down
Aileron deflection, deg . . . . 25 up, 20 down

The model was tested with the various wing configurations shown in figures 2 and 3. These configurations included the leading-edge droop and flap designs tested in the wind-tunnel investigation (see part I of this report).

38

TESTING TECHNIQUE

The tests were conducted at the airport located at West Point, Virginia. The testing technique consisted of a ground take-off of the model and flight in an oval pattern so that the model was always in front of the pilot and ground tracking site. The stall and spin entry were executed on the leg of the pattern nearest the pilot to aid the crew in keeping visual contact of the model and the photographer in tracking the model as it was maneuvered.

The flight maneuvers used to assess the stall and spin characteristics of the model were

1. 1g stall with idle power: The model was flown with the wings level while the power was reduced to idle and the stick was gradually pulled back. The stick was held full back and the ailerons and rudder were kept neutral.

2. 1g stall with full power: This maneuver was identical to maneuver 1, except that full power was gradually applied and maintained through the stall.

3. Accelerated stall with full power: The model was banked to about 45° (either left or right) with full power, and the stick was gradually pulled back.

4. Attempted spins with neutral ailerons: The power was reduced to idle and the model stalled. At the stall, the rudder was deflected sharply in the desired direction for the spin attempt with the ailerons neutral. If a rotary motion (spin or spiral) resulted from the attempted spin, it generally was allowed to continue for 5 to 6 turns before recovery was attempted. Recovery from the ensuing rotary motion was attempted by neutralizing the rudder and elevator or by reversing the rudder to full against the spin while simultaneously neutralizing the elevator.

5. Attempted spins with deflected ailerons: This maneuver was the same as maneuver 4, except that at the stall the ailerons were deflected against the attempted spin direction (opposite to the direction the rudder was deflected).

No instrumentation was carried in the model. A ground-based movie camera with a telephoto lens recorded the flight motions; and from pilot comments and ground crew observations, information regarding the stall characteristics, spin susceptibility, spin mode, rate of rotation, and turns for recovery was obtained. More detailed information on radio-controlled model operations is given in reference 3.

TEST CONDITIONS

The model was ballasted to obtain dynamic similarity to an airplane weighing 6672 N (1500 lb) flying at an altitude of 1980 m (6500 ft) with a relative density (μ) of 10.0. For this condition, the total flying weight of the model was about 64.5 N (14.5 lb). The mass characteristics and the mass parameters for the loading conditions tested on the model have been converted to corresponding full-scale values in table I. The value of the inertia yawing-moment

39

parameter $(I_X - I_Y)/mb^2$ for the tests was -50×10^{-4}. The center of gravity was located at $0.255\bar{c}$.

RESULTS AND DISCUSSION

The results obtained for the radio-controlled model with the various wing-leading-edge modifications are summarized in tables II and III in terms of stall and spin characteristics.

Basic Configuration

A 1g wings-level stall (neutral ailerons and rudder) caused the basic configuration to roll abruptly to the right or left at the stall and enter a steep spin. On some occasions, the model exhibited several cycles of "wing rock" (lateral oscillations) at the stall. The roll-off encountered at stall usually occurred before the elevator was deflected full up. The rudder was kept neutral during the steep spin which ensued following the roll-off, and recovery was quickly effected by neutralizing the elevator.

During accelerated (banked) stalls with power, the model exhibited an apparent 1/2 cycle of wing rock, rolled briefly to the inside of the turn, and then rapidly rolled in the opposite direction departing "over the top" away from the turn. Spinning characteristics of the basic low-wing configuration are presented in reference 4, which compares spin characteristics of the present configuration obtained from spin-tunnel tests, radio-controlled model tests, and airplane flight tests. The basic configuration (referred to as tail 4 in ref. 4) exhibited two spin modes: one mode was fast and flat with poor or no recovery, and the other mode was slower and steeper with satisfactory recovery. The flat mode occurred at an estimated angle of attack of $80°$ with 1.3 seconds (full-scale time) required per turn; the steeper mode was moderately flat at an angle of attack of $40°$ to $50°$ with 2 seconds required per turn.

Results (ref. 4) obtained with the radio-controlled model and the full-scale airplane correlated well, particularly with regard to susceptibility to enter the flat spin. With normal prospin controls and with any use of ailerons, the radio-controlled model and the airplane were reluctant to enter the flat spin mode which had been predicted by spin-tunnel tests; they exhibited only the steeper spins. When used during the moderately flat spin, a unique control technique developed during full-scale flight tests would aggravate the spin and drive the airplane into the flat spin. When a similar control technique was used on the radio-controlled model, it would enter a "locked-in" flat spin, requiring the emergency parachute for recovery.

Effect of Wing-Leading-Edge Droop

Full-span droop.- The tests conducted with full-span leading-edge droop (modification D1 in fig. 2) indicated that the stall characteristics of the model were somewhat improved, but the resistance of the model to enter the flat

40

spin was significantly degraded. During lg and accelerated stalls, the model exhibited characteristics similar to those of the basic configuration; that is, a tendency to roll off before the elevator was deflected full up. However, the model could be flown to noticeably higher angles of attack and lower speeds, as would be expected on the basis of the wind-tunnel results discussed in part I.

When spins were attempted with neutral ailerons, the model entered a spin which appeared to be flatter than the moderately flat spin of the basic configuration; however, the model was recovered with normal controls.

When spins were attempted with the ailerons deflected against the spin, the resistance of the model to enter the flat spin was obviously degraded. The model could be flown into the flat spin within 3 turns following application of prospin controls (back stick, rudder with the spin, ailerons against the spin). Thus, the resistance of the model to enter the flat spin was significantly less than that for the basic model, and the flat spin could be obtained on virtually every flight if such prospin controls were maintained beyond 3 turns after stall.

Outboard wing droop.- Eight different lengths of outer-wing droop were tested as indicated in figure 2 (modifications D2 to D9). Tests of these modifications indicated that the resistance of the model to enter a spin could be significantly improved by the proper length of outboard leading-edge droop. A general pattern emerged regarding the effects of the outboard modification; specifically, the spin resistance of the model improved as the length of the outer-panel modification increased from the tip inboard to 0.38b/2. When this length was exceeded, spin resistance was degraded compared with the basic configuration, and the spin characteristics became similar to those of the full-span droop modification.

Perhaps the most impressive results were obtained with modification D2 which was sized on the basis of the promising results of the earlier wind-tunnel tests. When a lg wings-level stall was attempted with idle power, the model generally exhibited a slight amount of wing rock upon reaching what appeared to be the initial stall. This stall was reached with less than full-up elevator deflection. When the elevator was deflected full up, the model exhibited no tendency to roll off and could be flown for extended periods of time. The model was observed to be quite stable laterally while flying at an extremely high angle of attack. During such flights with full-up elevator deflection, the ailerons were relatively ineffective and the rudder was used for lateral control. When full power was applied after the primary stall, no wing rock was observed and the characteristics were similar to the idle power stall.

When the model with modification D2 was banked to the right with full power to produce an accelerated stall, it rolled left to a wings-level attitude with full-up elevator deflection. When banked to the left, it tended to stay in a slight left bank after stalling.

When spins were attempted for configuration D2 with the ailerons neutral, the model did not enter the moderately flat spin as did the basic or full-span droop configurations. Instead, the model entered what appeared to be a steep

41

spiral or extremely steep spin with a rotation rate of about 4 seconds per turn. Rapid recoveries were obtained from such motions by neutralizing either the rudder or the elevator. Spins attempted with ailerons held against the spin produced similar results.

The foregoing results for configuration D2 were considered extremely significant in that the overall resistance of the model to spin was markedly improved, as was suggested by wind-tunnel tests. Subsequent flights with the model indicated that numerous aerobatic maneuvers, aggravated control inputs as stall, and aborted maneuvers could be flown without roll-off or inadvertent spins.

Additional tests were conducted to determine the sensitivity of the improved stall/spin characteristics to the geometry of the outer-wing droop modification. The leading-edge discontinuity at the inboard edge of modification D2 was eliminated by the addition of a fairing (modification D3). Results of stalls and spins with neutral ailerons for modification D3 were similar to those for modification D2, including stable stalls with full-up elevator deflection and a spiral-type motion obtained during deliberate spins. However, when spins were attempted with ailerons against the spin, the spin resistance was extremely poor. Spinning to the right produced a flat spin; recovery was obtained in 4 turns by full rudder reversal and movement of the elevators and ailerons to neutral. Spinning to the left also produced a flat spin; however, recovery controls were ineffective, and the spin was terminated by the emergency recovery parachute. The spin entry and spin resistance of the model with modification D3 were similar to those with the full-span droop configuration (modification D1) and were obviously degraded from configuration D2. Apparently, the fairing eliminated a very beneficial aerodynamic phenomenon which had produced the desirable characteristics obtained with the notched end of modification D2.

When the outer droop was extended inboard an amount equal to the fairing (modification D4), the model exhibited a roll-off tendency during accelerated stalls, and it sometimes entered moderately flat spins to the right, during spin attempts even with ailerons neutral. Thus, extending the outer-panel droop inboard beyond the position used for modification D2 was definitely detrimental to stall/spin behavior.

The results obtained with wing modifications D5 to D8 indicated that the beneficial effects produced by modification D2 could be maintained as the length of the outer modifications was reduced to configuration D6. When the droop was further shortened (as in modifications D7 and D8), the model behavior was essentially the same as that of the basic configuration, including roll-off during stalls at partial-up elevator positions.

As mentioned in a previous discussion of wind-tunnel results, it appears that modifications such as D2 cause the outer wing panel to act as a low-aspect-ratio wing at high angles of attack, with an attendant delay in flow separation and stall. Wing-tip shapes may have an influence on this effect, and a triangular, or "raked," tip (modification D9 of fig. 2) was therefore tested to evaluate the effects of wing-tip shape in combination with the outer droop. When 1g stalls were attempted with idle power, a slight amount of wing rock was

42

evident, but modification D9 appeared to result in more roll damping than the other wing modifications tested. The model exhibited no tendency to roll off or to enter a spin or spiral, even with full-up elevator deflection. The ailerons were ineffective in controlling the model; the rudder was used for lateral control.

Application of full power to the model after it had exceeded the primary stall resulted in no wing rock. The ailerons appeared to be more effective with the triangular wing tips on the model than for the other wing modifications during power-on stalls.

When the model with triangular tips was banked to the right with full power to produce an accelerated stall, the model stayed in a right turn. When banked to the left, the model rolled to the right to a wings-level attitude very quickly and remained there.

For right and left spin attempts with the ailerons neutral, slow, steep spirals or spins with a rate of rotation of about 4.5 seconds per turn resulted when the raked tips were on the model. Rapid recoveries from the motions were obtained by neutralizing the controls. Spin attempts with the ailerons deflected full against the spin gave results similar to those obtained with ailerons neutral.

Segmented droop.- Wind-tunnel studies at NASA Ames Research Center and the University of Michigan had indicated that segmented wing-leading-edge modifications including both inner and outer segments would improve stall and spin entry characteristics. Accordingly, segmented droop modifications (D10 to D14 in fig. 2) were tested to determine the effects of the length of the gap between the inner and outer segments.

When 1g stalls at idle power were attempted for modifications D10 to D14, a slight amount of wing rock was noted after passing through the primary stall. There was no tendency, however, for the model to roll off into a spiral or spin; for some cases a gentle, wide-radius turn was evident. The ailerons were ineffective but the model could be controlled easily with the rudder.

Application of full power to the model after it had exceeded the primary stall from a wings-level condition resulted in reduced wing rock or no wing rock as compared with the stall at idle power. Again, the aileron effectiveness was poor. There was no tendency for the model to roll off into a spiral or spin; in some cases, the model circled slowly to the left.

During accelerated stalls to the right, the model rolled to the left to a wings-level attitude and then continued to roll to the left, gradually going into a left turn. When banked to the left, the model generally remained in a gentle left bank.

For attempted spins with the ailerons neutral for modification D10, steep spins or spirals were obtained to the left, and a moderately flat spin was obtained to the right. Recovery from this spin was obtained in two turns by deflecting the rudder full against the spin and neutralizing the elevator. For modifications D11 and D13, flat spins were obtained which had to be terminated

by the spin-recovery parachute. For modifications D12 and D14, only very steep spirals or spins were obtained with neutral ailerons. Prompt recoveries were obtained by neutralizing the controls.

Spins also were attempted with the ailerons held full against the spin with modifications D10, D12, and D14. With modification D10, the model spun moderately flat to the right and flat to the left. Reversing the rudder against the spin and neutralizing the elevator and ailerons terminated the moderately flat spin but deployment of the parachute was required to terminate the flat spin. For modification D14, a flat spin was obtained to the left that had to be terminated with the parachute. Modification D12 was superior to the other segmented modifications in that only slow, steep spirals or spins were obtained to the right or left. Recovery was prompt by neutralizing the controls.

Results obtained with the various spanwise segmented wing-leading-edge modifications suggest that the beneficial effects of an outer-panel modification may not be obtained if an inner segment of too great a length is added.

Effect of Wing-Leading-Edge Flaps

Full-span flaps.- With the full-span leading-edge flaps (modification F1 in fig. 3) on the model, a 1g wings-level stall with idle power was attempted. The model entered a slow, moderately steep spiral or spin to the right. Recovery was accomplished quickly by moving the elevator to neutral (the rudder was held neutral throughout the flight).

For right and left spin attempts with neutral ailerons, the model entered a moderately steep spin or spiral with a rotation rate of about 3.4 seconds per turn. Recovery was accomplished in several turns by neutralizing the controls. No spins were attempted with ailerons against the spin.

Outboard flaps.- Two different lengths of leading-edge flaps were tested on the model (modifications F2 and F3). The shorter flap (modification F2) was equal in length to modification D2. When a 1g stall with idle power was attempted, a slight wing-rock motion was obtained after passing through the primary stall. There was no tendency of the model to enter a spiral or spin for either modification F2 or F3. The ailerons were fairly effective with modification F2 but less effective with the longer flap (modification F3).

When full power was applied to the model, some wing rock existed for both modifications. There was no tendency of the model to roll off into a spiral or spin with modification F2, but for modification F3, the model entered a moderately steep spin or spiral which was terminated by neutralizing the controls.

For right spin attempts, a slow steep spin or spiral was obtained with modification F2; recovery was prompt with neutralization of controls. However, with modification F3, a spin was obtained which started to flatten; recovery was obtained by full rudder reversal and neutralization of the elevator. For left spin attempts, a slow steep spin or spiral was obtained for both modifications.

44

Segmented flaps.- Two different lengths of the gap between flap segments on the wing were tested. The short gap was referred to as modification F4 and the longer one as modification F5. When a 1g stall was attempted with idle power, a slight amount of wing rock was noted with modification F4 and a larger amount of wing rock with modification F5. There was no tendency for the model to enter a spin or spiral. Aileron control was weak.

When full power was applied to the model under the preceding conditions, the wing rock for modification F4 was similar to that obtained at idle power. However, with modification F5, there was practically no wing rock. Again, there was no tendency for the model to roll off into a spin or spiral and aileron control was weak.

Right and left spins with the ailerons neutral were attempted for both modifications. Except for one case, only steep, slow spins or spirals were obtained for both spin directions, with rapid recoveries by neutralizing the controls. As the model with modification F4 entered a right spin, it quickly built up spin rotation and the attitude started to flatten. Recovery was accomplished in about 4 turns by moving the rudder full against the spin and moving the elevator to neutral.

SUMMARY OF RESULTS

The results of a radio-controlled model investigation of the effects of wing-leading-edge modifications on the stall and spin characteristics of the low-wing general aviation airplane may be summarized as follows:

1. The basic configuration (no leading-edge modifications) tended to roll off during 1g and accelerated stalls before the elevator could be deflected full up, and the model exhibited two developed spin modes. One mode was moderately flat and could be satisfactorily terminated. The other mode was fast and flat with poor or no recovery; however, the model was reluctant to enter this mode with normal prospin controls.

2. The addition of full-span leading-edge droop greatly reduced the resistance of the model to enter the flat spin mode.

3. Addition of a leading-edge flap or droop to the outer 40 percent of the wing improved the stall and spin characteristics of the model. The model could be stalled with the elevator deflected full up without a tendency to roll off, was reluctant to enter either spin mode exhibited by the basic configuration, and entered a steep, spiral-type spin from which it recovered immediately upon relaxing controls.

REFERENCES

1. Standard for Metric Practice. E 380-76, American Soc. Testing & Mater.,
     1976.

2. Burk, Sanger M., Jr.; Bowman, James S., Jr.; and White, William L.: Spin-
     Tunnel Investigation of the Spinning Characteristics of Typical Single-
     Engine General Aviation Airplane Designs. II - Low-Wing Model A: Tail
     Parachute Diameter and Canopy Distance for Emergency Spin Recovery. NASA
     TP-1076, 1977.

3. Burk, Sanger M., Jr.; and Wilson, Calvin F., Jr.: Radio-Controlled Model
     Design and Testing Techniques for Stall/Spin Evaluation of General-Aviation
     Aircraft. NASA TM-80510, 1975.

4. Bowman, James S., Jr.; Stough, Harry P.; Burk, Sanger M., Jr.; and Patton,
     James M., Jr.: Correlation of Model and Airplane Spin Characteristics for
     a Low-Wing General Aviation Research Airplane. AIAA Paper 78-1477, Aug.
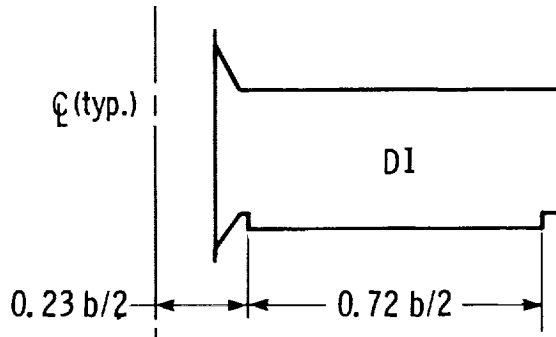   1978.

46

TABLE I.- MASS AND INERTIA CHARACTERISTICS OF RADIO-CONTROLLED

MODEL IN TERMS OF FULL-SCALE VALUES

Weight, N (lb) 6672 (1500)

Center of gravity, percent $\bar{c}$ 25.5

Relative density (μ), at altitude of 1980 m (6500 ft) 10.0

Moments of inertia, kg-m^2 (slug-ft^2):
  Pitch (I_Y) 827 (610)
  Roll (I_X) 643 (474)
  Yaw (I_Z) 1381 (1018)

Inertia yawing-moment parameter, $\dfrac{I_X - I_Y}{mb^2}$ . . . . -50×10^{-4}

TABLE II.- SUMMARY OF RADIO-CONTROLLED MODEL RESULTS FOR

LEADING-EDGE DROOP CONFIGURATIONS TESTED

(a) Configuration D1

$\mathcal{C}$ (typ.)

0.23 b/2   0.72 b/2

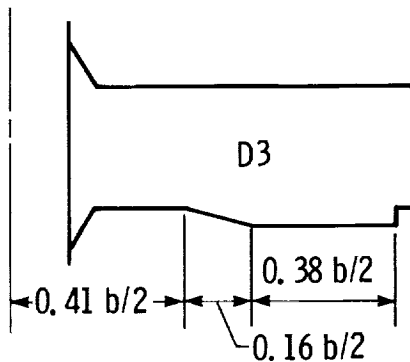| Stall			
Idle power, 1g	Full power		
Able to penetrate to higher angle of attack than with basic wing. Still noticeable wing rock and break, either to right or left, into spin.	1g	Accelerated	
	Slight wing rock and roll-off like basic configuration.	Left	Right
		Stayed in left bank. Slight wing rock.	Rolled out, then into left spin.
Spin, ailerons neutral			
Left		Right	
Moderately flat spin, flatter than with basic wing. Recovered in about 2 turns with neutral controls.		Same as left spin, ailerons neutral.	
Spin, ailerons against			
Left		Right	
Flat spin after 3 turns. Opposite controls used for recovery.		Same as left spin, ailerons against.	

48

TABLE II.- Continued

(b) Configuration D2

D2

|←— 0.57 b/2 —→|← 0.38 b/2 →|

Stall			
Idle power, 1g	Full power		
Wing rock, but no roll-off. Ailerons ineffective.	1g	Accelerated	
	No wing rock or roll-off. Ailerons ineffective.	Left	Right
		Stayed in left bank.	Rolled out to wings level.

Spin, ailerons neutral	
Left	Right
Slow, spiral-type spin. Recovered immediately after neutralizing controls.	Same as left spin, ailerons neutral.

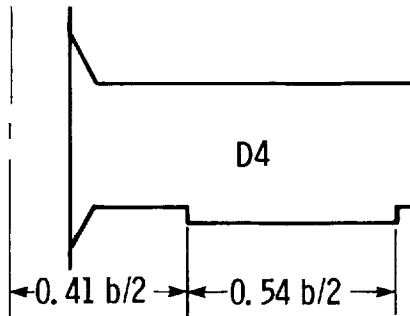| Spin, ailerons against	
Left	Right
Same as with neutral ailerons.	Same as with neutral ailerons.

TABLE II.- Continued

(c) Configuration D3

Stall			
Idle power, 1g	Full power		
Wing rock. Gentle left turn. Weak aileron response.	1g	Accelerated	
	No wing rock. Spiral to left. Weak aileron control.	Left	Right
		Stayed in left bank, with wing rock.	Wings leveled; then left turn.

Spin, ailerons neutral	
Left	Right
Spin with slightly faster turn rate than with configuration D2. Recovered with neutral controls.	Slow, spiral-type spin. Recovery with neutral controls.

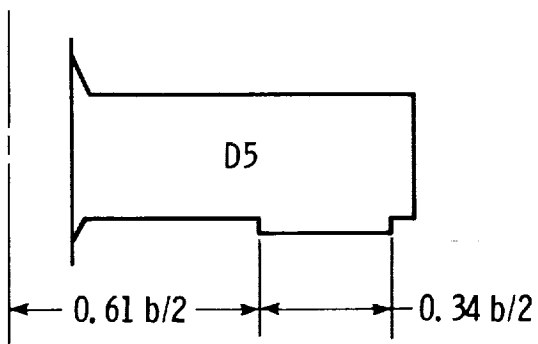| Spin, ailerons against	
Left	Right
Spin became flat. Recovery controls (rudder against, stick forward, ailerons neutral) ineffective. Used recovery parachute.	First attempt.- Flat spin, recovered in 4 turns (rudder against, stick forward, ailerons neutral). Second attempt.- Model recovered sooner with stick (elevator) neutral first, then forward.

50

TABLE II.- Continued

(d) Configuration D4

Stall			
Idle power, 1g	Full power		
Wing rock. Right turn. Ailerons ineffective.	1g	Accelerated	
	No wing rock. Broke left into spin. Recovered with neutral controls.	Left	Right
		Wings leveled; then slight roll-off.	Wings leveled; then broke into left spin. Recovered with neutral controls.

Spin, ailerons neutral	
Left	Right
Slow, steep, spiral-type spin. Recovery within 1/2 turn.	First attempt.- Moderately flat spin. Recovered in 2 turns. Second attempt.- Slow, steep, spiral spin. Recovered immediately.

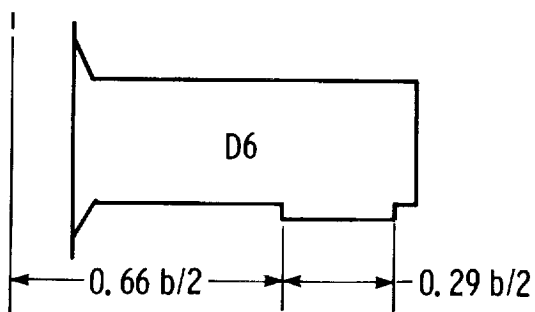| Spin, ailerons against	
Left	Right
Same as with ailerons neutral.	Same as with ailerons neutral.

TABLE II.- Continued

(e) Configuration D5

D5

$$\leftarrow 0.61\ b/2 \rightarrow \kern-0.5em\leftarrow \kern2em 0.34\ b/2$$

Stall			
Idle power, 1g	Full power		
Wing rock. No departure tendency. Ailerons ineffective.	1g	Accelerated	
	No wing rock. Left turn. Slight aileron effectiveness.	Left	Right
		Same as right stall, accelerated.	Slight pitch oscillation and wings slowly leveled.

Spin, ailerons neutral	
Left	Right
Same as right spin, ailerons neutral.	Slow, steep, spiral-type spin (like configuration D2).

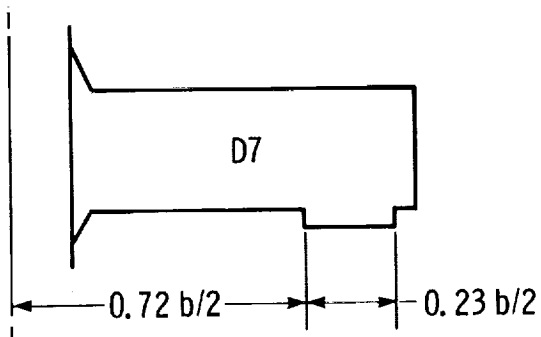| Spin, ailerons against	
Left	Right
Not attempted.	Not attempted.

TABLE II.- Continued

(f) Configuration D6

Stall			
Idle power, lg	Full power		
Less wing rock than configuration D5. Slight aileron effectiveness.	lg	Accelerated	
	Slight wing rock. Slow left turn; controllable with ailerons.	Left	Right
		Maintained slow left turn (like right accelerated stall).	Wings leveled; then slow left turn. Controllable, with slight pitch oscillation and wing rock.

Spin, ailerons neutral	
Left	Right
Same as right spin, ailerons neutral.	Steep, spiral-type motion, with rapid entry. Recovered immediately with neutral controls.

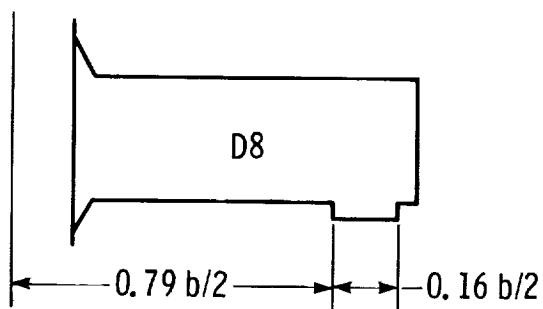| Spin, ailerons against	
Left	Right
Not attempted.	Not attempted.

TABLE II.- Continued

(g) Configuration D7

|--- 0.72 b/2 ---| |-- 0.23 b/2

Stall			
Idle power, 1g	Full power		
Wing rock (larger ampli- tude, slower frequency). Increased aileron effec- tiveness over configura- tion D6, but airplane less stable.	1g	Accelerated	
		Left	Right
	Airplane more docile, aile- ron effective and less wing rock.	Rolled out and into right spiral.	Departed right, nose dropped and entered right spiral.

Spin, ailerons neutral	
Left	Right
Same as right spin, ailerons neutral.	Still steep, spiral-type spin but faster turn rate. Recovered in 1 turn after neutral controls.

Spin, ailerons against	
Left	Right
Not attempted.	Not attempted.

54

TABLE II.- Continued

(h) Configuration D8

|←————0.79 b/2————→|←→|—0.16 b/2
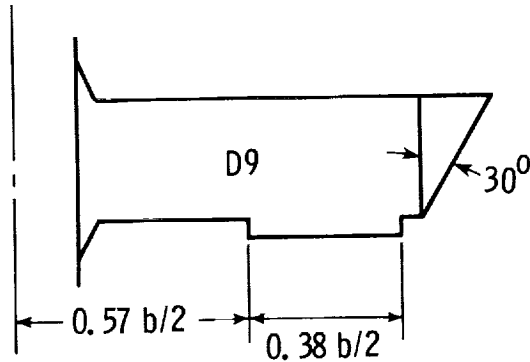
Stall			
Idle power, 1g	Full power		
More like basic aircraft. Unpredictable motion, either right or left steep spin.	1g	Accelerated	
	Motion a little more abrupt; broke left and tried to spin.	Left	Right
		Crossed over into right steep spin (like right, accelerated).	Entered right spin, like snap roll. Easily recovered.

Spin, ailerons neutral	
Left	Right
Same as right spin, ailerons neutral.	More like basic aircraft spin, although slightly steeper. Recovered in 1 turn with neutral controls.

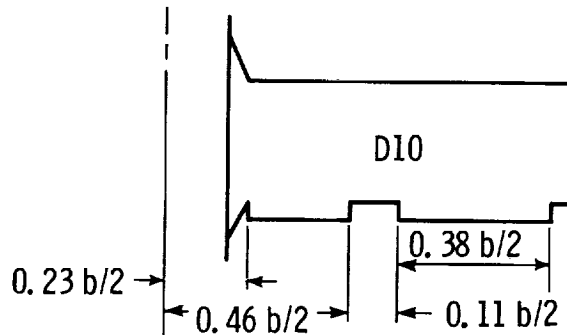| Spin, ailerons against	
Left	Right
Not attempted.	Not attempted.

TABLE II.- Continued

(i) Configuration D9

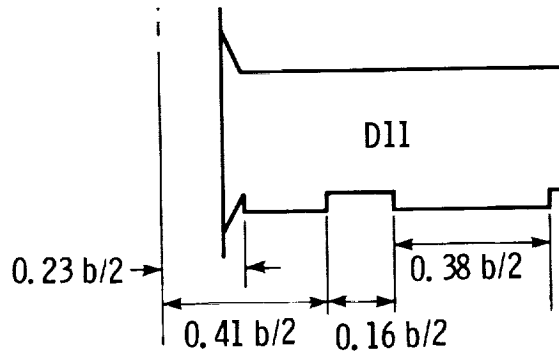| Stall			
Idle power, 1g	Full power		
Wing rock more random. Damped out, but reexcited. Aileron control weak.	1g	Accelerated	
		Left	Right
	No wing rock. Entered gentle left turn.	Quickly broke to wings level.	Stayed in right turn.
Spin, ailerons neutral			
Left		Right	
Steep spiral-type spin. Quick recovery (1/4-turn) after neutral controls.		Same as left spin, ailerons neutral.	
Spin, ailerons against			
Left		Right	
Same as right spin, ailerons against.		Steep spiral motion again; turn rate a little slower. Again quick recovery with neutral control.	

TABLE II.- Continued

(j) Configuration D10

D10

0.23 b/2 →

0.38 b/2

0.46 b/2 →

← 0.11 b/2

Stall			
Idle power, 1g	Full power		
Wing rock. Gentle left turn. Ailerons effective.	1g	Accelerated	
	Slight wing rock. Left turn. Ailerons ineffective.	Left	Right
		Stayed in left turn, with slight wing rock.	Broke level, then into left turn.

Spin, ailerons neutral	
Left	Right
Steep spiral (4 turns). Recovered in 1/2 turn with rudder against, elevator and ailerons neutral.	Moderately flat spin (12 turns). Recovered in 2 turns with rudder against, elevator and ailerons neutral.

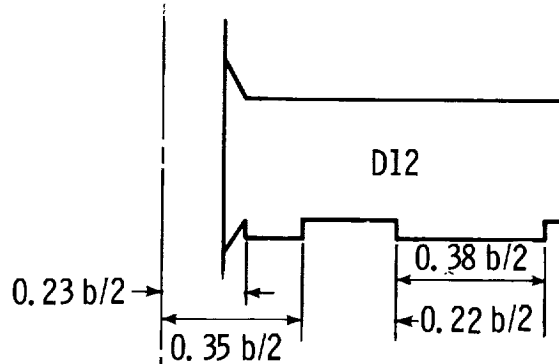| Spin, ailerons against	
Left	Right
Spin became flat in 6 turns. No recovery with controls. Recovery parachute used.	Moderately flat spin at 9 turns. Recovered in $3\frac{1}{2}$ turns. Repeat of a 12-turn spin recovered in $1\frac{1}{2}$ turns.

TABLE II.- Continued

(k) Configuration D11

$0.23\ b/2 \rightarrow$

$0.38\ b/2$

$0.41\ b/2 \qquad 0.16\ b/2$

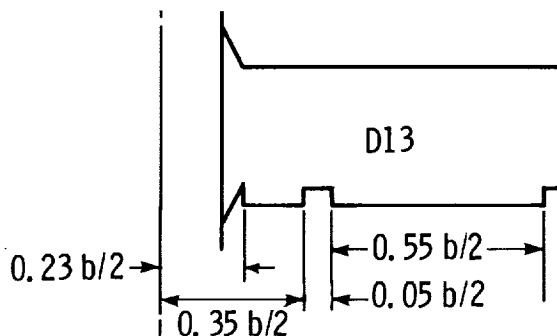| Stall			
Idle power, 1g	Full power		
Intermittent wing rock, but no roll-off. Ailerons ineffective.	1g	Accelerated	
	No wing rock, ailerons weak.	Left	Right
		No wing rock. Wings leveled slowly.	Broke level, and into left turn.
Spin, ailerons neutral			
Left		Right	
First attempt.- Spin building up after 6 turns. Slow recovery in 8 turns with rudder against, elevator neutral. Second attempt.- Spin became flat. Unrecoverable with controls. Used recovery parachute.		Not attempted.	
Spin, ailerons against			
Left		Right	
Not attempted.		Not attempted.	

TABLE II.- Continued

(l) Configuration D12

Stall		
Idle power, 1g	Full power	
Slight wing rock. Tendency to diverge left, but settled with no roll-off.	1g	Accelerated

		Left	Right
Slight wing rock. Tendency to diverge left, but settled with no roll-off.	No wing rock. Ailerons weak. Power caused slow left circle with no roll-off.	Stayed in left circle.	Wings leveled, and no roll-off.

Spin, ailerons neutral	
Left	Right
Steep, spiral-type spin - (very tight turn). Recovery in 1/4 to 1/2 turn with neutral controls.	Steep spiral spin. Same as left spin with neutral ailerons except recovery in 1/2 to 1 turn with neutral controls.

Spin, ailerons against	
Left	Right
Slow, steep spiral-type spin. Immediate recovery with neutral controls.	Same as left spin, ailerons against.

TABLE II.- Continued

(m) Configuration D13

Stall			
Idle power, 1g	Full power		
Not attempted.	1g	Accelerated	
	Not attempted.	Left	Right
		Not attempted.	Not attempted.

Spin, ailerons neutral	
Left	Right
Spin became flat in 3 to 4 turns. No recovery with controls. Used recovery parachute.	Steep spin; faster rotation rate with recovery using neutral controls.

Spin, ailerons against	
Left	Right
Not attempted.	Not attempted.

TABLE II.- Concluded

(n) Configuration D14

Stall			
Idle power, 1g	Full power		
Slight wing rock - weak aileron control. No roll-off.	1g	Accelerated	
	No wing rock, into left turn. Ailerons slightly effective.	Left	Right
		Stayed in left turn. No tendency to level off.	Broke level, then rolled to left. Slight wing rock.

Spin, ailerons neutral	
Left	Right
Moderately flat spin. Slow recovery in 2 to 3 turns with rudder against and elevator neutral.	Steep spiral-type spin. Recovery in 1/4 turn with neutral controls.

Spin, ailerons against	
Left	Right
Went flat immediately. No recovery with controls. Used recovery parachute.	Not attempted.

TABLE III.- SUMMARY OF RADIO-CONTROLLED MODEL RESULTS FOR

LEADING-EDGE FLAP CONFIGURATIONS TESTED

(a) Configuration F1

Stall			
Idle power, 1g	Full power		
No wing rock. Slow turn to right.	1g	Accelerated	
	Not attempted.	Left	Right
		Not attempted.	Not attempted.

Spin, ailerons neutral	
Left	Right
Steep spin, possible spiral. Recovery in 1 to 2 turns with neutral controls.	Same as left spin, ailerons neutral.

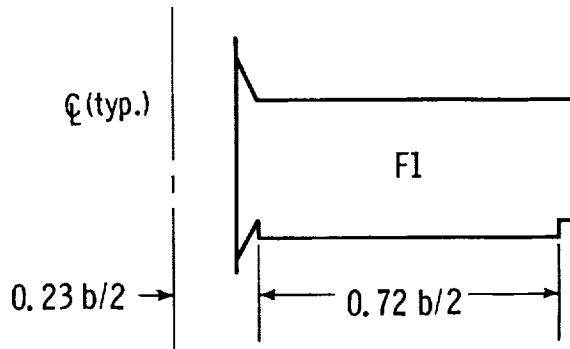| Spin, ailerons against	
Left	Right
Not attempted.	Not attempted.

TABLE III.- Continued

(b) Configuration F2
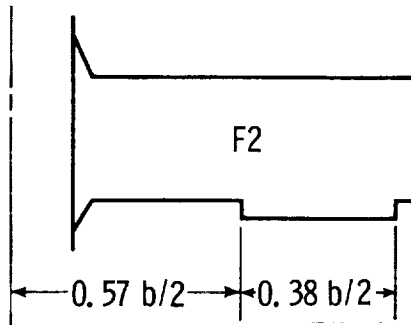
Stall			
Idle power, 1g	Full power		
Slight wing rock, but no tendency to roll-off. Ailerons fairly effective.	1g	Accelerated	
	Still slight wing rock, and no tendency to roll-off.	Left	Right
		Not attempted.	Not attempted.
Spin, ailerons neutral			
Left		Right	
Same as right spin, ailerons neutral.		Slow, steep, spiral-type spin. Quick recovery with neutral controls.	
Spin, ailerons against			
Left		Right	
Not attempted.		Not attempted.	

TABLE III.- Continued

(c) Configuration F3

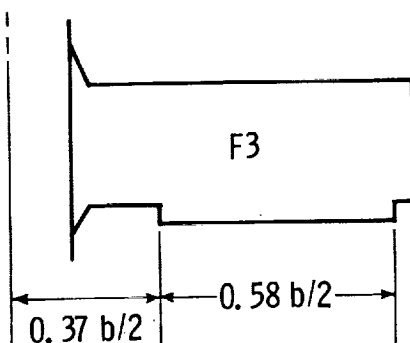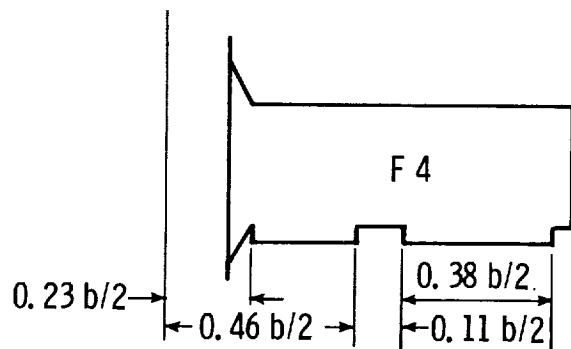| Stall			
Idle power, 1g	Full power		
Slight wing rock. No tendency to roll off. Ailerons less effective than with configuration F2.	1g	Accelerated	
		Left	Right
	Slight wing rock; rolled off into spin or spiral.	Not attempted.	Not attempted.
Spin, ailerons neutral			
Left		Right	
Slow, steep spiral-type spin. Immediate recovery.		Moderately flat spin. Recovery with rudder against, elevators neutral.	
Spin, ailerons against			
Left		Right	
Not attempted.		Not attempted.	

TABLE III.- Continued

(d) Configuration F4

F 4

0. 23 b/2 →

|← 0. 46 b/2 →|

0. 38 b/2.

|← 0. 11 b/2|

Stall			
Idle power, 1g	Full power		
Slight wing rock. No roll-off. Aileron control weak.	1g	Accelerated	
	Slight wing rock and no roll- off tendency. Ailerons weak.	Left	Rudder
		Not attempted.	Not attempted.

Spin, ailerons neutral	
Left	Right
Steep, slow spin - or spiral-type motion. Recovery rapid with neutral controls.	Moderately flat spin with higher rotation rate. Recovered in about 4 turns with rudder against, elevators neutral.

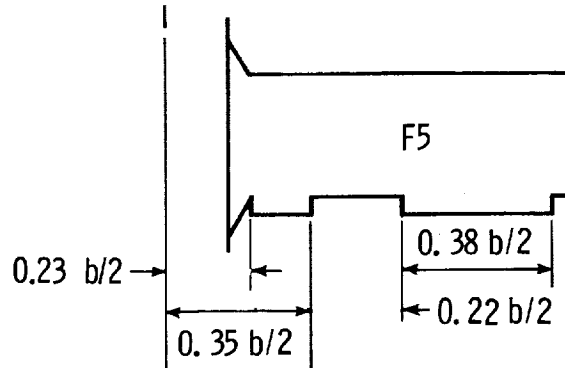| Spin, ailerons against	
Left	Right
Not attempted.	Not attempted.

TABLE III.- Concluded

(e) Configuration F5

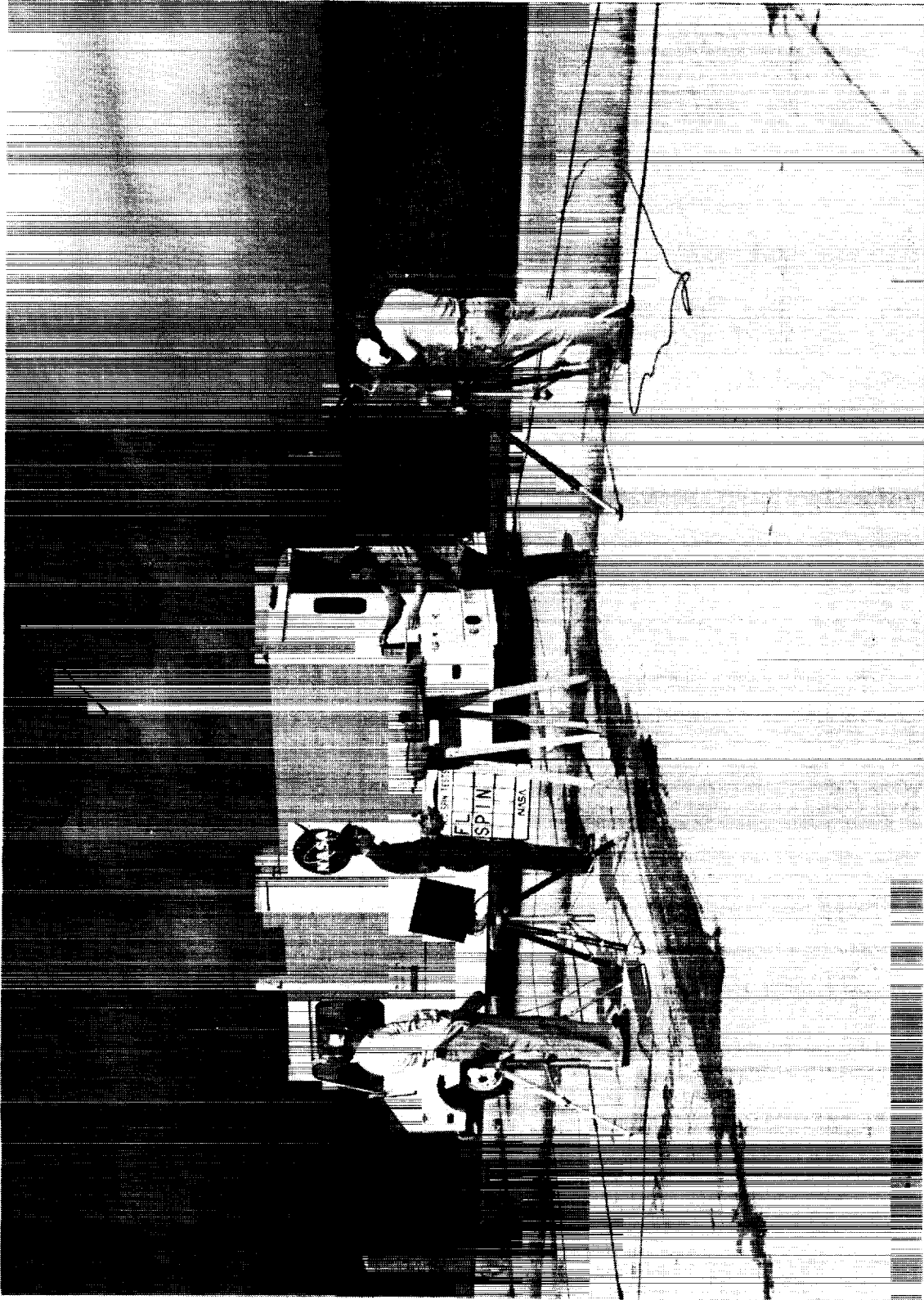| Stall			
Idle power, 1g	Full power		
Noticeable wing rock, but no roll-off. Aileron control weak.	1g	Accelerated	
	Very little or no wing rock, no roll-off, and ailerons still weak.	Left	Right
		Not attempted.	Not attempted.
Spin, ailerons neutral			
Left		Right	
Steep, spiral-type spin. Recovery very rapid with neutral controls.		Same as left spin, ailerons neutral.	
Spin, ailerons against			
Left		Right	
Not attempted.		Not attempted.	

66

Figure 1.- Radio-controlled model and test crew.

L-76-6774

Section A-A, enlarged

D1
0.23 b/2 ← → 0.72 b/2

D5
← 0.61 b/2 → 0.34 b/2

D2
0.57 b/2 → 0.38 b/2

D6
← 0.66 b/2 → 0.29 b/2

D3
0.41 b/2 → 0.38 b/2
0.16 b/2

D7
0.72 b/2 → 0.23 b/2

D4
0.41 b/2 → 0.54 b/2

D8
0.79 b/2 → 0.16 b/2
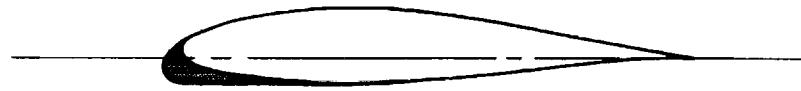
Figure 2.- Location and dimensions of wing-leading-edge droop
configurations tested.

Section A-A, enlarged

Figure 2.- Concluded.

Section A-A, enlarged

Figure 3.- Location and dimensions of wing-leading-edge
flap configurations tested.

III. AIRPLANE FLIGHT TESTS

Daniel J. DiCarlo; James M. Patton, Jr.;
and H. Paul Stough III

SUMMARY

A flight investigation was conducted to determine effects of leading-edge modifications on the stall/spin characteristics of a light single-engine general aviation airplane. Both the stall and spin characteristics were significantly improved with leading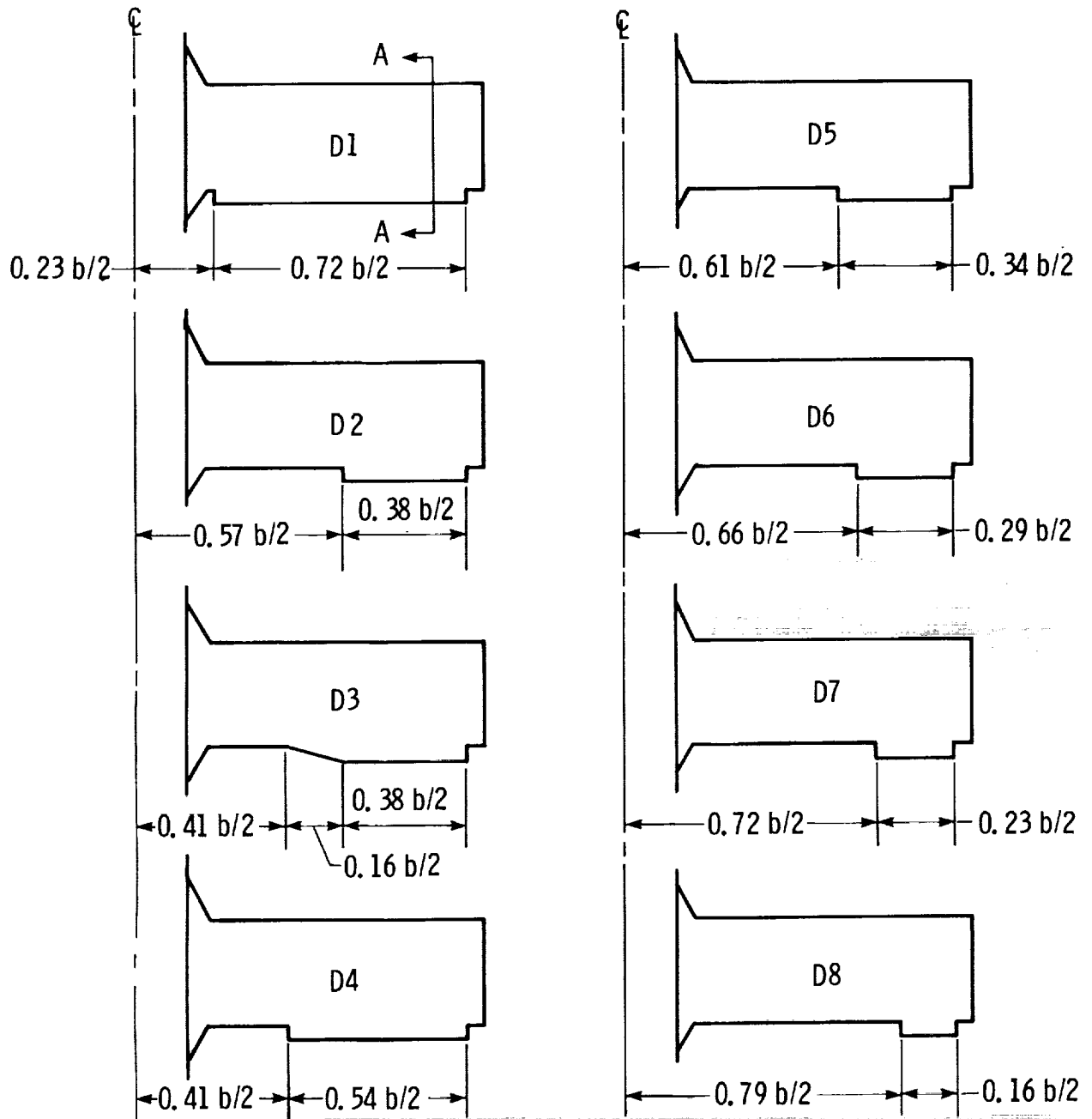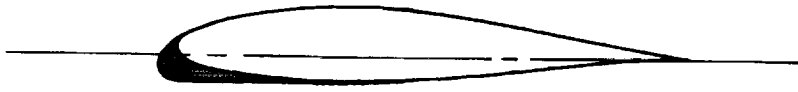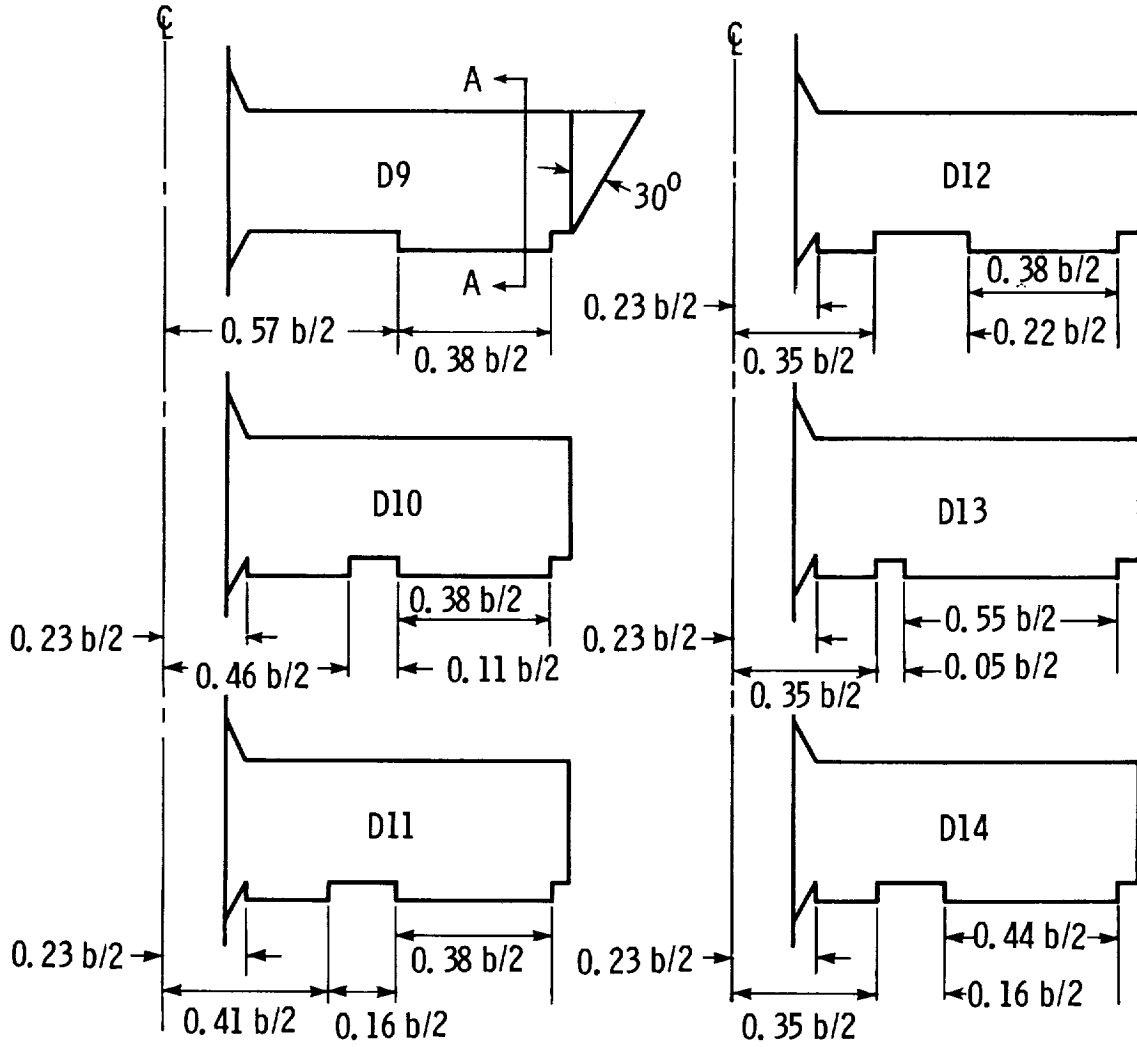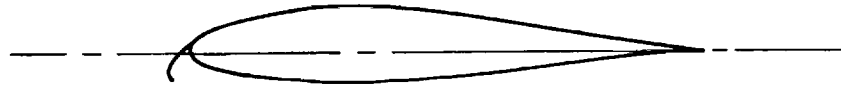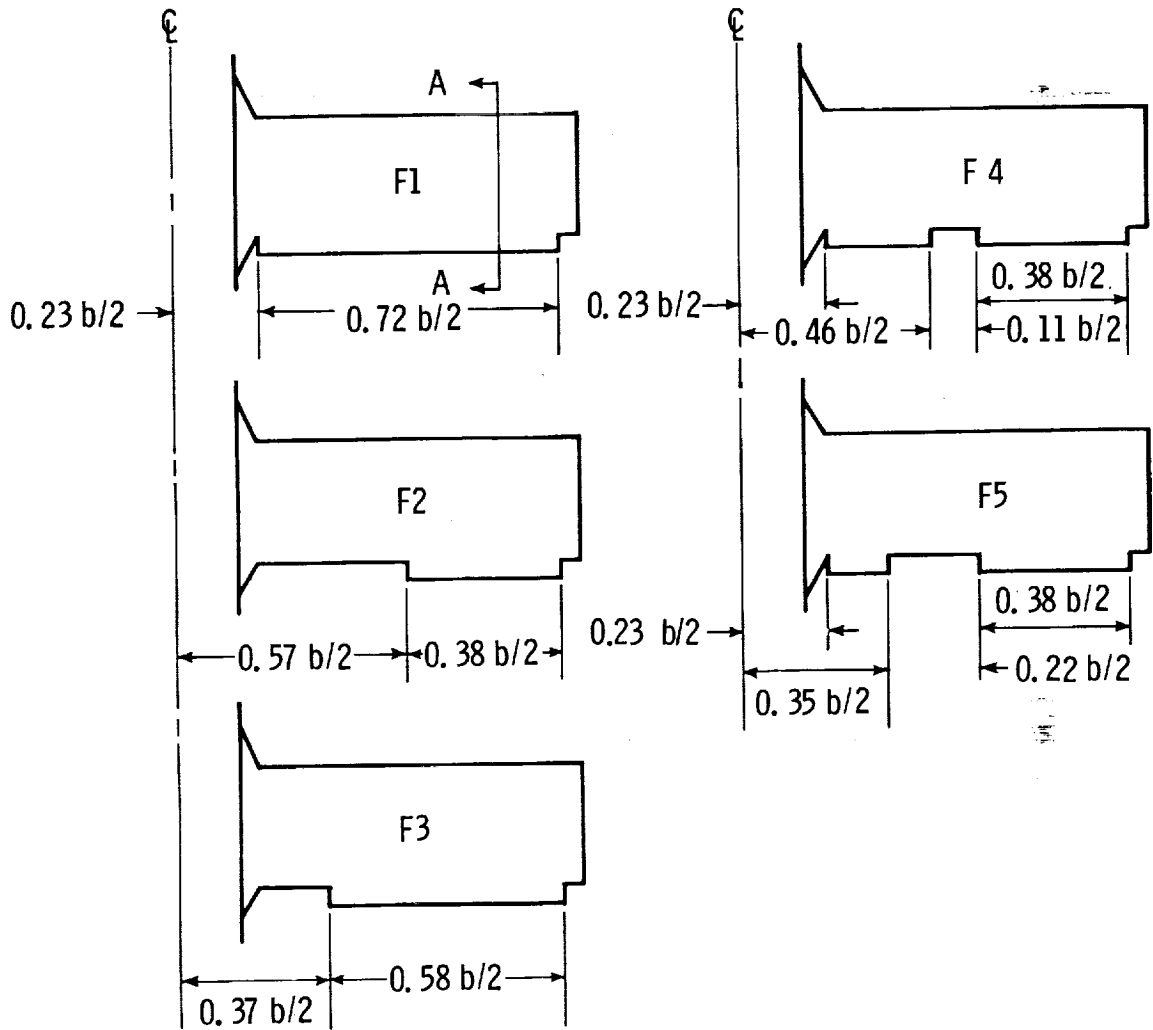-edge droop added to only the outboard sections of the wing. Full, deep stalls, beyond the stall angle of attack of the basic airplane, were maintained with little tendency to roll off into a spin. When prospin controls were applied and held, the airplane would eventually enter a very steep, diving spiral-type of motion at an angle of attack of about 28°. Recovery from this steep "spin" mode was effected immediately upon relaxing prospin controls. Full-span droop, on the other hand, resulted in markedly poorer stall/spin characteristics: the airplane would readily enter a fast, flat spin from which recovery could not be effected with normal airplane controls.

INTRODUCTION

This part of the report discusses the results of stall/spin flight tests of a low-wing, single-engine general aviation airplane with several wing-leading-edge configurations. These flight tests were undertaken to determine the influence of the most promising leading-edge modification, identified by wind-tunnel and radio-controlled model tests discussed in parts I and II of this report, on the stall/spin characteristics of the full-scale airplane. The modification consisted of adding a drooped leading edge, which enlarged the radius of the lower forward surface of the airfoil, to approximately the outer 40 percent of the wing span. Comparisons are made with the basic airplane configuration having a full-span conventional, small-radius leading edge and with a configuration having a full-span, large-radius, drooped leading edge. Flight-test results are presented in terms of pilot commentary and time histories of selected flight parameters.

SYMBOLS

Aerodynamic data are presented with respect to the body axes. Dimensions are given both in the International System of Units (SI) and in U.S. Customary Units. Measurements were made in U.S. Customary Units and converted using factors given in reference 1.

a_n	normal acceleration, g units
b	wing span, m (ft)
$\bar{c}$	mean aerodynamic chord, m (ft)
$\dot{h}_p$	vertical velocity based on pressure altitude, m/sec (ft/sec)
m	mass of airplane, kg (slugs)
p	rolling velocity, positive for right wing down, rad/sec or deg/sec
q	pitching velocity, positive for nose up, rad/sec or deg/sec
r	yawing velocity, positive for nose right, rad/sec or deg/sec
t	time, sec
V	velocity along flight path, m/sec (ft/sec)
α	angle of attack, rad or deg
δ_a	average aileron control-surface deflection, positive for right aileron trailing edge down, rad or deg
δ_e	elevator control-surface deflection, positive for trailing edge down, rad or deg
δ_r	rudder control-surface deflection, positive for trailing edge left, rad or deg
θ	pitch attitude, positive for nose up, rad or deg
ϕ	roll attitude, positive for right wing down, rad or deg
ψ	yaw attitude, positive for nose right, rad or deg

Subscripts:

stall	value at stall
steady	value at steady-state conditions

DESCRIPTION OF EQUIPMENT AND TESTS

Airplane

Tests were conducted using the general aviation research airplane shown in figure 1. Dimensions of the airplane are given in figure 1, with additional physical characteristics listed in table I. Throughout all phases of the

72

flight-test program, the airplane was equipped with a tail-mounted spin-recovery parachute system.

Instrumentation

The airplane was instrumented to measure true airspeed and flow angles at each wing tip, control positions and forces, linear accelerations, angular rates and attitudes about the body axes, altitude, engine speed, manifold pressure, and spin-recovery parachute load. Data were recorded onboard the airplane and were telemetered to the ground. Airplane data were supplemented by pilot commentary and motion picture film from both ground-tracking and wing-tip cameras. Wings were tufted for flow visualization. Selected flight parameters telemetered from the airplane, a video signal from a ground-tracking television camera, and pilot commentary were monitored in real time in a ground station. All data, including motion picture films and the video signal, were time-correlated.

Wing-Leading-Edge Modifications

The basic wing had a NACA 64_2-415 airfoil section modified to remove the concavity of the undersurface near the trailing edge. This airfoil had a small leading-edge radius and a modest camber. The modifications consisted of a glove over the forward part of the airfoil which provided a 3-percent chord extension and a droop which increased the leading-edge camber and radius. The principal modification was one which markedly improved stall/spin characteristics in the foregoing small-scale model tests. In this configuration, which is shown in figure 2, the leading-edge droop was applied to the outboard section of each wing (from 57 to 95 percent b/2) with sharp discontinuities at the junctures between the two airfoil sections. Dimensions of this outboard leading-edge modification are given in figure 3.

Several flight tests were conducted with a tapered fairing added to the inboard juncture to smooth the transition between the two airfoil shapes. This fairing, which is shown in figure 4, extended 0.61 m (2 ft) inboard from the juncture at 57 percent b/2.

A full-span drooped leading-edge wing having corresponding drooped leading edges on the root fillet and wing tip was also flight-tested.

TEST CONDITIONS

Flight tests were conducted at NASA Wallops Flight Center. Stalls with and without power were performed with trailing-edge flaps retracted and extended at an altitude of 914 m (3000 ft) or higher. Unaccelerated and accelerated stalls, which included slipping and skidding entries, were investigated.

Spin tests were conducted at altitudes of 2900 m (9500 ft) to 2040 m (6700 ft). Spins were entered by slowly decelerating at idle power to a

1g wings-level stall with flaps retracted and abruptly applying prospin controls. A variety of prospin control inputs were investigated. Right and left spins of 1, 3, and 6 turns were performed. Power on, accelerated, slipping and skidding spin entries were also attempted. Recovery control techniques included reversing the rudder and elevator, reversing the rudder only, reversing the elevator only, and neutralizing the controls.

RESULTS AND DISCUSSIONS

Stalls

Only stalls conducted with the power off and flaps retracted are discussed, since the use of power and flaps did not result in significant differences in stall characteristics. Also, entry conditions are limited to a slow decelerating approach to the stall while maintaining balanced (zero sideslip) flight, since accelerated and unbalanced flight had the same slightly degrading effect on the stall for all configurations tested. In addition, the pilot noted that for all wing configurations, whatever roll-off tendency existed was strongest at the initial stall break which occurred before the elevator was deflected full up (less roll-off at full aft stick). Roll-off tendencies were to the right in all cases. Another common characteristic was that very light initial stall buffet commenced 2 to 3 knots above the stall speed of 63 knots (72 mph), and increased to moderate buffet at full aft stick.

The stall characteristics are presented in figure 5 as time histories of selected flight parameters. The basic airplane stall (fig. 5(a)) was characterized by a roll-off tendency before the elevator could be deflected full up. Full-up elevator could not be held even for a short time without experiencing a roll-off tendency that would, in most cases, lead to an incipient spin. For the stall noted in figure 5(a), the pilot countered a right roll tendency with left rudder deflection which was held too long and caused what appears to be a left roll-off tendency. The pilot did indicate that a wings-level condition could be maintained for a limited time providing that sufficient control power was available and the pilot anticipated, or at least responded quickly to, the airplane motions.

The airplane's stall characteristics with the modified outboard leading edge are shown in figure 5(b). In contrast to the stall behavior with the basic wing, no roll-off is noted throughout the period the elevator was deflected full up. Instead, a slight wing rock developed, but the bank angle never exceeded 25°. The pilot noted that the reduced roll-off tendency could easily be prevented by small control inputs, and in some cases, the airplane exhibited no roll-off tendency whatsoever and entered a wings-level high-sink-rate flight condition with full aft stick.

Limited flight tests conducted with the tapered fairing added at the inboard juncture between the modified and basic airfoils indicated that stall characteristics were the same as those with the sharp discontinuity between the two sections.

74

Stall behavior with the full-span drooped wing was similar to that of the basic wing, though oscillatory and slightly more docile, as shown in figure 5(c). Again, brisk, anticipatory rudder and aileron deflections were necessary to prevent rapid roll at the stall, though the pilot indicated that the airplane eventually rolled off in every case, despite maximum preventive effort.

Although the stall characteristics associated with either the basic or the drooped leading-edge wing were acceptable, the pilot indicated that the airplane behavior with the drooped outboard leading edge was more predictable, better controlled, and hence, much improved. These results were anticipated from the wind-tunnel and radio-controlled model tests which indicated improved lateral stability for the drooped outboard leading-edge configuration. The improved air flow over the outer panel of each wing was substantiated by pilot observations and photographic records of tuft patterns on the wing at angles of attack above the stall. As shown in figure 6, the flow did not separate outboard of a line from the leading edge just outboard of the airfoil juncture point to the trailing edge near the outer edge of the aileron.

Even though no performance tests were conducted, pilot comments, climb times, and operating speeds indicated that performance was not degraded by addition of the outboard leading-edge droop.

Spins

For the spins discussed in this section, prospin controls consisted of full aft stick, full rudder deflection, and full aileron deflection against the desired spin direction. These controls were applied 1 to 2 knots above the stall speed and power remained idle throughout the spins with flaps retracted. Ailerons were deflected against the spin because the resulting spin was slightly flatter than the spin entered with ailerons neutral but had about the same rotation rate; this was considered the most critical condition. Recovery controls, which consisted of full antispin rudder deflection, full forward stick, and neutral ailerons, were applied at the 6-turn point and held until the airplane was obviously either recovering or not responding.

With the basic wing, the airplane had two spin modes: one moderately flat and the other flat. The moderately flat spin mode, shown in figure 7(a), was characterized by an angle of attack of 50° to 52°, a rate of descent of 32 to 38 m/sec (105 to 126 ft/sec), and a turn rate of 2.3 to 2.4 seconds per turn. The pilot indicated that this spin was entered readily with no hesitation. Pitch attitude was very steep at the 1/2-turn point, and increased to about 20° below the horizon at the 1-turn point. Pitch oscillations decreased as the spin progressed and eventually damped to zero. Airspeed stabilized at about 76 knots (88 mph) and recovery occurred $1\frac{1}{2}$ turns after applying normal recovery controls.

The flat spin mode was characterized by an angle of attack of 70°, a rate of descent of 30 m/sec (100 ft/sec), and a turn rate of 1.8 seconds per turn. Airplane controls did not recover the airplane from this flat mode and the spin-

recovery parachute was needed. More information on the airplane spin charac-
teristics with the basic wing and a comparison with spin-tunnel and radio-
controlled model test results can be found in reference 2.

With the drooped outboard wing leading edge, the airplane spun very
steeply (fig. 7(b)) with an angle of attack of approximately 28°, a rate of
descent of 30 to 55 m/sec (100 to 180 ft/sec), and a turn rate of 3.5 seconds
per turn. The characteristics of the various spins are given in table II, where
aileron deflection during the spin is also indicated. The resultant airplane
motion was the same regardless of the type of spin entry attempted and required
about 2 or 3 turns to achieve steady-state conditions. The pilot noted that
with the drooped outboard leading edge, the airplane was reluctant to enter a
spin, and the resultant motion was of a different character. After application
of prospin controls, the airplane slowly rolled and yawed in the direction the
rudder was deflected, hesitated at the 1/4-turn point, then entered a steep,
slow spiral-type mode. The buffet level remained high in contrast to the spin
of the basic configuration, pitch and roll oscillations disappeared quickly, and
airspeed increased during the first 3 turns and stabilized at about 101 knots
(116 mph). Normal acceleration was noticeably higher than in the basic spin,
about 2.2g versus 1.7g. At the 6-turn point, simply relaxing either prospin
rudder or elevator resulted in immediate recovery (less than 1/8 turn).

Because of the foregoing results with the drooped outboard leading edge,
the question arises as to whether or not the airplane was spinning. A spin is a
maneuver of an airplane in which it descends in a helical path with an angle of
attack greater than the angle of maximum lift. As noted in part I, the modified
wing configuration did have a double-peaked lift curve, the first peak occurring
at the expected lower angle of attack ($\alpha \simeq 14°$) and the second occurring at an
angle of attack of about 35°. The steady-state angle of attack during the spin
was about 28°, which is below that corresponding to maximum lift, and tufts
showed the outboard part of the wing to be unstalled. Also, the rotation would
stop if the controls were not held in the prospin position. On the basis of
these characteristics, the motion might be regarded as a steep controlled spiral
dive. However, since the airplane appeared to the pilot to have flown through a
stall corresponding to the first peak in the lift curve, this flight mode is
referred to herein as a spin.

An example of the results obtained with the full-span drooped leading-edge
wing is shown in figure 7(c). For this configuration, the airplane spun flat,
regardless of the prospin controls employed, and at times, required the use of
the spin-recovery parachute. This flat spin mode was characterized by an angle
of attack of 60° to 70° and a turn rate of 1.8 to 2.2 seconds per turn, which
was comparable with the flat spin mode with the basic configuration. However,
the pilot indicated that the airplane readily entered the flat spin and reached
a steady-state condition by the fourth or fifth turn. At about the second or
third turn, the rotation rate increased along with the nose-up attitude.
Details of the airplane spin characteristics with the full-span drooped leading
edge are included in reference 3.

Although the addition of a drooped leading edge to the outboard part of the
wing obviously resulted in an increased stall angle of attack at the wing tip,

the mechanism by which the outer-panel lift is maintained to yield such improved stall/spin characteristics has been unclear. It could be the result of the modified outer airfoil section itself, the abrupt discontinuity at the inboard juncture of the two airfoil sections, which might act as a vortex generator, or both. To obtain additional information in this regard, a metal fairing was added at the inboard juncture to smooth the discontinuity. A similar configuration was subsequently tested on the radio-controlled model as discussed in part II of this report.

Addition of the fairing to the drooped outboard leading edge caused the spin characteristics to be severely degraded. From pilot commentary, the spin entry appeared identical to the modified outboard leading-edge configuration with the sharp discontinuity, except that at the $1\frac{1}{2}$-turn point the spin character-ter suddenly changed. Rotation rate increased rapidly, pitch attitude flattened, and the airplane "locked-in" to a flat spin within 2 additional turns. In fact, the pilot noted that this flat spin was quite stable and more severe than that associated with the basic airplane configuration which had to be driven into a flat spin using a series of elevator control inputs (ref. 2).

Time histories of selected parameters from this particular flat spin are presented in figure 8. Of particular interest is the angular yaw rate which dramatically increases at about the 1- to $1\frac{1}{2}$-turn point as the airplane enters a flat spin. The spin mode was characterized by an angle of attack of 74°, a rate of descent of 31 m/sec (103 ft/sec), and a turn rate of 1.6 seconds per turn. (Comparative data are given in table II.) Airspeed stabilized at 59 knots (68 mph). Recovery controls were applied after 5 turns, but the airplane continued to spin. After 10 turns the spin-recovery parachute was deployed, at an altitude of 1676 m (5500 ft), effecting recovery in an additional $2\frac{1}{2}$ turns. Apparently, eliminating the abrupt airfoil discontinuity also eliminated the attendant spin resistance.

An interesting feature of the spin behavior during the first several seconds (or turns) for the drooped outboard leading-edge configurations is the similarity in angle of attack, yaw rate, and other flight parameters. Time histories of two spins have been superimposed in figure 9 to highlight these similar initial trends. This points out another aspect of the spin test results which is quite significant. Specifically, all the configurations tested complied with the spin requirements specified in the Federal Aviation Regulations for normal and utility category airplanes (ref. 4); that is, all recovered from a 1-turn spin within the prescribed additional turn. This fact should serve as a warning to operators of this class of airplane; acceptable 1-turn spin characteristics do not necessarily imply good or acceptable behavior for multiturn spins. When a flat spin such as that shown in figure 8 exists, there is the likelihood that recovery will be impossible through the use of normal controls.

CORRELATION WITH MODEL RESULTS

The marked improvement in the airplane stall and spin behavior with the drooped outboard leading edge agreed well with the earlier experimental model results. This agreement is particularly noteworthy in view of the large difference between model and full-scale Reynolds numbers. Although it is recognized that Reynolds number affects the value of maximum lift coefficient and the shape of the lift curve, the increased damping in roll (lateral stability) and improved stall characteristics identified by the static and forced-oscillation tests (part I) were realized in the airplane tests. Also, the flight data substantiated the characteristics predicted by the radio-controlled model tests conducted with corresponding configurations. In fact, the stall characteristics, spin modes, and recovery characteristics of the radio-controlled model for the full-span drooped leading-edge wing and for the outboard drooped leading-edge wings (with and without the tapered fairing at the inboard airfoil juncture) were practically identical to the full-scale results.

SUMMARY OF RESULTS

Flight tests have been conducted to determine the effect of wing-leading-edge modifications on the stall/spin characteristics of a light, single-engine, low-wing, general aviation airplane. From the flight data and pilot observations, the following results have been obtained:

1. Stall behavior of the test airplane with outboard leading-edge droop (without a fairing at the airfoil discontinuity) was much improved over that of the airplane with no leading-edge modification.

2. Regardless of the entry technique employed, the spin mode of the airplane with this outboard leading-edge droop was characterized by a steep, slow, spiral-type motion from which recovery was effected immediately by relaxing prospin controls.

3. A tapered fairing to eliminate the airfoil discontinuity at the 57-percent semispan location did not alter the improved stall characteristics, but eliminated the improvements in spin characteristics realized with the discontinuity present.

4. Full-span leading-edge droop resulted in markedly poorer spin characteristics: the airplane would readily enter a fast flat spin from which no recovery was possible with the normal controls.

5. The stall/spin characteristics obtained during the flight tests substantiated the results predicted from the radio-controlled model flight tests conducted for the same configurations.

Langley Research Center
National Aeronautics and Space Administration
Hampton, VA 23665
November 19, 1979

REFERENCES

1. Standard for Metric Practice. E 380-76, American Soc. Testing & Mater., 1976.

2. Bowman, James S., Jr.; Stough, Harry P.; Burk, Sanger M., Jr.; and Patton, James M., Jr.: Correlation of Model and Airplane Spin Characteristics for a Low-Wing General Aviation Research Airplane. AIAA Paper 78-1477, Aug. 1978.

3. Patton, James M., Jr.; Stough, H. Paul, III; and Dicarlo, Daniel J.: Spin Flight Research Summary. [Paper] 790565, Soc. Automot. Eng., 1979.

4. Airworthiness Standards: Normal, Utility and Acrobatic Category Airplanes. Federal Aviation Regulations, vol. III, pt. 23, FAA, June 1974.

TABLE I.- TEST AIRPLANE CHARACTERISTICS

Gross weight, N (lb) at test altitude 6863 (1543)

Moments of inertia, kg-m^2 (slug-ft^2):
  Pitch (I_Y) 826 (609)
  Roll (I_X) 1010 (745)
  Yaw (I_Z) 1741 (1284)

Inertia yawing-moment parameter, $\dfrac{I_X - I_Y}{mb^2}$ . . . . -47×10^{-4}

Center of gravity, percent $\bar{c}$ 26

Wing:
  Span, m (ft) 7.46 (24.46)
  Area, m^2 (ft^2):
    Basic wing 9.11 (98.11)
    With drooped outboard leading edge 9.21 (99.13)
  Root chord, m (ft) 1.22 (4.0)
  Tip chord, m (ft) 1.22 (4.0)
  Mean aerodynamic chord, m (ft):
    Basic wing 1.22 (4.0)
    With drooped outboard leading edge 1.23 (4.03)
  Aspect ratio:
    Basic wing 6.10
    With drooped outboard leading edge 6.04
  Dihedral, deg 5.0
  Incidence:
    At root, deg 3.5
    At tip, deg 3.5
  Airfoil section . . . .   NACA 64_2-415 (modified)

Horizontal tail:
  Span, m (ft) 2.34 (7.69)
  Incidence, deg . . . .   -3.0
  Root chord, m (ft) 1.10 (3.6)
  Tip chord, m (ft) 0.51 (1.67)
  Airfoil section . . . .   NACA 65_1-012

Maximum control deflections:
  Rudder, deg . . . .   25 right, 25 left
  Elevator, deg . . . .   25 up, 15 down
  Ailerons, deg . . . .   25 up, 20 down

TABLE II.- SPIN CHARACTERISTICS WITH DROOPED OUTBOARD LEADING EDGE

	α_{stall}, deg	α_{steady}, deg	V_{steady}, m/sec	a_n, g units	*p, deg/sec	q, deg/sec	r, deg/sec	$\dot{h}_p$, m/sec	Turn rate, sec/turn
Ailerons with spin									
1 turn	13.5	23.0	46.3	1.6	29	18	31	12.2	7.8
3 to 6 turns	15.0	26.0	56.4	2.1	78	20	30	33.5	4.2
	19.0	23.0	54.9	2.6	71	21	30	51.8	4.5
	12.5	22.5	54.9	2.5	76	25	30	45.7	4.2
	14.0	26.0	55.5	2.5	67	23	30	43.6	4.7
Average . . .	15.1	24.4	55.5	2.4	73	22	30	43.6	4.4
Ailerons neutral									
1 turn	18.0	25.0	44.2	1.5	43	15	30	10.1	6.6
	17.5	27.0	42.7	1.5	48	18	27	7.6	6.2
	17.0	33.0	42.7	1.5	29	15	40	15.2	7.0
	17.0	27.0	41.2	1.5	22	18	35	19.5	8.0
Average . . .	17.4	28.0	42.7	1.5	36	17	33	13.1	7.0
3 to 6 turns	17.5	27.5	54.9	2.6	87	18	40	47.9	3.7
	15.5	22.0	56.4	2.5	68	12	25	36.6	4.9
	14.5	25.0	54.9	2.5	96	20	40	50.6	3.4
	17.0	25.5	57.9	2.4	81	18	35	48.8	4.0
	17.0	26.0	54.9	1.4	50	15	45	39.6	5.2
Average . . .	16.3	25.2	55.8	2.3	76	17	37	44.8	4.2
†5 turns	17.0	30.0	54.9	2.4	102	25	50	45.7	3.1
Ailerons against spin									
1 turn	13.5	25.5	47.3	1.3	47	8	30	15.2	6.4
	14.5	36.0	40.5	1.5	53	15	40	4.3	5.3
Average . . .	14.0	30.8	43.9	1.4	50	17	35	9.8	5.9
3 to 6 turns	12.5	27.5	51.8	2.2	99	5	45	45.7	3.3
	13.5	25.0	55.5	2.3	83	10	40	54.9	3.9
	13.5	28.0	51.8	2.3	93	8	44	40.5	3.5
	16.0	28.0	51.2	2.2	73	8	48	42.7	4.1
	17.0	28.5	51.8	2.2	96	10	50	45.7	3.3
	17.5	29.5	53.4	2.5	89	10	45	42.7	3.6
	13.0	28.0	51.8	2.4	89	5	45	30.5	3.6
Average . . .	14.7	27.8	52.5	2.3	89	8	45	43.2	3.6
‡6 turns	14.0	74.0	30.5	2.3	74	10	220	31.4	1.6

*Calculated.
†Configuration with fairing at inboard airfoil juncture.
‡Flat spin developed by 3-turn point with configuration with fairing at inboard airfoil juncture.

2.34
(7.69)

1.22
(4.0)

1.30
(4.26)

Flow direction
and velocity
sensor

Diameter 1.80
(5.92)

Camera

7.46
(24.46)

2.05
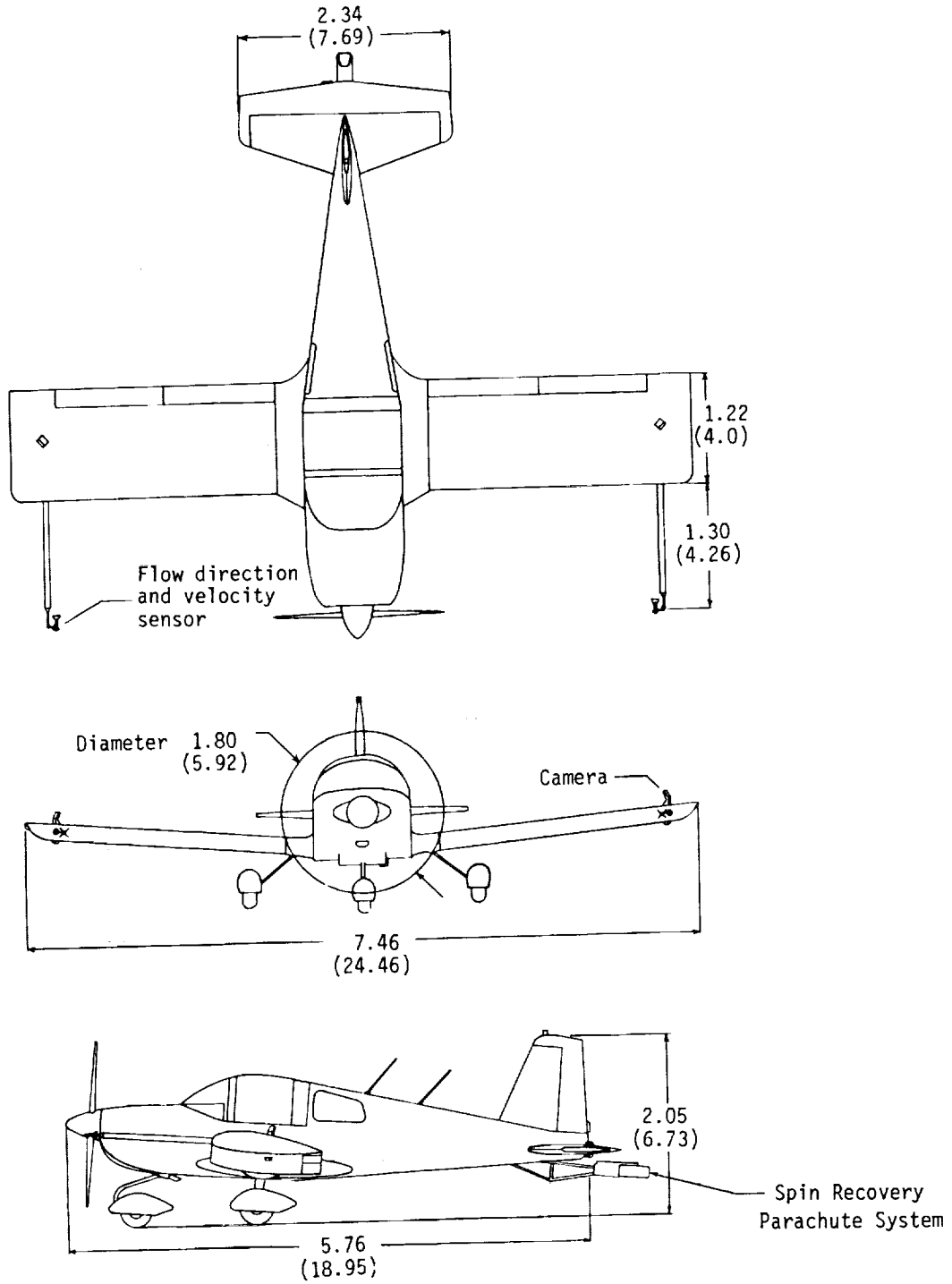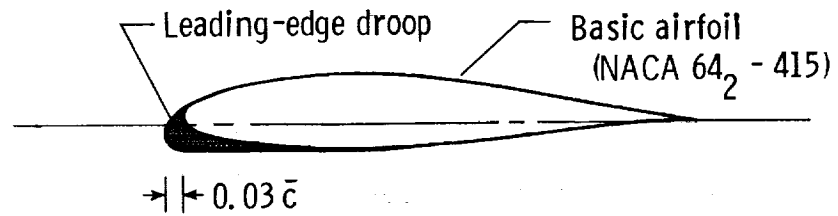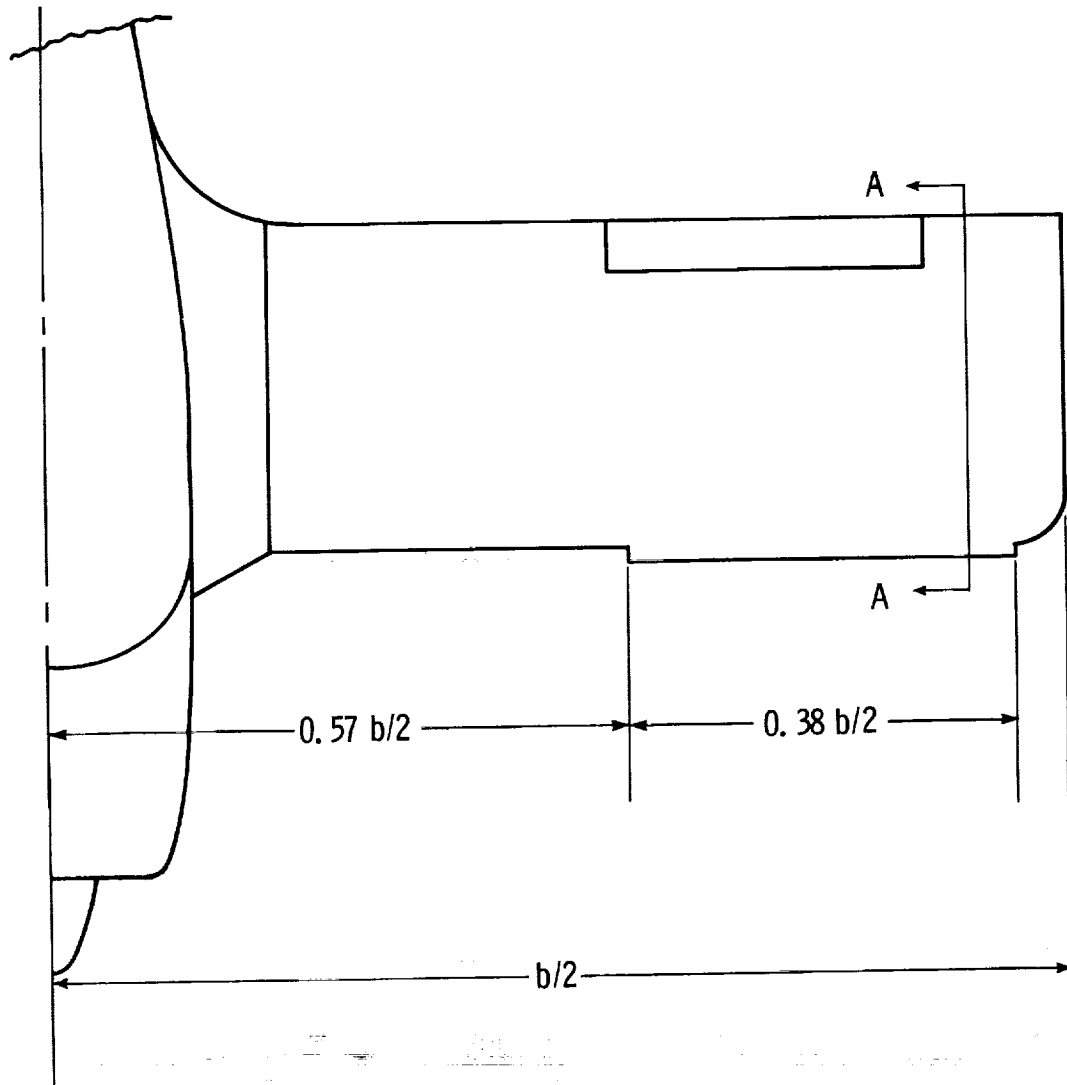(6.73)

Spin Recovery
Parachute System

5.76
(18.95)

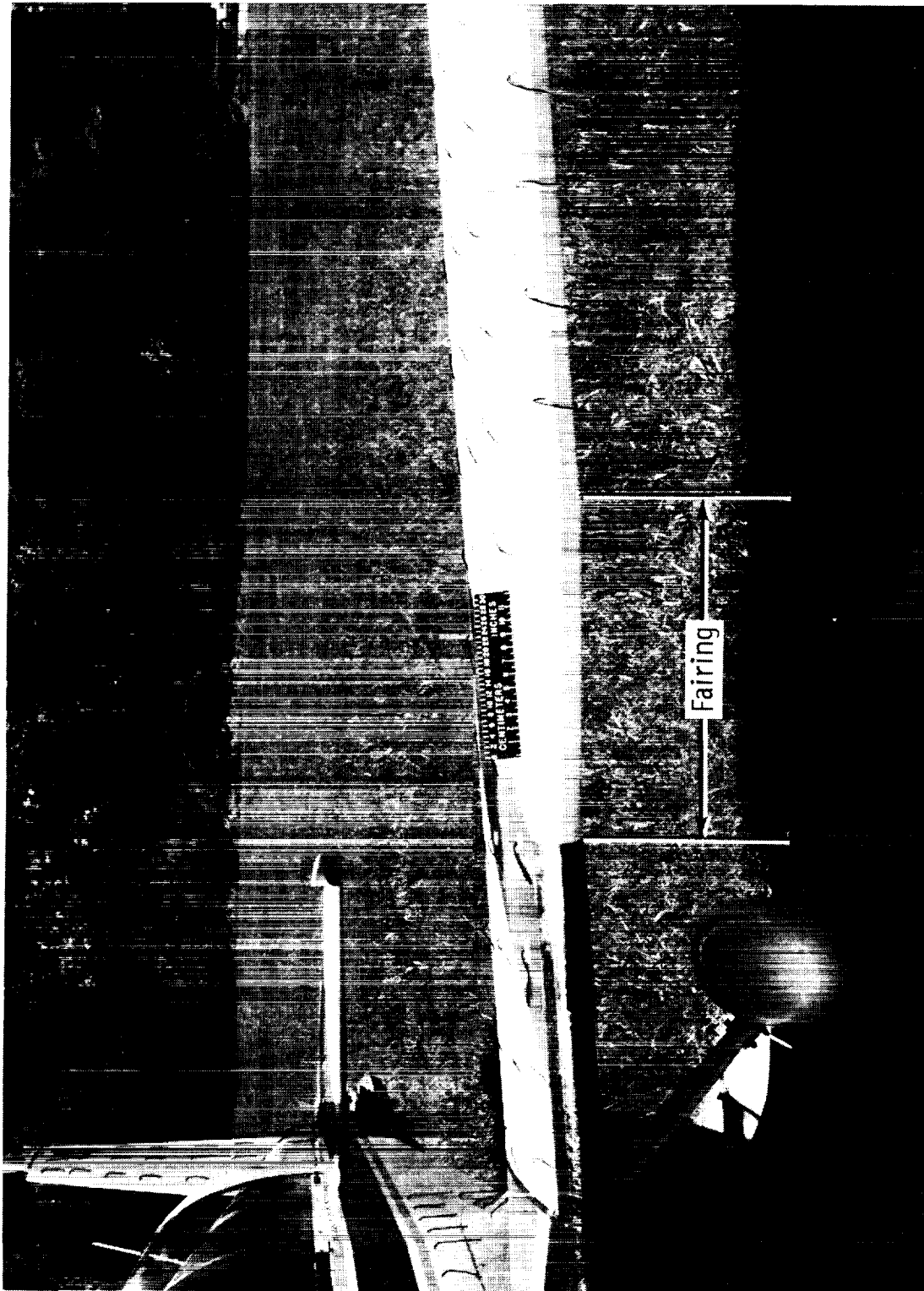Figure 1.- Flight test airplane. Dimensions
are in meters (feet).

82

DROOPED LEADING EDGE

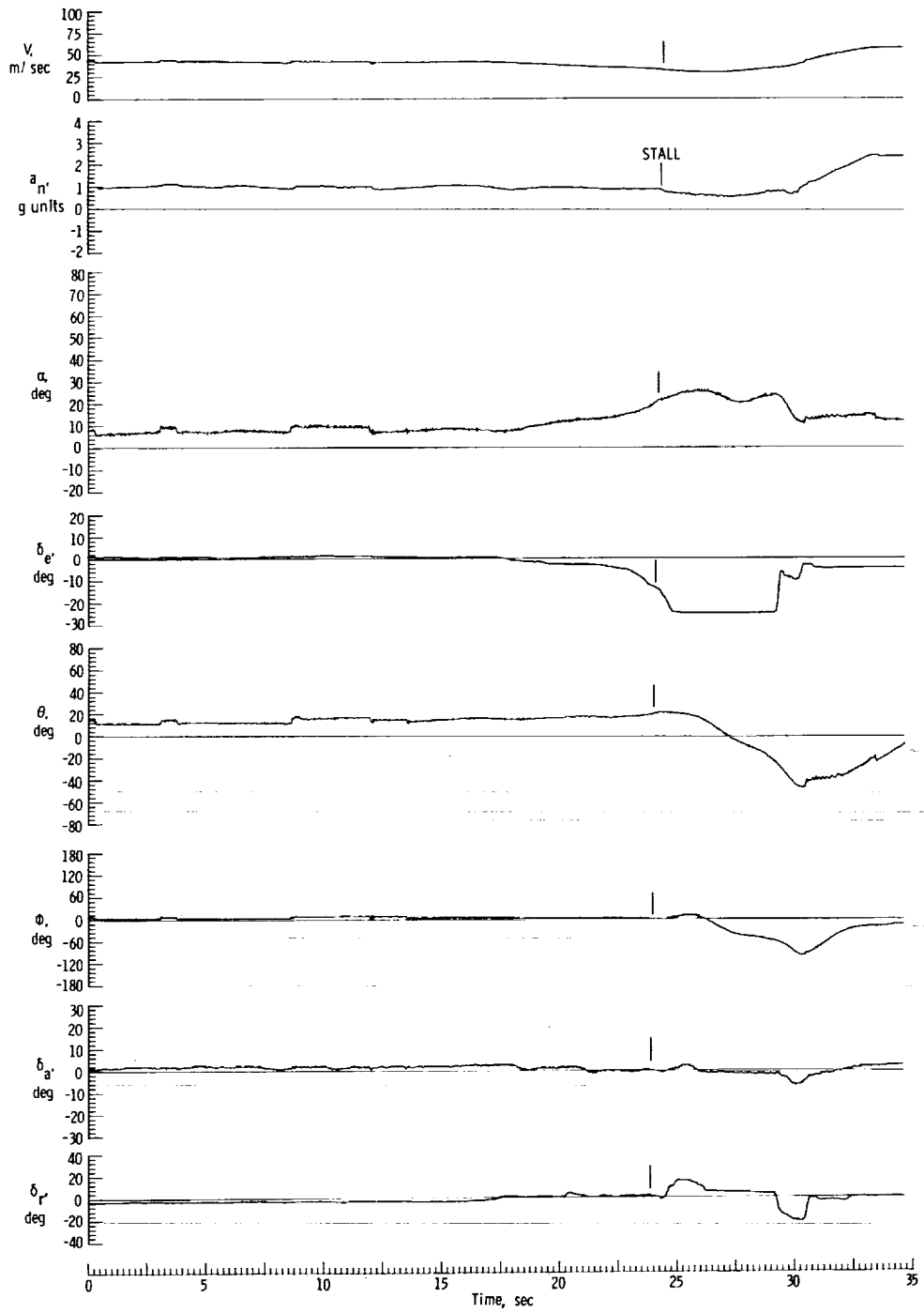BASIC LEADING EDGE

L-79-348

Figure 2.- Test airplane with drooped outboard leading edge.

83

Section A-A
(enlarged)

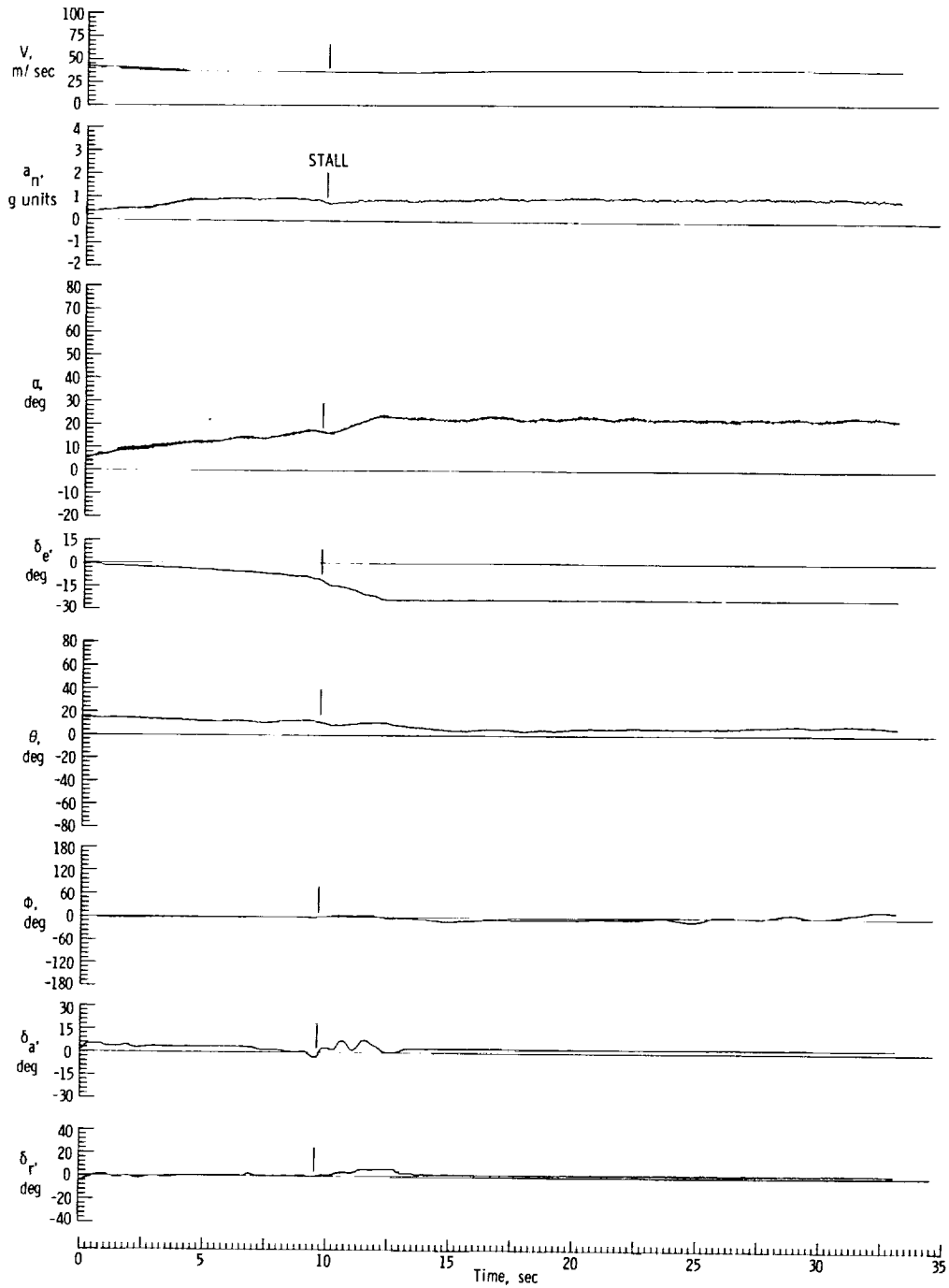Figure 3.- Configuration with drooped outboard leading edge.

Figure 4.- Fairing installation at inboard juncture of leading-edge modification.

L-78-4184.1

85

(a) Basic airplane (unmodified).

Figure 5.- Stall characteristics.

(b) Airplane with drooped outboard wing leading edge.

Figure 5.- Continued.
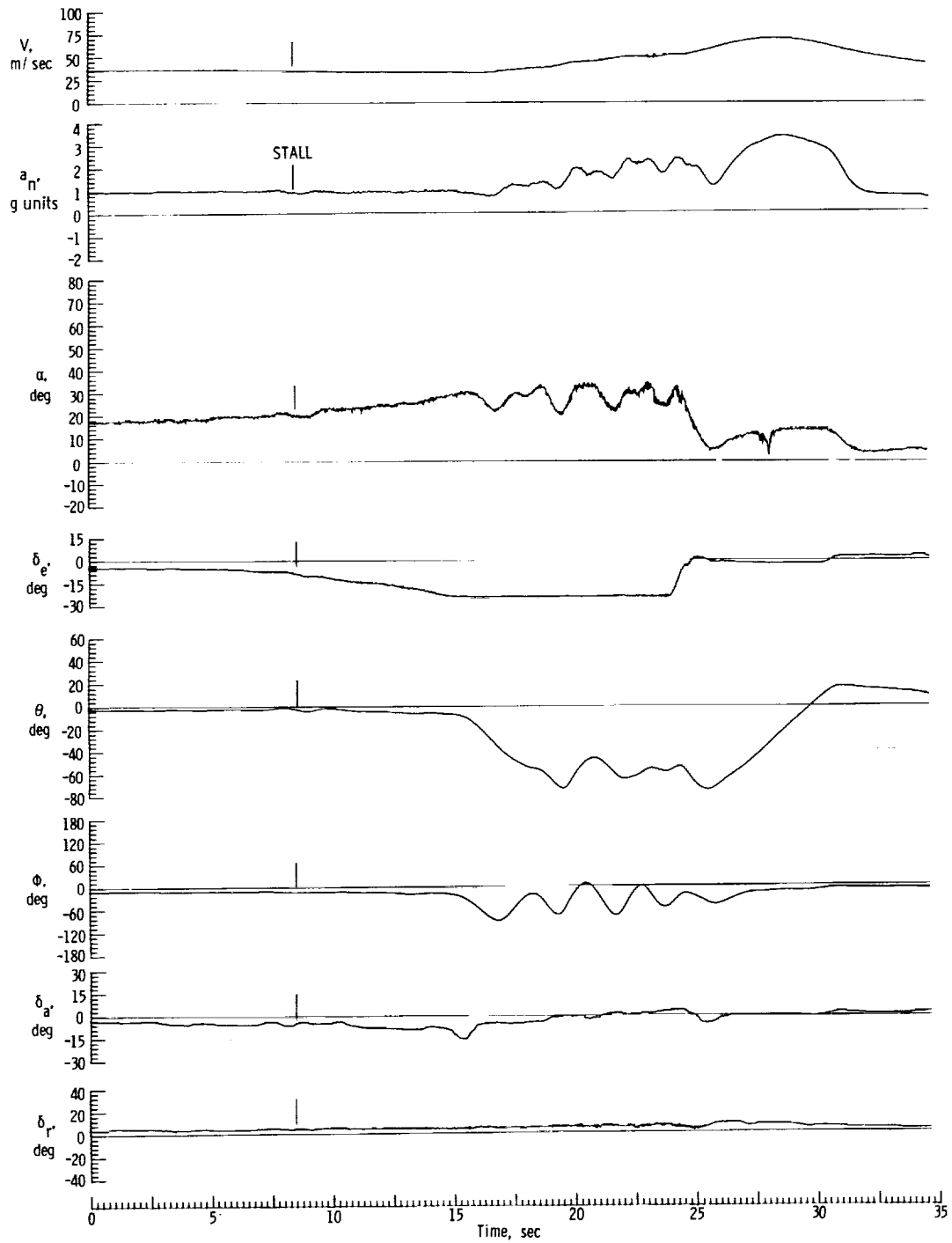
(c) Airplane with full-span drooped wing leading edge.

Figure 5.- Concluded.
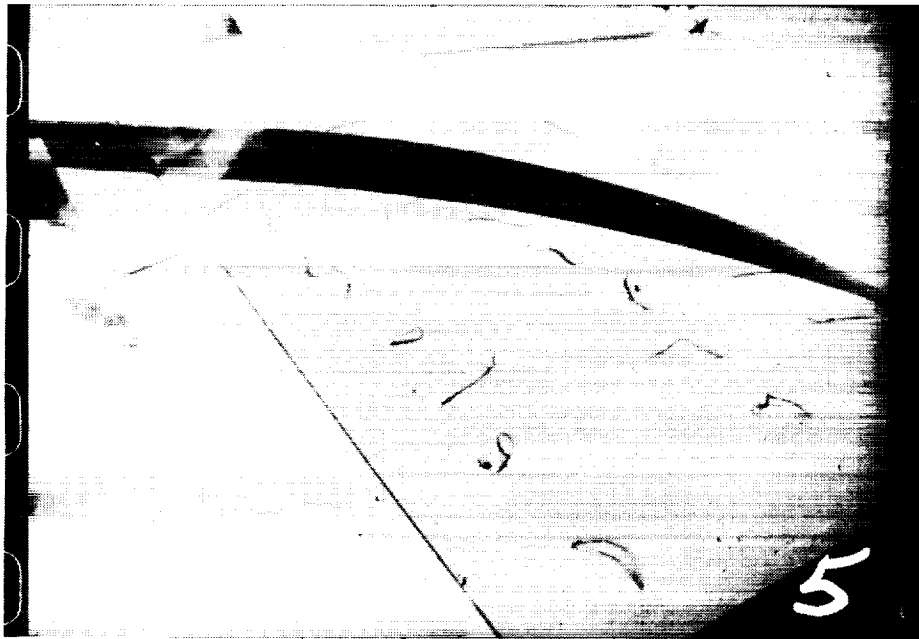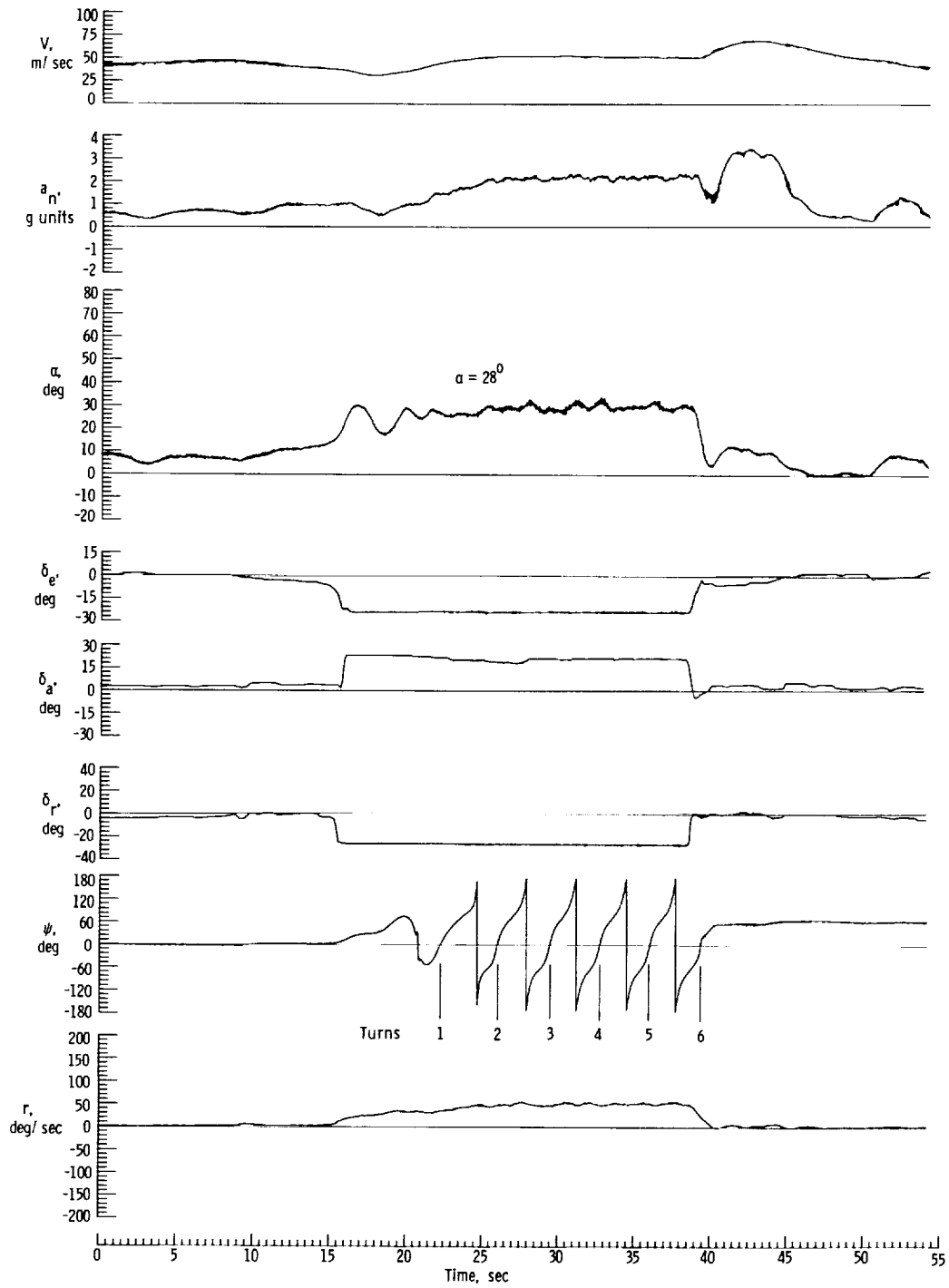
(a) Left wing.

(b) Right wing.

L-79-349

Figure 6.- Tuft patterns on wing upper surface
above stall angle of attack with drooped
outboard leading edge.

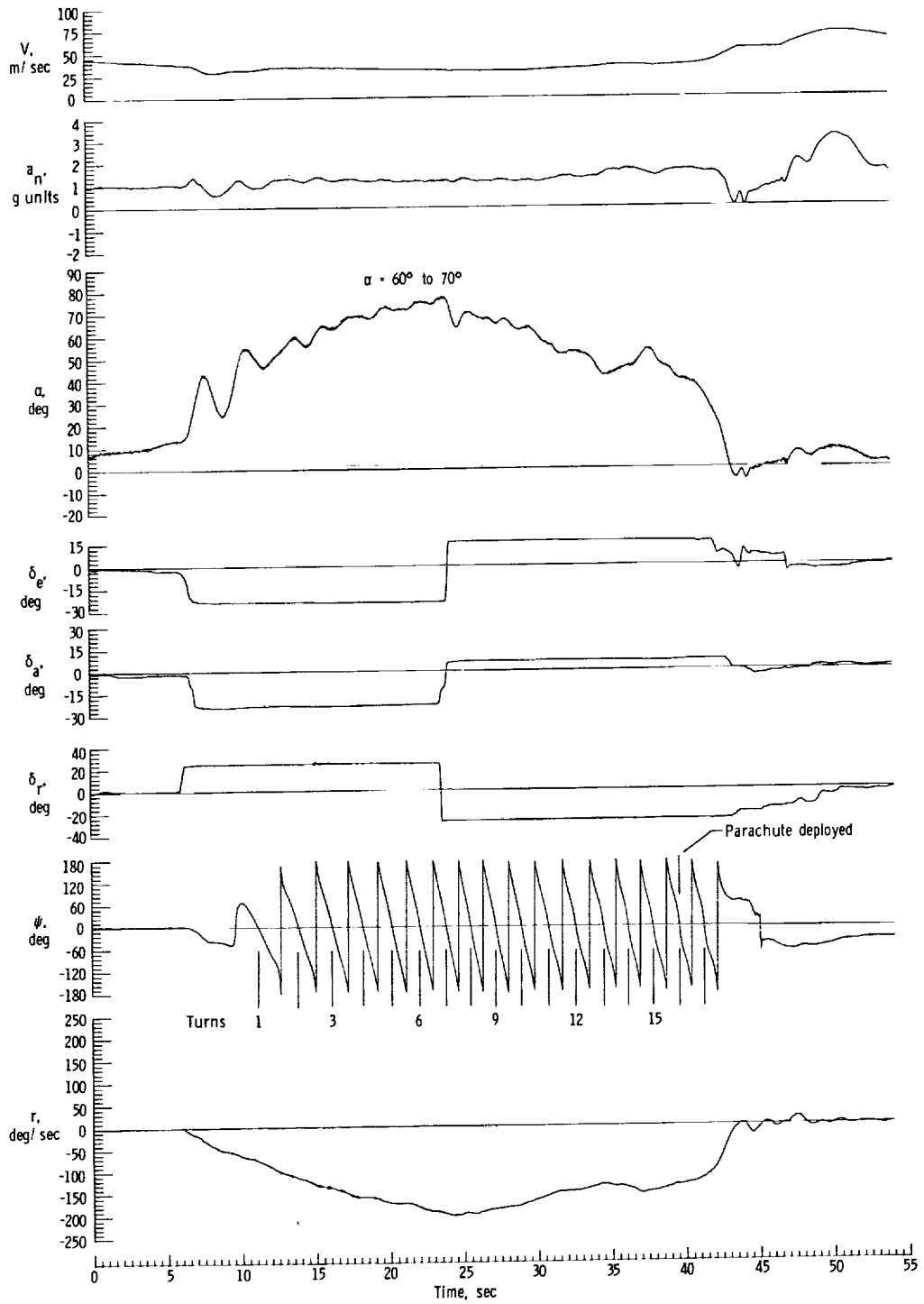α = 50° to 52°

Turns 1 2 3 4 5 6

Time, sec
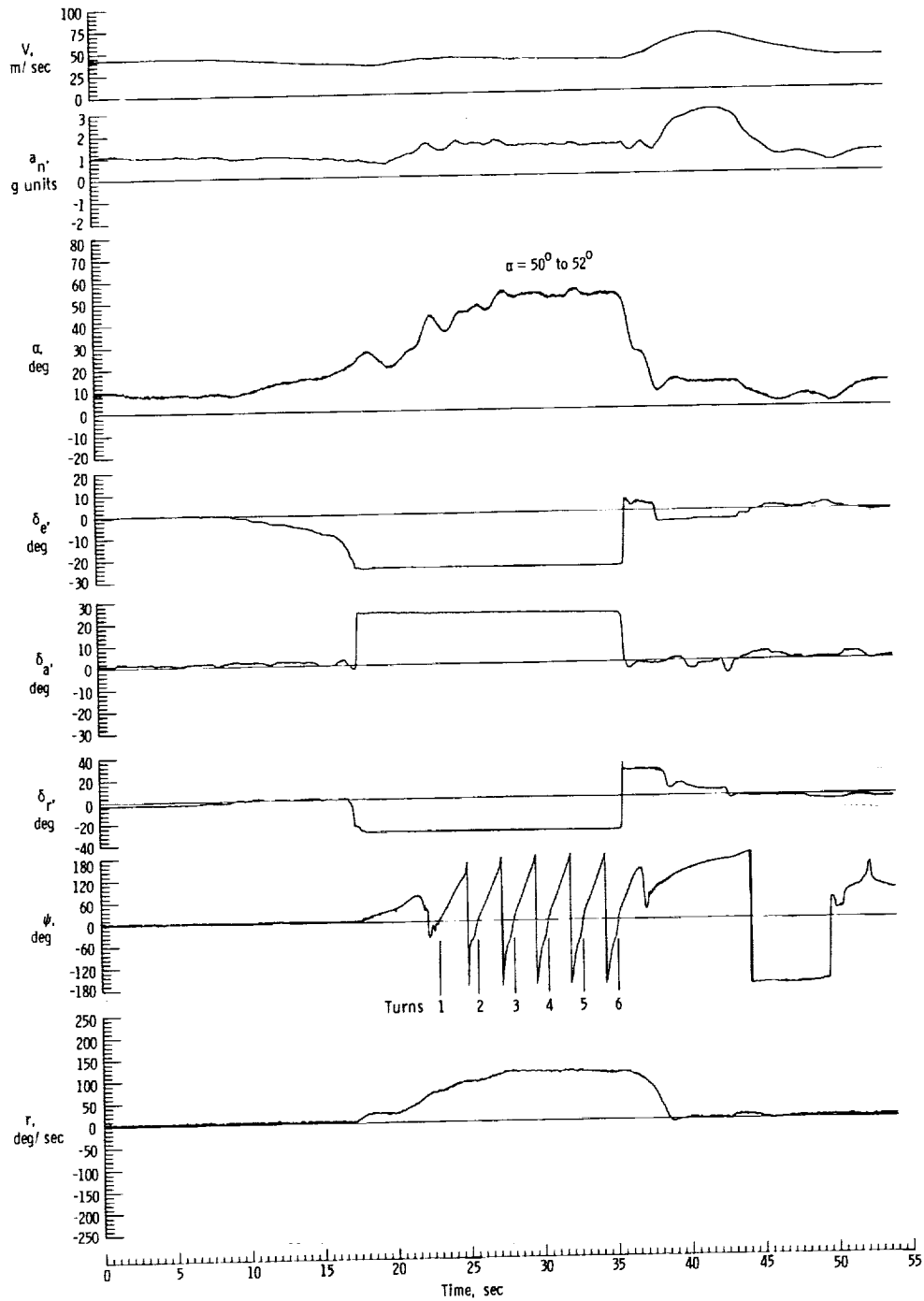
(a) Basic airplane (unmodified wing)
in moderately flat spin.

Figure 7.- Selected time histories of spin modes.   Prospin
controls include ailerons deflected against spin.

90

(b) Airplane with drooped outboard wing leading edge.

Figure 7.- Continued.

(c) Airplane with full-span drooped wing leading edge.
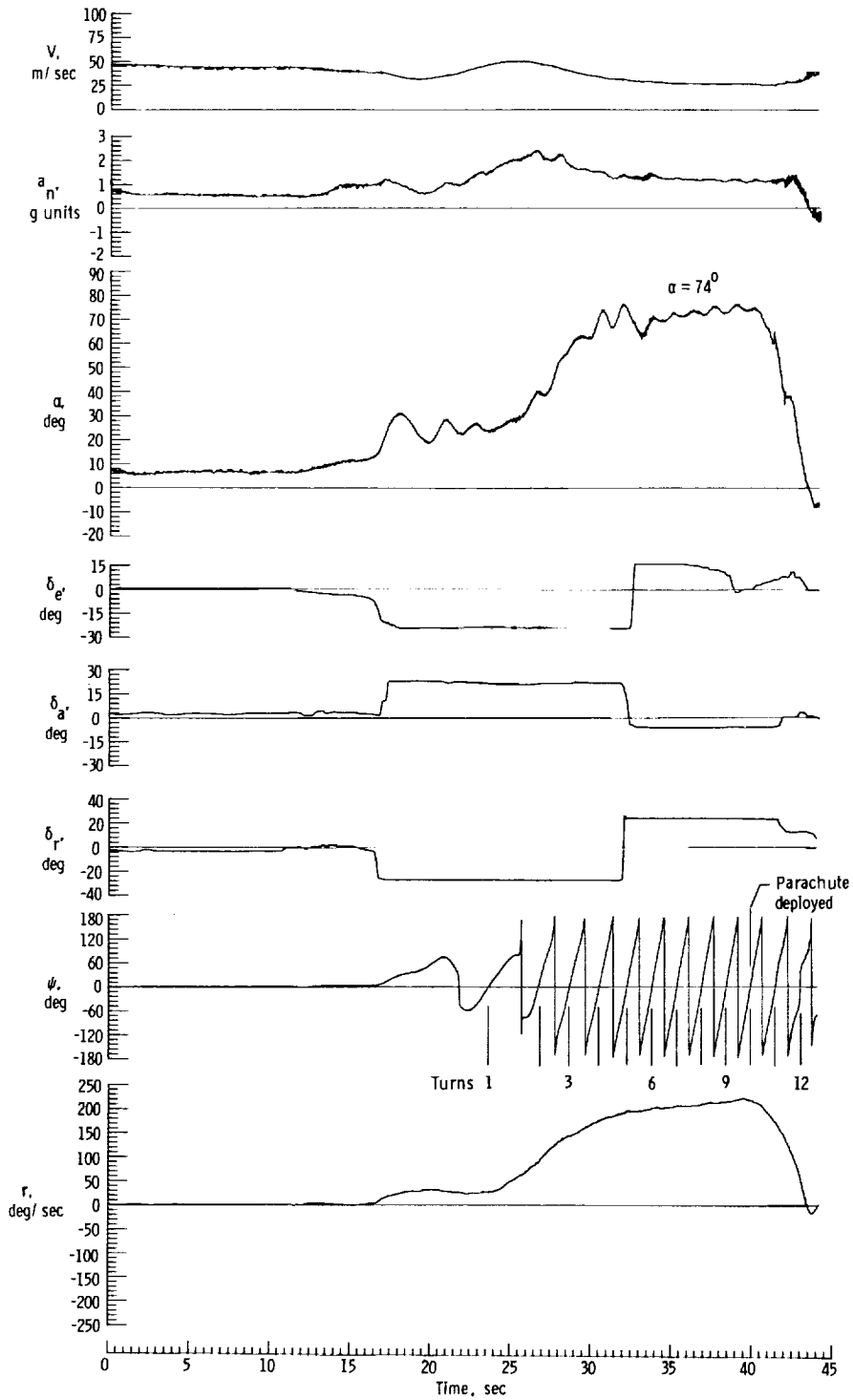
Figure 7.- Concluded.

Figure 8.- Flat spin characteristics for airplane with
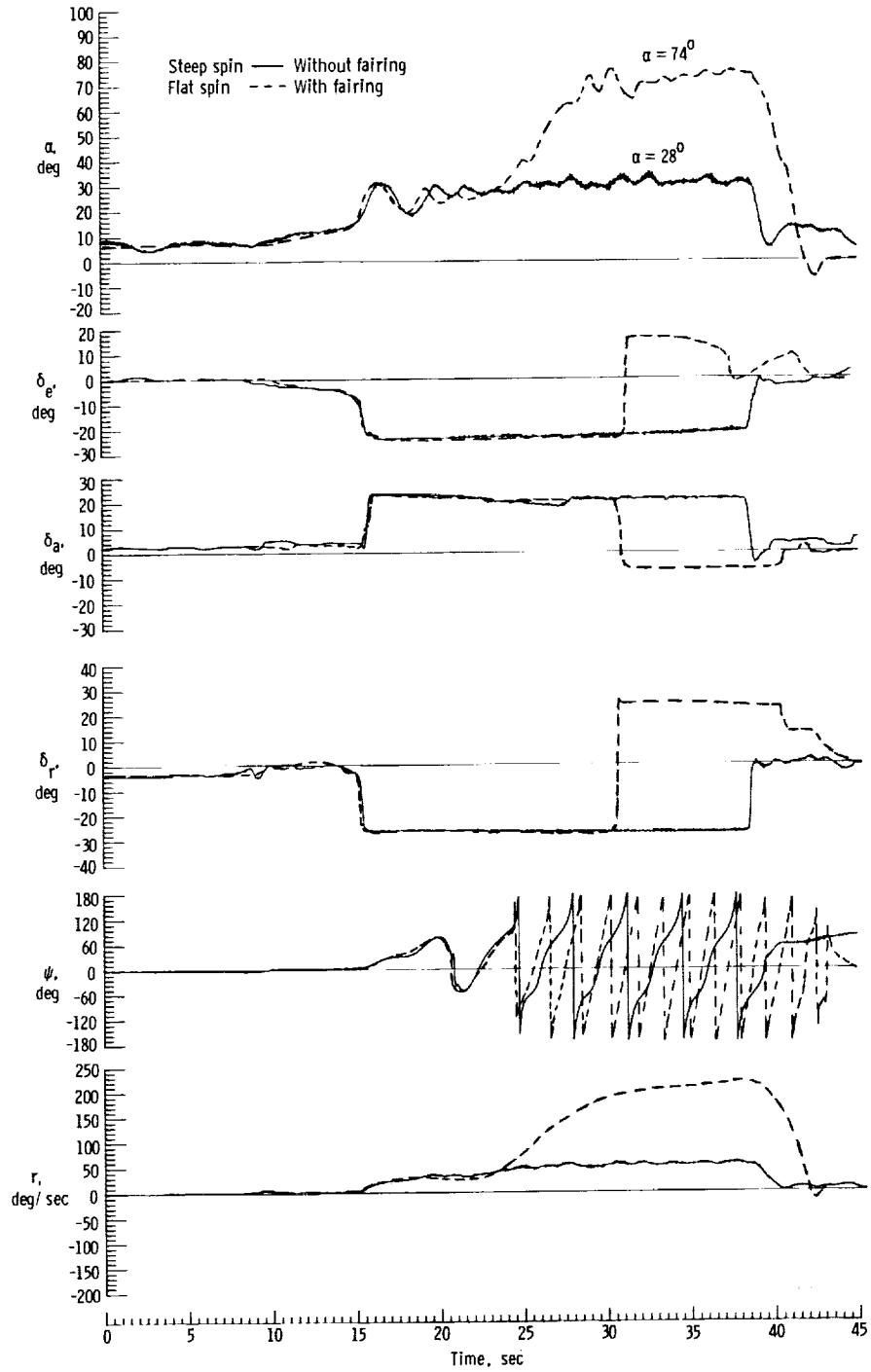   fairing at inboard juncture between drooped leading
    edge and the basic wing.

Figure 9.- Selected time history comparison of spins
of airplane with drooped outboard leading edge
with and without fairing at inboard juncture.

1. Report No. NASA TP-1589	2. Government Accession No.	3. Recipient's Catalog No.
4. Title and Subtitle EXPLORATORY STUDY OF THE EFFECTS OF WING-LEADING-EDGE MODIFICATIONS ON THE STALL/SPIN BEHAVIOR OF A LIGHT GENERAL AVIATION AIRPLANE		5. Report Date December 1979
		6. Performing Organization Code
7. Author(s) Staff of Langley Research Center		8. Performing Organization Report No. L-13143
		10. Work Unit No. 505-41-13-06
9. Performing Organization Name and Address NASA Langley Research Center Hampton, VA 23665		11. Contract or Grant No.
		13. Type of Report and Period Covered Technical Paper
12. Sponsoring Agency Name and Address National Aeronautics and Space Administration Washington, DC 20546		14. Sponsoring Agency Code

15. Supplementary Notes

16. Abstract

An exploratory study was conducted to determine the effects of several wing-leading-edge modifications on the stalling and spinning characteristics of a light general aviation airplane. Configurations with full-span and segmented leading-edge flaps and full-span and segmented leading-edge droop were tested. Studies were conducted with wind-tunnel models, with an outdoor radio-controlled model, and with a full-scale airplane. Results showed that wing-leading-edge modifications can produce large effects on stall/spin characteristics, particularly on spin resistance. One outboard wing-leading-edge modification tested significantly improved lateral stability at stall, spin resistance, and developed spin characteristics.

17. Key Words (Suggested by Author(s))		18. Distribution Statement
Stall/spin Wing design Aerodynamics General aviation	Radio-control model testing Flight testing Flight safety	Unclassified - Unlimited Subject Category 05

19. Security Classif. (of this report) Unclassified	20. Security Classif. (of this page) Unclassified	21. No. of Pages 96	22. Price* $6.00